PETROLOGY AND ENVIRONMENTS OF DEPOSITION OF THE PERCHA FORMATION, UPPER DEVONIAN, SOUTHWESTERN NEW MEXICO

by
Gary Kocurek

A Thesis
Presented to the
Faculty of the Department of Geology
The University of Houston
in Partial Fulfillment
of the Requirements of the
Degree of Master of Science

The University of Houston
August, 1977

ACKNOWLEDGMENTS

I am greatly indebted to Dr. Henry S. Chafetz, the principal thesis advisor. Hank Chafetz has freely given of his time and energy in the field, in the lab, in many discussions, and in the editing of this manuscript. It is a pleasure to acknowledge his many contributions to this study and to thank him for his guidance throughout my graduate work. I wish to thank Dr. Rosalie F. Maddocks for her eagerness to discuss aspects of this study and for her many suggestions made during the entire study. Dr. Victor L. Mote offered many helpful suggestions in the editing of this manuscript. Dr. John C. Butler has enthusiastically supported my work and was most helpful with the x-ray diffraction procedures. Dr. James E. Canright of Arizona State University kindly offered his aid in the identification of the microbiota from organic residues. Dr. Dietmar Schumacher of the University of Arizona provided encouragement and some "inaccessible" literature.

I wish to thank M.T. Everhart of the Hatchet Ranch, Sterling Roberts of Hillsboro and Homer White of Silver City for allowing me access to their land. A special thanks is extended to M.T. Everhart for his interest in this study and for his kind hospitality. This study was funded in part by grants from the University of Houston Geology Foundation and a Sigma Xi grant-in-aid of research.

Special thanks are extended to Keith Myers for his field assistance and discussion, and to Bernie Huysman for typing early drafts of this report. Very special thanks are given to Dianna Stalinsky for her assistance in drafting and for her tolerance during this period.

ABSTRACT

The Upper Devonian Percha Formation of the southwestern New Mexico is a transgressive terrigenous-carbonate deposit that accumulated in a complex of depositional environments that grade laterally and vertically from tidal flat to shallow lagoon to carbonate platform. The Percha unconformably overlies Silurian strata. The basal 0 to 32 m of strata consist of a variable sequence of distinct lithofacies. In the northern part of the study area, these deposits show a vertical gradation from fissile shale, showing an irregular alternation of silty lenticular and clayey laminae, to more regularly laminated interbedded siltstone and mudstone. This sequence of strata was deposited on a transgressive tidal flat. In the southern part of the study area, this tidal sequence is repeated, but the shales and mudstones are calcareous and overlie quartz sandstone. Carbonate accumulation may have been initiated by diminished terrigenous influx, resulting in tidal flat progradation after the initial deposition of a transgressive beach sand. Rhythmically laminated carbonaceous limestone beds occur at both the northern and southern study areas and were deposited in lagoons isolated from terrigenous influx.

Tidal deposits in the northern area are overlain by 44 to 74 m of carbonaceous finely laminated, fissile, black shale that grades upward into silty lenticularly laminated, bioturbated, green shale. This shale sequence was deposited in a transgressive, shallow, euxinic

lagoon barred from open circulation by the offshore carbonate buildup. At the southern area, where this lagoonal sequence is 30 m thick, the shale is highly calcareous, fossiliferous, and shows a greater abundance of current-deposited silty laminae. Lagoonal conditions were less restricted at the southern area because carbonate accumulation, initiated during tidal flat deposition, maintained the lagoon bottom at a shallow depth, where it was stirred by wind-generated waves and currents.

In the northern area, the upper 4 to 14 m of the shale sequence contains horizontal rows of discrete carbonate lenses a few centimeters in length. In the southern area, this zone is 18 m thick, and carbonate units occur as discontinuous layers several meters long. These carbonate lenses and layers formed in shallow channels filled by fine skeletal debris. This fine carbonate sediment was derived from the offshore carbonate buildup and transported into the outer edge of the lagoon. Channel-fills at the northern area have broken up into discrete lenses by loading.

Shale with carbonate lenses and layers grades upward into 8 to 28 m of strata composed of crinoidal ripples separated by a few centimeters of carbonate mud. This zone of flaser bedding is cut by numerous, shallow, migrating channels. This sequence of strata was deposited on the inner carbonate platform.

Flaser bedded carbonates grade upward into 1 to 38 m of crinoidal and bryozoan skeletal sand beds separated by a few centimeters of carbonate mud. Individual skeletal sand beds are up to 1 m thick but are highly variable in thickness, and they show wavy, flaser, and lenticular bedding, cross-stratification, and parallel laminations. These strata were deposited in the high energy outer carbonate platform where a broad crinoidal and bryozoan garden formed a wave-baffling bank maintained at or near wave base. The Percha carbonate buildup was unlike most modern platform margin buildups because it lacked a major boundstone wave barrier. As a result, upwelling currents at the platform edge were only gradually diminished over the broad platform, and outer platform conditions extended over a broad area of the craton.

The lithology and sedimentary structures of the Percha are transitional into the overlying Mississippian strata, and no break in the depositional package is present. This contact has been described by previous workers as unconformable, based on the fauna. The absence of a complete "time record" is the result of submarine erosion and the nature of sedimentation.

CONTENTS

TEXT

Tables

Figures

Page

INTRODUCTION

Purpose

This study was undertaken to determine the environments of deposition of the Upper Devonian Percha Formation. The formation has been divided into five lithofacies, which are defined by the sedimentary structures and lithology of the strata. The vertical and lateral relations of lithofacies have been interpreted to provide an understanding of the sequence of changes in the environment of deposition of the Percha Formation.

Location

This study was conducted in southwestern New Mexico, in the counties of Grant, Hidalgo, and Sierra. Sections were measured at Bear Mountain and Cain Spring Canyon in the Silver City Range, northwest of Silver City; at the "ghost town" of Georgetown; directly south of Percha Creek near Hillsboro; and at the Big Hatchet Mountains (Fig. 1). The sections at Bear Mountain, Cain Spring, Georgetown, and Hillsboro are collectively referred to throughout this study as the "northern sections".

Figure 1. Location map showing the study area in southwestern New Mexico. Locations of measured sections are indicated.

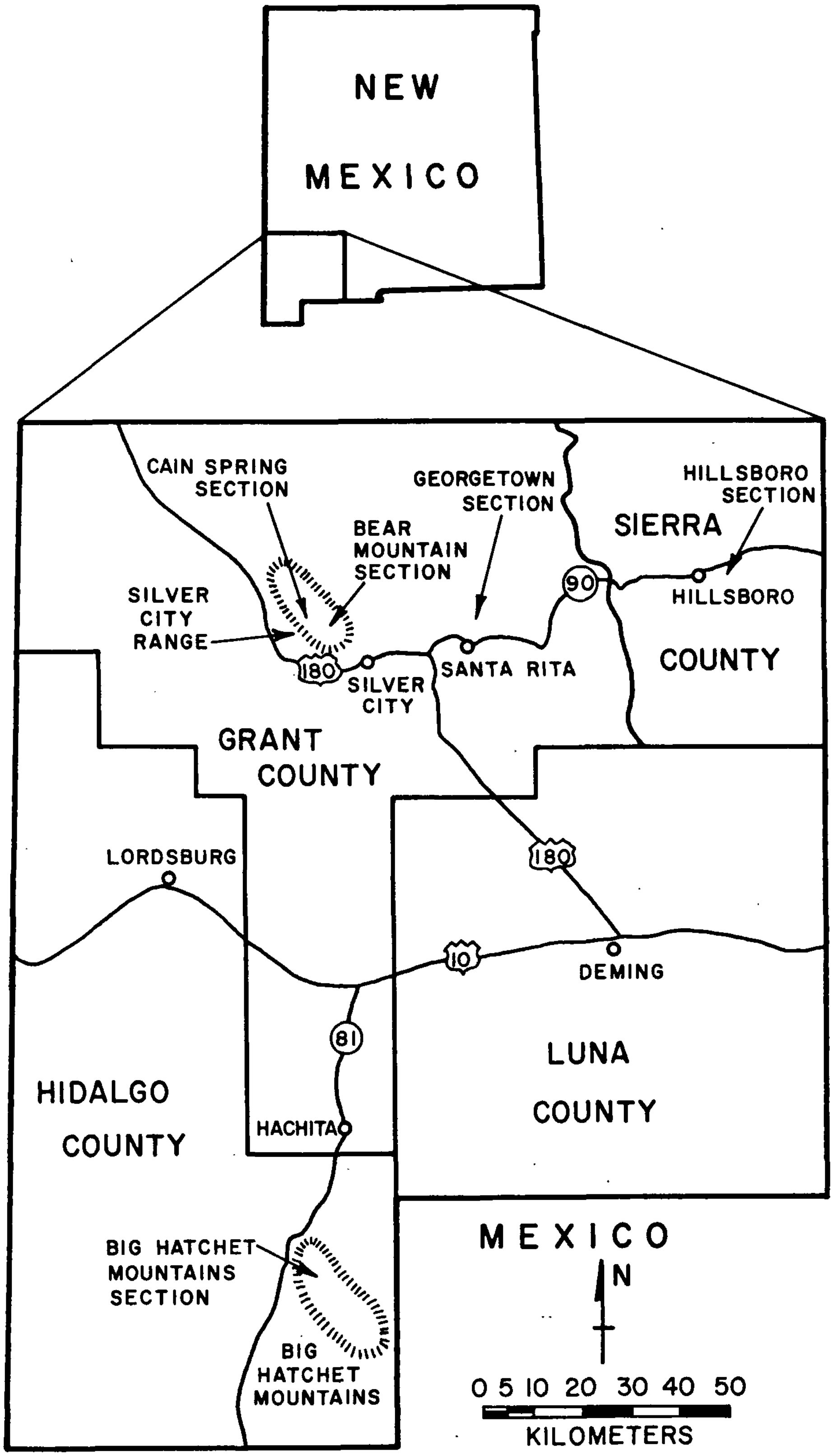

NEW
MEXICO
CAIN SPRING
SECTION
GEORGETOWN
SECTION
HILLSBORO
SECTION
BEAR
MOUNTAIN
SECTION
SIERRA
SILVER
CITY
RANGE
90
HILLSBORO
180
SILVER
CITY
SANTA RITA
COUNTY
GRANT
COUNTY
LORDSBURG
180
10
DEMING
81
LUNA
COUNTY
HIDALGO
COUNTY
HACHITA
MEXICO
BIG HATCHET
MOUNTAINS
SECTION
N
BIG
HATCHET
MOUNTAINS
0 5 10 20 30 40 50
KILOMETERS

Methods of Study

Field work was conducted during the summers of 1975 and 1976 and February of 1977. Five sections were described, photographed, sampled, and measured with a Jacob Staff and Brunton Compass. Field study of the sedimentary structures, bed forms, and vertical and lateral relationships between the various lithologic components making up the Percha Formation form the core of this study.

Laboratory work was conducted at the Geology Department of the University of Houston. Samples were slabbed, etched, and studied through a binocular microscope with emphasis on "micro-sedimentary structures". Over 200 thin-sections were examined petrographically in order to determine lithology and to investigate sedimentary structures too small to be adequately studied with the binocular microscope. Point-counts were made where deemed necessary and consisted of 100 points per thin-section. Accessory use was made of stains and x-ray radiography. Over 100 x-ray diffraction analyses were made, primarily of the shales, to determine mineralogy. Clay minerals present were "semi-quantified" by methods described by Hawkins (1970). Because the Hawkins method is unpublished, it, as well as the results of clay mineral quantification, are presented in the Appendix. For fine-grained carbonates, a "semi-quantification" of the relative abundance of dolomite versus calcite was performed according to Tennant and Berger (1957).

Carbonaceous material forms a significant fraction of the Percha shales. In order to determine the nature of the carbonaceous material, shale samples were dissolved in hydrochloric acid, then in hydrofluoric acid, with the residue sieved on a #400 (.037 mm) mesh sieve, mounted, and studied.

Carbonate and terrigenous rocks in this study are classified according to Folk (1962, 1974a). Bed and laminae thickness are described according to terminologies proposed by Ingram (1954) and Campbell (1967), respectively. Those sedimentary structures described as wavy-, flaser-, or lenticular bedded, are classified according to Reineck and Wunderlich (1968).

Previous Work

Significant previous work on the Percha Formation of southwestern New Mexico consists of stratigraphic and paleontological reports. Gordon (1907) first applied the name Percha to all Devonian strata in the Kingston-Hillsboro-Lake Valley region of New Mexico. Dunham (1935) divided the formation into two distinct members consisting of a lower dark shale and an upper shale with nodular limestone beds. After 1940, Stevenson and others divided the original Percha Formation of Gorgon (1907) into several different formations (see Stevenson, 1945, for discussion). For that portion of Devonian strata retaining the Percha name, Stevenson (1945) proposed the names Ready Pay Member and Box Member for the lower and upper members of Dunham (1935), respectively. An overall discussion of the stratigraphy is found in Kottlowski (1963).

Zeller (1965) provides an excellent coverage of the stratigraphy of the Big Hatchet Mountains. Bowsher (1967) relates thickness of Devonian strata in the area to the overall tectonics of the region.

Numerous descriptions of the fauna of the Percha have been published, but many are highly fragmental and report only occurrences of a particular fossil from a single location. Pioneer faunal lists are by Kindle (1909) and Darton (1917). Later significant studies on the megafauna include Fritz (1944), Stainbrook (1947), and Miller and Cullison (1951).

Geological Setting and Stratigraphy

The Percha Formation is an Upper Devonian-Lower Mississippian shale-carbonate unit cropping out in southwestern New Mexico and eastern Arizona, and in the Franklin and Hueco Mountains of west Texas. The Percha Formation unconformably overlies the Silurian Montoya Dolomite and is gradational into the overlying Mississippian Lake Valley Formation in the northern sections and the Escabrosa Formation in the Big Hatchet Mountains.

Thicknesses of Percha strata measured in this report are:

Bear Mountain	113 m
Cain Spring	104 m
Georgetown	93 m
Hillsboro	71 m
Big Hatchet Mountains	137 m

The top of the Percha, as used in this report, does not correspond to the same stratigraphic horizon traditionally used in mapping. The upper contact used previously in mapping the Percha does not correspond to genetic depositional packages within this formation. Evidence indicates that the Percha Formation and the overlying Lake Valley or Escabrosa Formations are part of the same depositional package and gradational at all points. On the measured sections and in this study, however, only the basal member of the Lake Valley Formation (Andrecito Member) at the northern sections is included, and the sections are arbitrarily ended at the base of the Alamogordo Member. At the Big Hatchet Mountains, the section is again arbitrarily ended at the first oolite bed in the Escabrosa Formation. Figure 2 illustrates the traditional mapping boundaries and that part of the section considered here. Schematic stratigraphic columns for these sections are provided as figures 3 to 7.

On a much broader scope, the Percha Formation belongs to an extensive Devonian-Mississippian belt of black shales overlain by carbonates. The Percha forms the southwestern extent of this belt, which includes the Woodford, Chattanooga, Ohio, New Albany and other dark shales (see discussions by Amsden and others, 1967; Collinson and others, 1967; McGlasson, 1967; Pool and others, 1967).

Figure 2. Stratigraphic columns of part of the Devonian and Mississippian strata of southwestern New Mexico, showing that part of the section considered in this study.

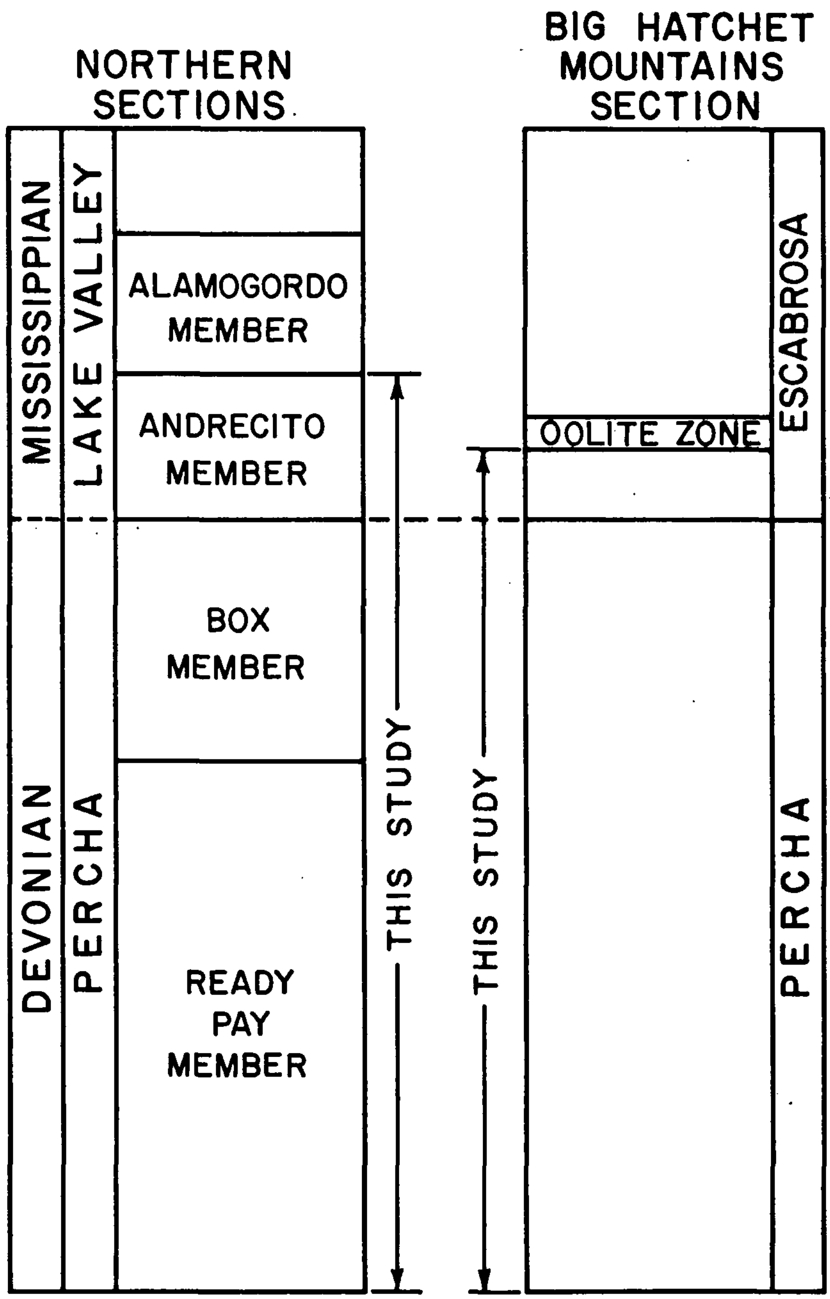
NORTHERN SECTIONS
BIG HATCHET MOUNTAINS SECTION
MISSISSIPPIAN
LAKE VALLEY
ALAMOGORDO MEMBER
ANDRECITO MEMBER
DEVONIAN
PERCHA
BOX MEMBER
READY PAY MEMBER
THIS STUDY
THIS STUDY
OOLITE ZONE
ESCABROSA
PERCHA

Figure 3. Schematic illustration of the Cain Spring measured section located within Cane Spring Canyon, White Ranch, Silver City Range, approximately 14.4 km northwest of Silver City.

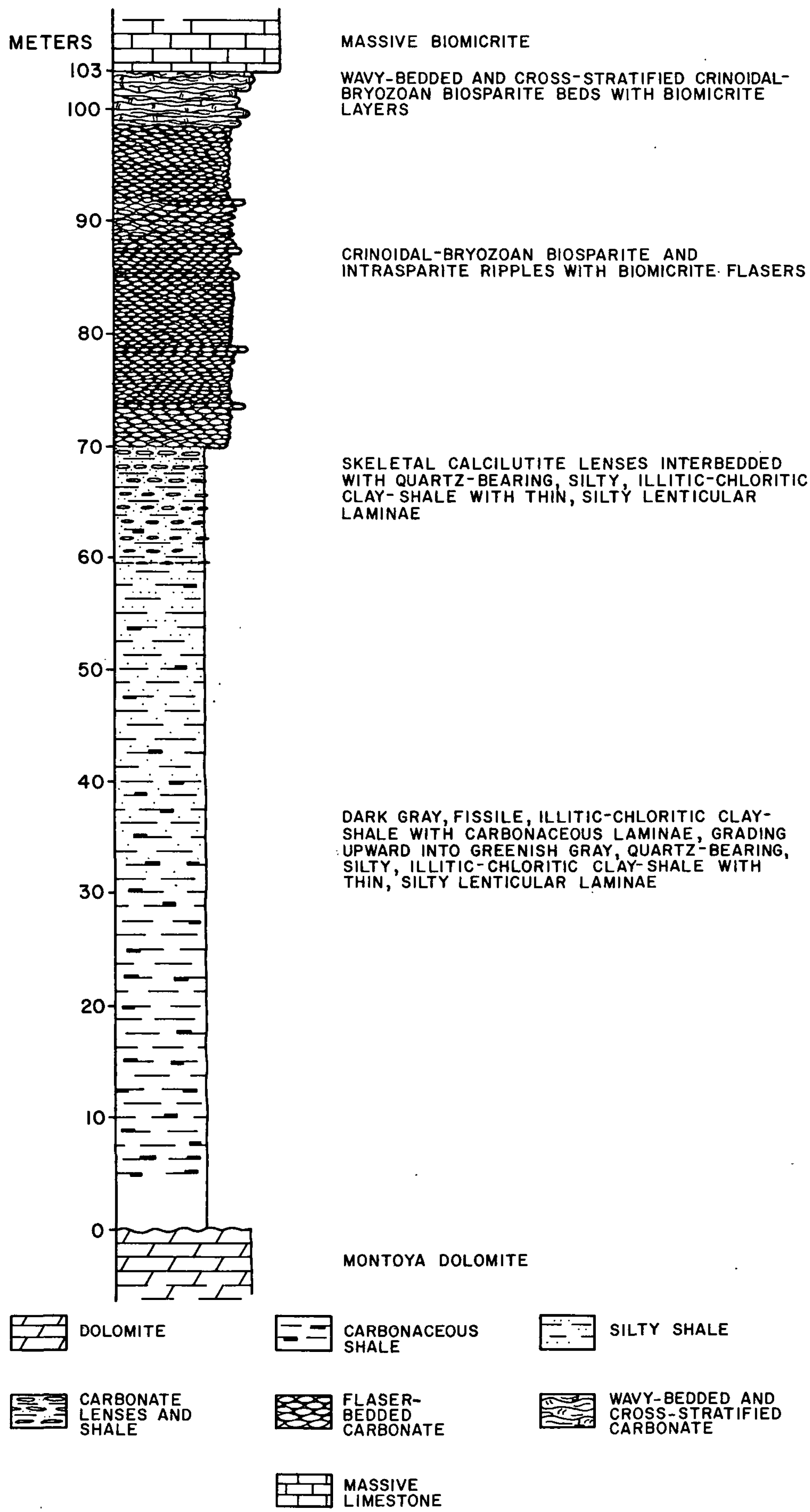
METERS
103
100
90
80
70
60
50
40
30
20
10
0
MASSIVE BIOMICRITE
WAVY-BEDDED AND CROSS-STRATIFIED CRINOIDAL-BRYOZOAN BIOSPARITE BEDS WITH BIOMICRITE LAYERS
CRINOIDAL-BRYOZOAN BIOSPARITE AND INTRASPARITE RIPPLES WITH BIOMICRITE FLASERS
SKELETAL CALCILUTITE LENSES INTERBEDDED WITH QUARTZ-BEARING, SILTY, ILLITIC-CHLORITIC CLAY-SHALE WITH THIN, SILTY LENTICULAR LAMINAE
DARK GRAY, FISSILE, ILLITIC-CHLORITIC CLAY-SHALE WITH CARBONACEOUS LAMINAE, GRADING UPWARD INTO GREENISH GRAY, QUARTZ-BEARING, SILTY, ILLITIC-CHLORITIC CLAY-SHALE WITH THIN, SILTY LENTICULAR LAMINAE
MONTOYA DOLOMITE
DOLOMITE
CARBONACEOUS SHALE
SILTY SHALE
CARBONATE LENSES AND SHALE
FLASER-BEDDED CARBONATE
WAVY-BEDDED AND CROSS-STRATIFIED CARBONATE
MASSIVE LIMESTONE

Figure 4. Schematic illustration of the Bear Mountain measured section, located on Bear Mountain, within the Gila National Forest, Silver City Range, approximately 9.6 km northwest of Silver City. The base of the section is located directly below Bear Mountain road.

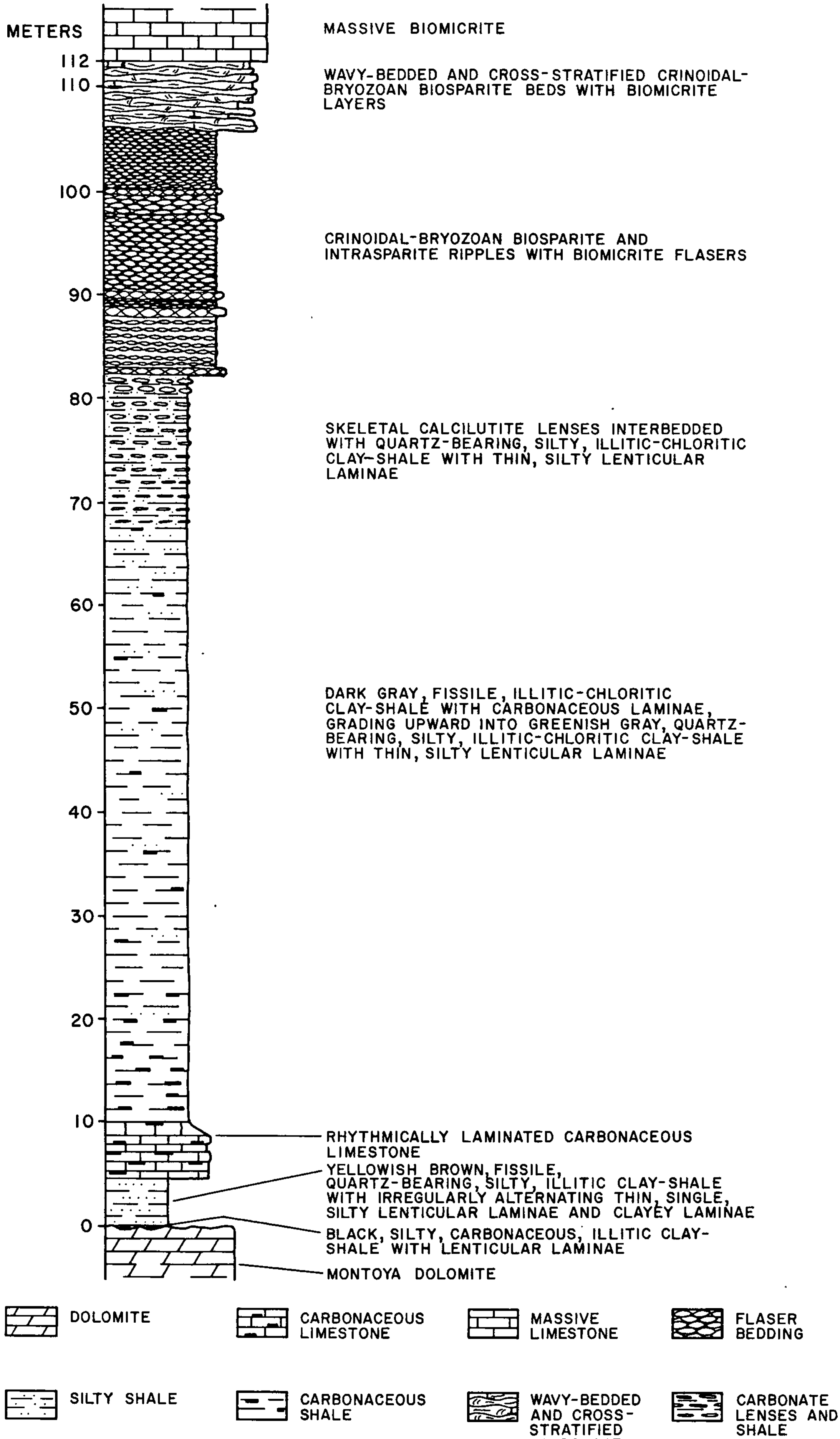

METERS
112
110
100
90
80
70
60
50
40
30
20
10
0
MASSIVE BIOMICRITE
WAVY-BEDDED AND CROSS-STRATIFIED CRINOIDAL-BRYOZOAN BIOSPARITE BEDS WITH BIOMICRITE LAYERS
CRINOIDAL-BRYOZOAN BIOSPARITE AND INTRASPARITE RIPPLES WITH BIOMICRITE FLASERS
SKELETAL CALCILUTITE LENSES INTERBEDDED WITH QUARTZ-BEARING, SILTY, ILLITIC-CHLORITIC CLAY-SHALE WITH THIN, SILTY LENTICULAR LAMINAE
DARK GRAY, FISSILE, ILLITIC-CHLORITIC CLAY-SHALE WITH CARBONACEOUS LAMINAE, GRADING UPWARD INTO GREENISH GRAY, QUARTZ-BEARING, SILTY, ILLITIC-CHLORITIC CLAY-SHALE WITH THIN, SILTY LENTICULAR LAMINAE
RHYTHMICALLY LAMINATED CARBONACEOUS LIMESTONE
YELLOWISH BROWN, FISSILE, QUARTZ-BEARING, SILTY, ILLITIC CLAY-SHALE WITH IRREGULARLY ALTERNATING THIN, SINGLE, SILTY LENTICULAR LAMINAE AND CLAYEY LAMINAE
BLACK, SILTY, CARBONACEOUS, ILLITIC CLAY-SHALE WITH LENTICULAR LAMINAE
MONTOYA DOLOMITE
DOLOMITE
CARBONACEOUS LIMESTONE
MASSIVE LIMESTONE
FLASER BEDDING
SILTY SHALE
CARBONACEOUS SHALE
WAVY-BEDDED AND CROSS-STRATIFIED CARBONATE
CARBONATE LENSES AND SHALE

Figure 5. Schematic illustration of the Georgetown measured section, located adjacent to the Georgetown cemetery, within the Gila National Forest.

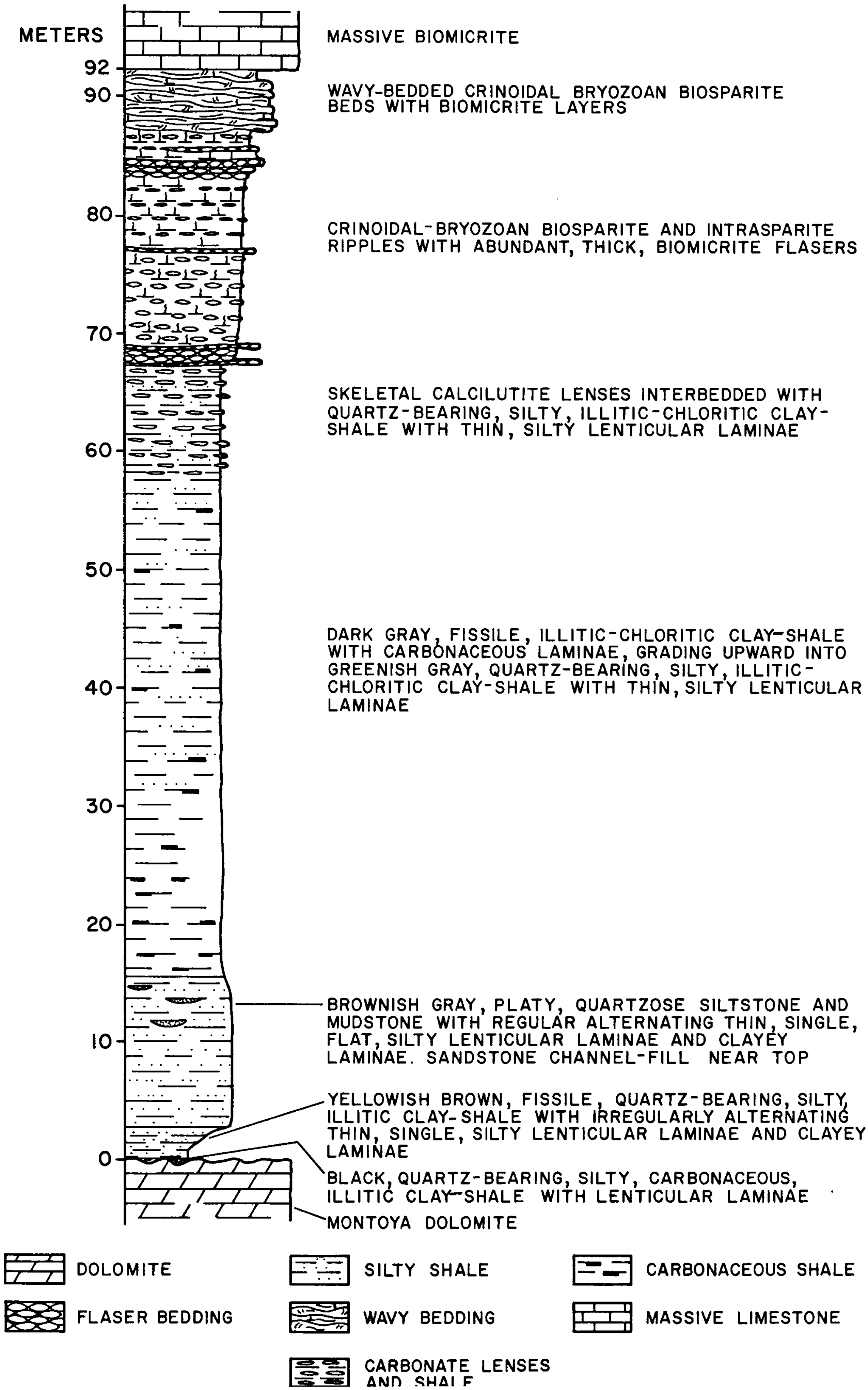

METERS
92
90
80
70
60
50
40
30
20
10
0
MASSIVE BIOMICRITE
WAVY-BEDDED CRINOIDAL BRYOZOAN BIOSPARITE BEDS WITH BIOMICRITE LAYERS
CRINOIDAL-BRYOZOAN BIOSPARITE AND INTRASPARITE RIPPLES WITH ABUNDANT, THICK, BIOMICRITE FLASERS
SKELETAL CALCILUTITE LENSES INTERBEDDED WITH QUARTZ-BEARING, SILTY, ILLITIC-CHLORITIC CLAY-SHALE WITH THIN, SILTY LENTICULAR LAMINAE
DARK GRAY, FISSILE, ILLITIC-CHLORITIC CLAY-SHALE WITH CARBONACEOUS LAMINAE, GRADING UPWARD INTO GREENISH GRAY, QUARTZ-BEARING, SILTY, ILLITIC-CHLORITIC CLAY-SHALE WITH THIN, SILTY LENTICULAR LAMINAE
BROWNISH GRAY, PLATY, QUARTZOSE SILTSTONE AND MUDSTONE WITH REGULAR ALTERNATING THIN, SINGLE, FLAT, SILTY LENTICULAR LAMINAE AND CLAYEY LAMINAE. SANDSTONE CHANNEL-FILL NEAR TOP
YELLOWISH BROWN, FISSILE, QUARTZ-BEARING, SILTY, ILLITIC CLAY-SHALE WITH IRREGULARLY ALTERNATING THIN, SINGLE, SILTY LENTICULAR LAMINAE AND CLAYEY LAMINAE
BLACK, QUARTZ-BEARING, SILTY, CARBONACEOUS, ILLITIC CLAY-SHALE WITH LENTICULAR LAMINAE
MONTOYA DOLOMITE
DOLOMITE
SILTY SHALE
CARBONACEOUS SHALE
FLASER BEDDING
WAVY BEDDING
MASSIVE LIMESTONE
CARBONATE LENSES AND SHALE

Figure 6. Schematic illustration of the Hillsboro measured section, located on the Roberts Ranch, directly south of that part of Percha Creek called "The Box", approximately 5 km southeast of Hillsboro.

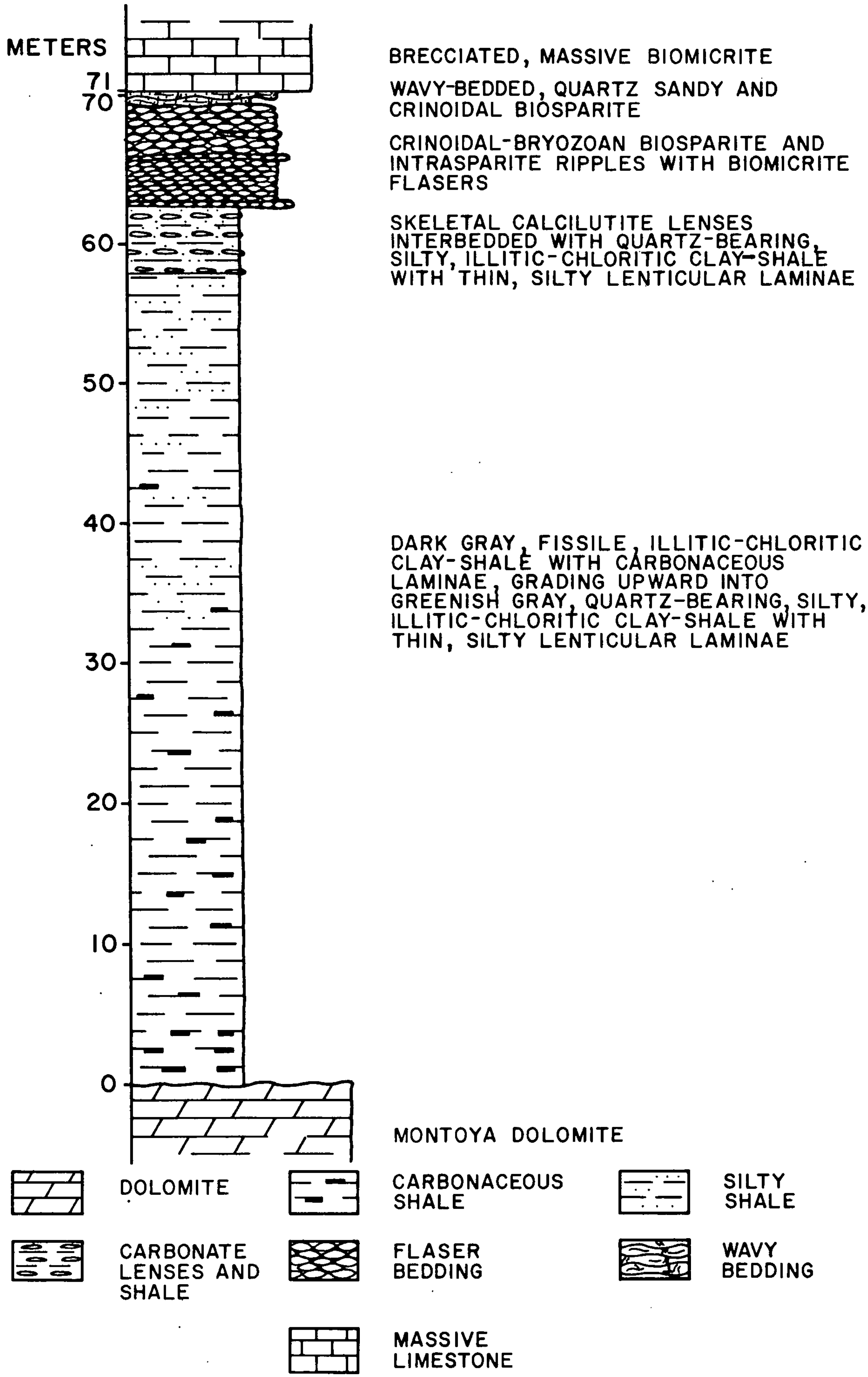
METERS
71
70
60
50
40
30
20
10
0
BRECCIATED, MASSIVE BIOMICRITE
WAVY-BEDDED, QUARTZ SANDY AND CRINOIDAL BIOSPARITE
CRINOIDAL-BRYOZOAN BIOSPARITE AND INTRASPARITE RIPPLES WITH BIOMICRITE FLASERS
SKELETAL CALCILUTITE LENSES INTERBEDDED WITH QUARTZ-BEARING, SILTY, ILLITIC-CHLORITIC CLAY-SHALE WITH THIN, SILTY LENTICULAR LAMINAE
DARK GRAY, FISSILE, ILLITIC-CHLORITIC CLAY-SHALE WITH CARBONACEOUS LAMINAE, GRADING UPWARD INTO GREENISH GRAY, QUARTZ-BEARING, SILTY, ILLITIC-CHLORITIC CLAY-SHALE WITH THIN, SILTY LENTICULAR LAMINAE
MONTOYA DOLOMITE
DOLOMITE
CARBONACEOUS SHALE
SILTY SHALE
CARBONATE LENSES AND SHALE
FLASER BEDDING
WAVY BEDDING
MASSIVE LIMESTONE

Figure 7. Schematic illustration of the Big Hatchet Mountains section, located along the northern flank of Big Hatchet Peak on the Everhart Ranch. The section is a composite of outcrops in Horse Pasture and Mescal Canyons, with the lower half of the section best exposed in Horse Pasture Canyon and the upper half best exposed in Mescal Canyon. The section parallels that of Zeller (1965).

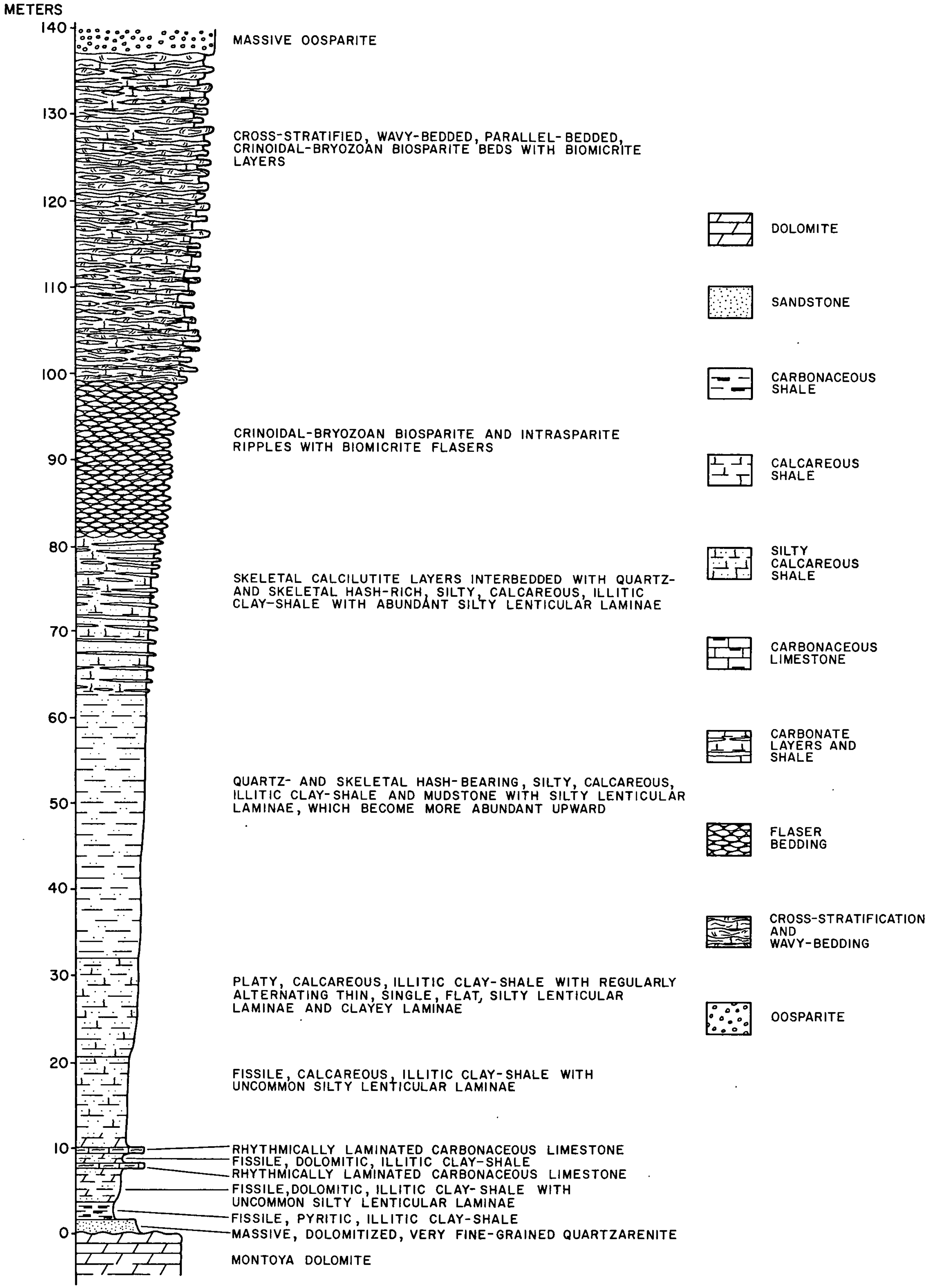
METERS
140
130
120
110
100
90
80
70
60
50
40
30
20
10
0
MASSIVE OOSPARITE
CROSS-STRATIFIED, WAVY-BEDDED, PARALLEL-BEDDED, CRINOIDAL-BRYOZOAN BIOSPARITE BEDS WITH BIOMICRITE LAYERS
CRINOIDAL-BRYOZOAN BIOSPARITE AND INTRASPARITE RIPPLES WITH BIOMICRITE FLASERS
SKELETAL CALCILUTITE LAYERS INTERBEDDED WITH QUARTZ- AND SKELETAL HASH-RICH, SILTY, CALCAREOUS, ILLITIC CLAY-SHALE WITH ABUNDANT SILTY LENTICULAR LAMINAE
QUARTZ- AND SKELETAL HASH-BEARING, SILTY, CALCAREOUS, ILLITIC CLAY-SHALE AND MUDSTONE WITH SILTY LENTICULAR LAMINAE, WHICH BECOME MORE ABUNDANT UPWARD
PLATY, CALCAREOUS, ILLITIC CLAY-SHALE WITH REGULARLY ALTERNATING THIN, SINGLE, FLAT, SILTY LENTICULAR LAMINAE AND CLAYEY LAMINAE
FISSILE, CALCAREOUS, ILLITIC CLAY-SHALE WITH UNCOMMON SILTY LENTICULAR LAMINAE
RHYTHMICALLY LAMINATED CARBONACEOUS LIMESTONE
FISSILE, DOLOMITIC, ILLITIC CLAY-SHALE
RHYTHMICALLY LAMINATED CARBONACEOUS LIMESTONE
FISSILE, DOLOMITIC, ILLITIC CLAY-SHALE WITH UNCOMMON SILTY LENTICULAR LAMINAE
FISSILE, PYRITIC, ILLITIC CLAY-SHALE
MASSIVE, DOLOMITIZED, VERY FINE-GRAINED QUARTZARENITE
MONTOYA DOLOMITE
DOLOMITE
SANDSTONE
CARBONACEOUS SHALE
CALCAREOUS SHALE
SILTY CALCAREOUS SHALE
CARBONACEOUS LIMESTONE
CARBONATE LAYERS AND SHALE
FLASER BEDDING
CROSS-STRATIFICATION AND WAVY-BEDDING
OOSPARITE

MONTOYA - PERCHA UNCONFORMITY

The unconformity between the Percha Formation and the underlying Montoya Group is commonly marked by a weathered surface and/or a basal conglomerate. A slightly irregular surface with shallow depressions exists locally, but nowhere is the contact sufficiently well-exposed to observe relief on the erosional surface over a broad area.

At Hillsboro, the unconformity is marked by a chert-cemented, chert pebble conglomerate up to several meters thick. Coarse sand- to pebble-sized angular chert fragments form the bulk of the conglomerate, but shale rock fragments are sparingly present. Quartz crystal-lined cavities are common in the conglomerate. It was not determined to what extent the conglomerate reflects development of karst topography on the Montoya Dolomite before deposition of the Percha or subsequent mineralization and fault brecciation along the contact after deposition of the Percha. The area is heavily mineralized, however, and at least part of the chert conglomerate is the result of later mineralization and faulting.

The unconformity at Georgetown is marked by a blackish red (5 R 2/2), crystalline hematite crust up to several centimeters thick. The hematite crust is probably the result of mineralization along the contact after deposition of the Percha Formation. Hematite nodules and chert pebbles are present along the unconformity at Bear Mountain, but a hematite crust is not present.

LITHOFACIES OF THE PERCHA FORMATION

Introduction

The Percha Formation is divided into five lithofacies based on sedimentary structures and lithology. From the base upward, the Percha lithofacies are:

(1) "basal deposits"

(2) shale

(3) lens and shale

(4) flaser-bedded carbonate

(5) wavy-bedded and cross-stratified carbonate

With the exception of the "basal deposits", all lithofacies are distinct rock units occurring at all sections. "Basal deposits" is a collective term referring to all deposits underlying the shale lithofacies. Table 2 summarizes the Percha lithofacies and their characteristics.

"Basal Deposits"

"Basal deposits" consist of less than 1 to 32 m of a laterally and vertically variable sequence of distinctive lithofacies. In total, nine lithofacies comprise the basal deposits. These nine lithofacies, characterized in Table 1, are:

(1) basal shale

(2) shale and dolomite

(3) interbedded siltstone and mudstone

(4) rhythmically laminated carbonaceous limestone

(5) sandstone

(6) grayish black shale

(7) dolomitic shale

(8) fissile calcareous shale

(9) platy calcareous shale

"Basal deposits" are highly variable laterally. None of the nine lithofacies is found at all sections, and most are confined to one or two sections (Fig. 8).

At the northern sections, "basal deposits" are best developed at Bear Mountain and Georgetown, where the lithofacies are 10 and 15 m thick, respectively. At Bear Mountain, a few centimeters of basal shale are overlain by 5 m of shale and dolomite, which is overlain by 5 m of rhythmically laminated carbonaceous limestone. At Georgetown, a few centimeters of basal shale are overlain by 3 m of shale and dolomite, which grade into 13 m of interbedded siltstone and mudstone. At Hillsboro, only the chert conglomerate underlies the shale lithofacies.

Table 1: Summary chart of the characteristics of the lithofacies of the "basal deposits" of the Percha Formation

Lithofacies	Thickness	Color	Nature of Bedding
Platy calcareous shale	0-10.7 m	Light gray	Platy thin beds
Fissile calcareous shale	0-10.7 m	Light gray	Fissile
Dolomitic shale	0-5.7 m	Yellowish gray	Fissile
Grayish black shale	0-2.6 m	Grayish black	Fissile
Sandstone	0-1.5 m	Light brownish gray	Massive
Rhythmically laminated carbonaceous limestone	0-4.2 m	Medium bluish gray	Brittle, thick beds
Interbedded siltstone and mudstone	0-12.2 m	Brownish gray	Platy interbedded siltstone and mudstone, sandstone channels
Shale and dolomite	0-4.6 m	Pale yellowish brown	Weakly fissile
Basal shale	0-15 cm	Grayish black	Fissile shale filling shallow depressions

Micro-sedimentary Structures	Lithology	Biota	Environment of Deposition
Regular alternation of thin, single, flat, silty lenticular laminae and clayey laminae	Calcareous, illitic, quartz-bearing, silty clay-shale	Skeletal "hash". No *in situ* fauna	Lower tidal flat
Very thin, single, flat, silty lenticular laminae in a clay matrix	Calcareous, illitic clay-shale	Uncommon skeletal "hash". No *in situ* fauna	Upper tidal flat
Very thin, single, flat silty lenticular laminae in clay matrix	Dolomitic, illitic clay-shale	None	Upper tidal flat
Probably finely laminated	Pyritic, carbonaceous illitic clay-shale	Carbonaceous detritus	Lagoon
Massive	Siliceous, mature, dolomitized, very fine-grained quartzarenite	Phosphatic shell material	Transgressive beach
Regular alternation of continuous, thin calcite and carbonaceous laminae	Carbonaceous limestone	Carbonaceous detritus	Isolated lagoons
Regular alternation of thin, single, flat silty lenticular laminae and clayey laminae	Illitic, micaceous, quartzose siltstone and mudstone	Carbonaceous detritus, rare brachiopods	Lower tidal flat
Irregular alternation of very thin, single, flat, silty lenticular laminae and clayey laminae	Quartz-bearing, medium silty, micaceous, illitic clay-shale	Plant imprints, spores, *Protosalvinia*	Upper tidal flat
Very thin, single, flat lenticular laminae in clay matrix	Quartz-bearing, coarse silty, carbonaceous illitic clay-shale	Carbonaceous detritus, spores, chitinozoans	Ponds

Table 2: Summary chart of the characteristics of the lithofacies of the Percha Formation

<table>
<tr><th colspan="2">Lithofacies</th><th>Thickness</th><th>Color</th><th>Nature of Bedding</th><th>Mode of Occurrence and Sedimentary Structures</th></tr>
<tr><td colspan="2">Wavy-bedded and cross-stratified carbonate</td><td>1-37.8 m</td><td>Light gray</td><td>Thin to thick wavy, discontin-uous beds</td><td>Cross-stratified, wavy-, parallel-, and lenticular-bedded skeletal sand beds, some thin muddy layers</td></tr>
<tr><td colspan="2">Flaser-bedded carbonate</td><td>7.5-28.3 m</td><td>Light gray</td><td>Flaser bedding with medium to thick resistant beds</td><td>Ripple-deposited skeletal sand with mud flasers, migrating channels</td></tr>
<tr><td rowspan="2">Lens and shale</td><td>North-ern sec-tions</td><td>4.3-14 m</td><td>Greenish gray shale and med-ium gray limestone</td><td>Rows of discrete carbonate lenses and fissile shale</td><td>Carbonate-filled channels in terri-genous shale</td></tr>
<tr><td>Big Hat-chet Moun-tains</td><td>18.3 m</td><td>Light gray shale and med-ium gray limestone</td><td>Discontinu-ous carbon-ate layers and fissile shale</td><td>Carbonate-filled channels in terri-genous shale</td></tr>
<tr><td rowspan="2">Shale</td><td>North-ern sec-tions</td><td>43.6-59.7 m</td><td>Dark, greenish gray, dark gray to medium gray</td><td>Fissile</td><td>Thick shale sequence</td></tr>
<tr><td>Big Hat-chet Moun-tains</td><td>30.5 m</td><td>Light gray</td><td>Fissile shale and thin mudstone beds</td><td>Thick shale and mudstone sequence</td></tr>
<tr><td colspan="2">"Basal deposits"</td><td>0-32 m</td><td colspan="3">Table 1</td></tr>
</table>

Micro-sedimentary Structures	Lithology	Dominant Biota	Environment of Deposition
Correspond to mega-sedimentary structures. Muddy units bioturbated	Crinoidal-bryozoan biosparite, some biomicrite layers	Clastic and in situ crinoids and bryozoans	Outer carbonate platform
Ripples show faint internal cross-stratification. Mud flasers commonly bioturbated	Crinoidal-bryozoan biosparite and intrasparite ripples with biomicrite mud flasers	Clastic and in situ braciopods, crinoids and bryozoans	Inner carbonate platform
Homogenous carbonate lenses. Thin, single, flat, silty lenticular laminae in clay matrix in shale	Skeletal calcilutite lenses and quartz-bearing, silty, illitic-chloritic clay-shale	Skeletal "hash" lenses, linguloid brachiopods in shale	Channeled outer lagoon
Homogeneous carbonate layers. Very common, thin, single to connected, flat, silty lenticular laminae in clay matrix in shale	Skeletal calcilutite layers and quartz- and skeletal "hash"-rich, illitic, calcareous clay shale	Skeletal "hash" layers, linguloid brachiopods in shale	Channeled outer lagoon
Thin, carbonaceous laminae in clay matrix, grading upward to thin, single, flat, silty lenticular laminae in clay matrix	Carbonaceous, illitic-chloritic clay-shale grading upward into quartz-bearing, silty, illitic-chloritic clay-shale	Linguloid brachiopods	Lagoon
Common, thin, single, flat, silty lenticular laminae in clay matrix	Quartz- and skeletal "hash"-rich, silty, illitic, calcareous clay-shale and mudstone	Brachiopods	Lagoon

Table 1

Figure 8. Stratigraphic columns showing the sequence of lithofacies within the "basal deposits" at the Bear Mountain, Georgetown and Big Hatchet Mountains sections. No "basal deposits" occur at the Cain Spring and Hillsboro sections.

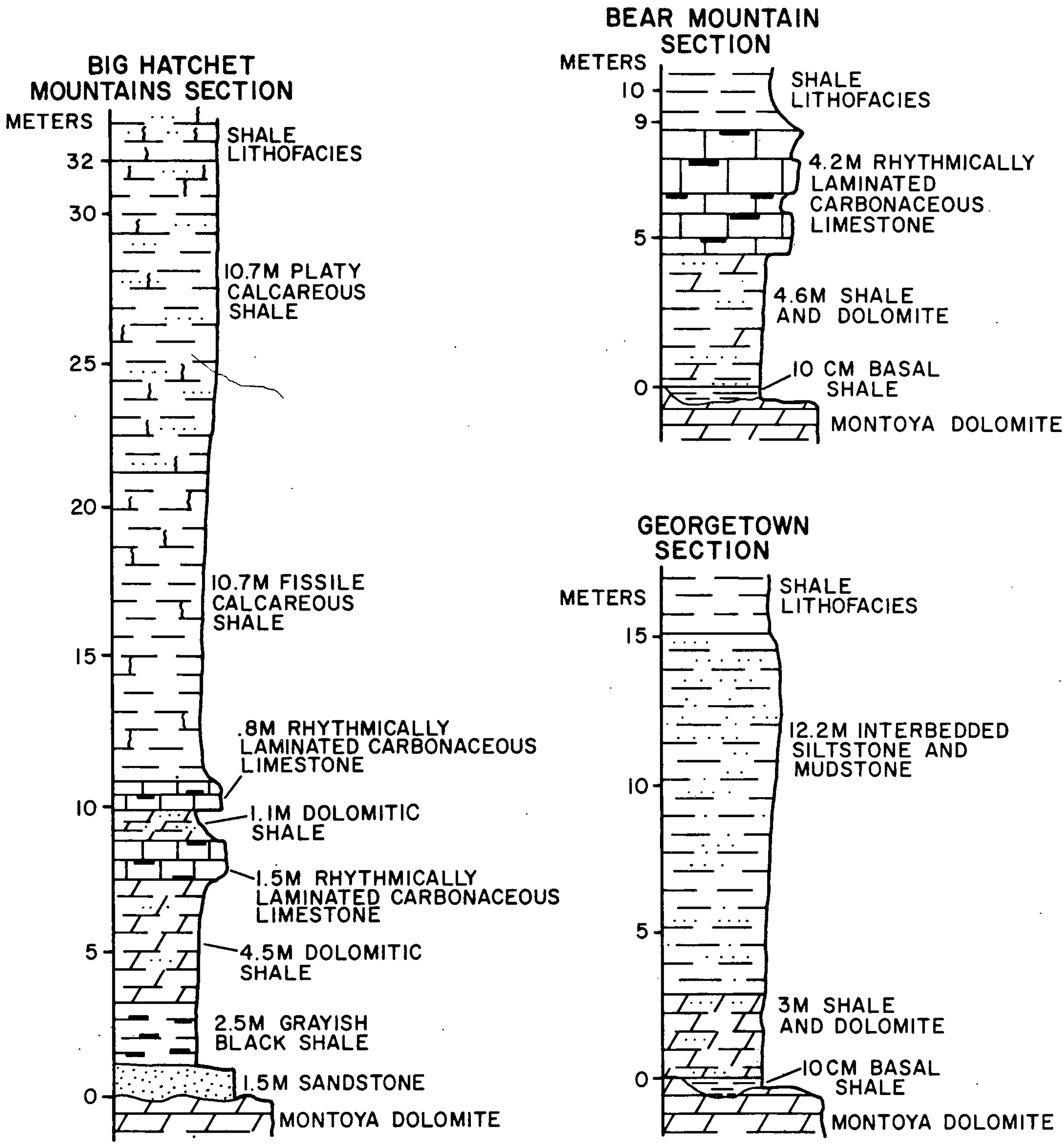
BIG HATCHET MOUNTAINS SECTION
METERS
0
5
10
15
20
25
30
32
SHALE LITHOFACIES
10.7M PLATY CALCAREOUS SHALE
10.7M FISSILE CALCAREOUS SHALE
.8M RHYTHMICALLY LAMINATED CARBONACEOUS LIMESTONE
1.1M DOLOMITIC SHALE
1.5M RHYTHMICALLY LAMINATED CARBONACEOUS LIMESTONE
4.5M DOLOMITIC SHALE
2.5M GRAYISH BLACK SHALE
1.5M SANDSTONE
MONTOYA DOLOMITE
BEAR MOUNTAIN SECTION
METERS
0
5
9
10
SHALE LITHOFACIES
4.2M RHYTHMICALLY LAMINATED CARBONACEOUS LIMESTONE
4.6M SHALE AND DOLOMITE
10 CM BASAL SHALE
MONTOYA DOLOMITE
GEORGETOWN SECTION
METERS
0
5
10
15
SHALE LITHOFACIES
12.2M INTERBEDDED SILTSTONE AND MUDSTONE
3M SHALE AND DOLOMITE
10CM BASAL SHALE
MONTOYA DOLOMITE

No "basal deposits" were found at Cain Spring, where the lowest few meters of the section are covered by recent stream gravel.

At the Big Hatchet Mountain, 32 m of "basal deposits" are present. About 1.5 m of sandstone underlie 3 m of grayish black shale. Grayish black shale grades upward into 3 m of dolomitic shale. Dolomitic shale is interbedded with two distinctive, resistant, 1 m thick beds of rhythmically laminated carbonaceous limestone. Dolomitic shale grades upward into 10.5 m of fissile calcareous shale, which grades upward into 10.5 m of platy calcareous shale.

"Basal" Lithofacies 1 - Basal Shale

At Bear Mountain and Georgetown, 12 to 15 cm of grayish black (N 2) to dark gray (N 3), fissile shale occur in shallow erosional depressions in Montoya Dolomite. These deposits are confined entirely to erosional depressions and extend laterally for several meters filling individual depressions, but end abruptly at highs in the erosional surface.

The internal structure of these shales consists of a clay matrix with uncommon or rare, very thin (.5 mm), flat, single, lenticular laminae several millimeters to a few centimeters long, consisting of black carbonaceous material or quartz silt.

In lithology, basal shales are quartz-bearing coarse silty, carbonaceous, illitic clay-shale. By point-count, 96 percent of the shale consists of fine carbonaceous material and illitic clay. Clay particles commonly occur as silt-sized clumps around carbonaceous material, probably resulting from the mode of depostion, in which clay particles flocculated around carbonaceous debris and settled out of suspension. The remaining 4 percent of the shale is quartz silt, confined primarily to lenticular laminae, and also randomly distributed throughout the shale. The identifiable portion of the carbonaceous material consists of spores and chitinozoans, primarily Ancyrochitina (Fig. 9).

"Basal" Lithofacies 2 - Shale and Dolomite

At Bear Mountain and Georgetown, basal shale is overlain by 3 to 4 m of pale yellowish brown (10 YR 6/2), weakly fissile shale and brownish gray (5 YR 4/1) dolomite (Fig. 10). Where erosional depressions are not developed in the Montoya Dolomite, the shale and dolomite lithofacies directly overlies the Silurian dolomite. Plant impressions, a few centimeters in length at a maximum, occur throughout the lithofacies, but are not common. Locally at Georgetown, circular flat hematite disks up to 1 cm in diameter (Fig. 11) occur in such abundance that the shale is stained a grayish red purple (5 RP 4/2). Canright (1977, personal communication) indicates that these structures may be Protosalvinia (Foerstia) selectively replaced by hematite.

Internally, shale and dolomite show irregularly alternating light-colored, very thin (<1 mm), single, flat, lenticular laminae a few millimeters to centimeters long, and dark-colored, thin (1 mm), more continuous laminae. Lenticular laminae consist of quartz silt and, rarely, very fine quartz sand. More continuous laminae consist of illitic clay, carbonaceous material, and mica flakes. Clay and clayey laminae dominate over silt and silty lenticular laminae. Where dolomitization has occurred, these sedimentary structures are present, but obscured.

Within this lithofacies, a complete gradation exists in lithology from quartz-bearing medium silty, micaceous, illitic clay-shale to quartz-bearing medium silty, medium crystalline dolomite. By point-count, about 85 percent of the clay-shale is illitic clay and fine silty mica. Medium to coarse silt-sized quartz, confined largely to lenticular laminae, constitutes up to 10 percent of the shale. Coarse silt-sized muscovite flakes comprise up to 7 percent of the shale. A trace of silt-sized feldspar occurs, consisting of plagioclase, orthoclase, and microcline. Carbonaceous material present is commonly partially replaced by hematite. Hematite and limonite staining of grains is common and hematite nodules up to 1 cm in diameter occur. Canright (1977, personal communication) identified spores form acid insoluable residues. Dolomite occurs as fine to medium crystalline rhombs replacing up to 70 percent of individual shale samples. At Georgetown, dolomite becomes more abundant upward in the lithofacies, but at Bear Mountain, no preferred trends in the occurrence of dolomite could be determined.

"Basal" Lithofacies 3 - Interbedded Siltstone and Mudstone

At Georgetown, the shale and dolomite lithofacies grades upward into 12 m of platy, brownish gray (5 YR 4/1), thinly bedded (2 - 5 cm) siltstone and mudstone, which grades upward into the shale lithofacies (Fig. 12). Siltstone predominates over mudstone. In the upper 4.5 m of the lithofacies, sandstone channel-fills, 15 cm thick and 1 m long, occur (Fig. 13). Episodes of channel filling are commonly separated by thin clay drapes (Fig. 14). The undersides of some channel-fills show well-developed burrows (Fig. 15). The adjacent siltstone and mudstone are generally free from burrows.

Both siltstone and mudstone beds show interlaminated dark-colored, very thin (.05 - 1 mm), clay laminae and light-colored, very thin to thin (.25 - 2 mm), commonly lenticular, coarse silty laminae.

The lithology of the siltstone and mudstone consists of illitic clayey, dolomitized, micaceous, quartzose coarse siltstone and quartz-bearing medium silty, dolomitized, micaceous, illitic clayey mudstone, respectively. Medium to coarse silty to, rarely, very fine sandy quartz and mica are concentrated in light-colored laminae and comprise up to 70 percent of the primary components of the siltstone. Feldspathic silt forms a trace in the light-colored laminae. Illitic clay, carbonaceous material, and medium silt-sized and finer micaceous flakes are concentrated in dark-colored laminae. Dolomite occurs throughout the lithofacies as very finely to finely crystalline rhombs replacing up to 30 percent of some samples.

Channel-fill sandstone shows poorly defined thin (1 mm), parallel laminations and rare ripple cross-stratification. In lithology,

Figure 9 — Ancyrochitina sp., the most common chitinozoan occurring in the basal shale lithofacies. This specimen is about 0.075 mm in length. Bear Mountain section biological mount.

Figure 10 — Outcrop of the shale and dolomite lithofacies, showing the fissile nature of the strata. Georgetown section.

Figure 11 — Small slabs (largest is 3 cm in length) showing disks of hematite on the bedding surface. The disks may have been Protosalvinia selectively replaced by hematite. Georgetown section, shale and dolomite lithofacies.

Figure 12 — Outcrop of the interbedded siltstone and mudstone lithofacies, showing the platy nature of the bedding. This platy bedding contrasts sharply with the fissile nature of the bedding in the underlying shale and dolomite lithofacies (Fig. 10). Georgetown section, rule is 15 cm long for scale.

Figure 13 — Sandstone channel-fill in the interbedded siltstone and mudstone lithofacies. Georgetown section.

Figure 14 — Sandstone channel-fill in the interbedded siltstone and mudstone lithofacies showing distinct episodes of channel-filling, each punctuated by the deposition of a clay drape. Georgetown section.

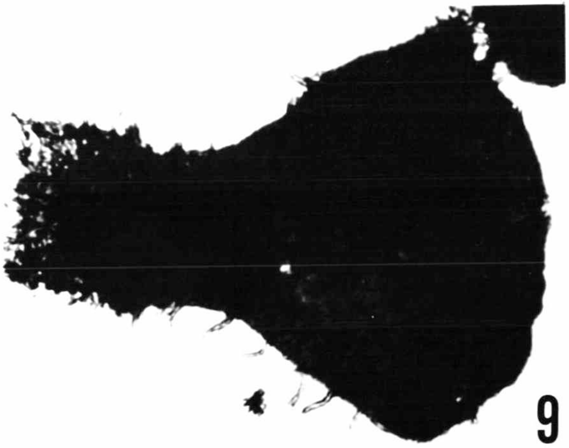
9

10
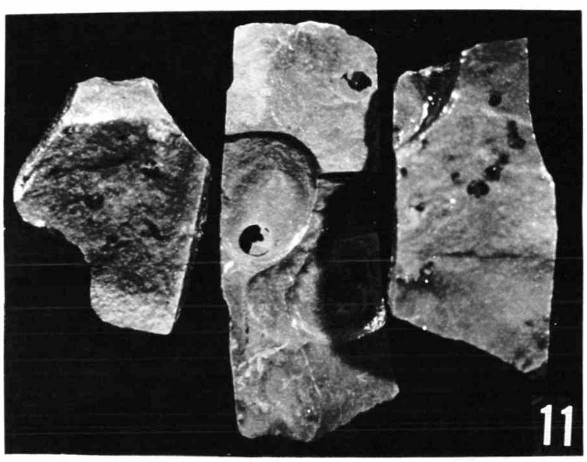
11



14

channel-fill is siliceous and limonitic, mature, feldspar-bearing quartzarenite. Feldspathic silt and very fine sand, consisting of plagioclase, orthoclase, and microcline, form up to 3 percent of the fill. No evidence of dolomitization of the quartzarenite was found.

"Basal" Lithofacies 4 - Rhythmically Laminated Carbonaceous Limestone

Resistant, thick-bedded (30-90 cm), dense, brittle, medium bluish gray (5 B 5/1) weathering to moderate yellow (5 Y 7/6), rhythmically laminated, carbonaceous limestone occurs at Bear Mountain and the Big Hatchet Mountains. At Bear Mountain, 4.5 m of this limestone rhythmite overlies the shale and dolomite lithofacies and grades into the overlying shale lithofacies. At the Big Hatchet Mountains, two distinct limestone rhythmites, each less than 1 m thick, occur within the dolomitic shale lithofacies.

Internally, the limestone rhythmite consists of a highly regular alternation of very thin to medium (<1 - 5 mm), light-colored and dark-colored laminations (Fig. 16, 17). Laminations are even to slightly wavy, but are continuous and individual lamina can be traced for several meters. Laminae are displaced only by fine "fractures" with displacement of a few millimeters.

Light-colored laminae consist of calcite and dark-colored laminae consist of carbonaceous material. At the Big Hatchet Mountains, calcite laminae are generally micritic. Calcite laminae at Bear Mountain, however, consist of very finely to finely crystalline calcite rhombs with a mean size of approximately 0.025 mm (Fig. 18, 19). Individual calcite laminae commonly show current formed structures, such as lenticular laminae several millimeters long, consisting of calcite rhombs somewhat coarser than the surrounding rhombic matrix (Fig. 20). Dark-colored laminae are concentrations of carbonaceous material, commonly replaced by pyrite. Both dark- and light-colored laminae are essentially devoid of terrigenous material.

"Basal" Lithofacies 5 - Sandstone

About 1.5 m of generally massive, light brownish gray (5 YR 6/1) sandstone occurs at the Big Hatchet Mountains where it overlies Montoya Dolomite. This sandstone is a siliceous, mature, dolomitized, very fine-grained quartzarentite. By point-count, terrigenous quartz constitutes just over 50 percent of the sandstone. Traces of plagioclase, microcline, and muscovite are present. Phosphatic shell material forms 1 or 2 percent of some samples. Dolomite, after quartz, occurs as finely crystalline rhombs forming up to 48 percent of some thin-sections.

"Basal" Lithofacies 6 - Grayish Black Shale

At the Big Hatchet Mountains, the sandstone lithofacies is overlain by about 2.5 m of fissile, grayish black (N 2), pyritic, carbonaceous, illitic clay-shale. Outcrops are very poor and samples suitable for thin-sectioning were not obtained. The weathering pattern of the shale into fine flakes, however, suggests that clay particles are oriented and bioturbation has not occurred. In general, the shale lightens in color and appears to grade upward into the dolomitic shale.

Figure 15 Undersurface of a sandstone channel-fill in the interbedded siltstone and mudstone lithofacies, showing well-developed burrows. The surrounding siltstone and mudstone are generally free from burrows. Georgetown section, slab is 18 cm long.

Figure 16 Slab (6 cm high) of rhythmically laminated carbonaceous limestone. Light-colored laminae consist of calcite. Dark-colored laminae are rich in carbonaceous material. Some of the laminae shown are displaced by fine fractures. Big Hatchet Mountains section.

Figure 17 Slab (13 cm high) of rhythmically laminated carbonaceous limestone. Individual laminae are very continuous. Bear Mountain section.

Figure 18 Photomicrograph of part of a calcite laminae in the rhythmically laminated carbonaceous limestone, showing the rhombic nature of the calcite making up the laminae. Bear Mountain section, X200.

Figure 19 Photomicrograph clearly showing the rhombic nature of a calcite crystal within a calcite lamina in the rhythmically laminated carbonaceous limestone. Bear Mountain section, X625.

Figure 20 Photomicrograph of a lenticular laminae about 1 mm long occurring within a thicker calcite lamination in the rhythmically laminated carbonaceous limestone. Bear Mountain section, X12.5.

15

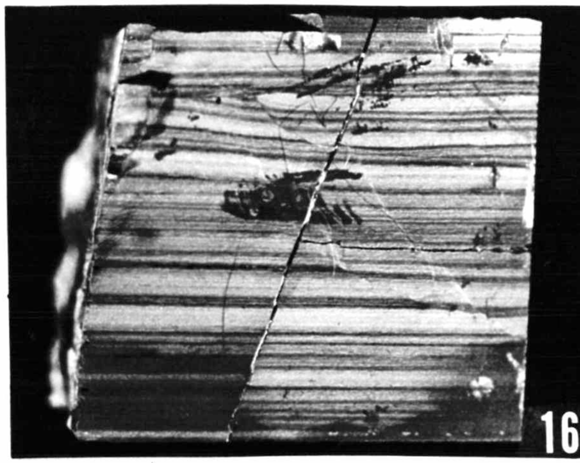

16

17

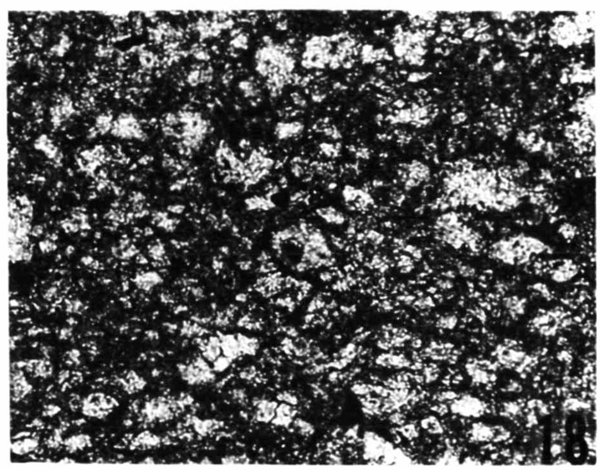

18

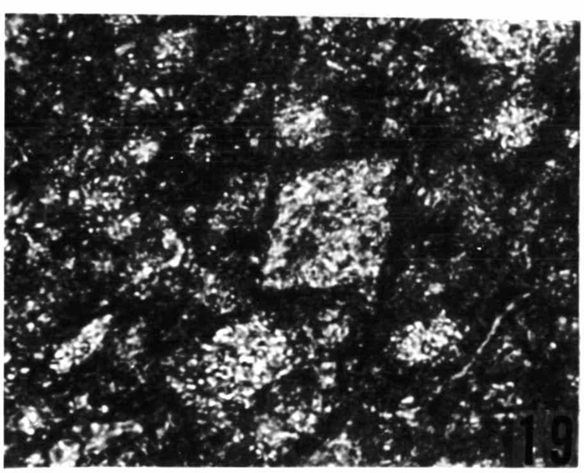

19

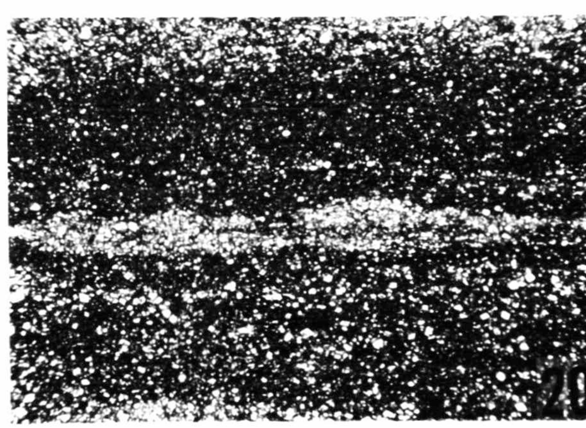

20

"Basal" Lithofacies 7 - Dolomitic Shale

About 6 m of fissile, yellowish gray (5 Y 7/2), dolomitic shale occurs in the Big Hatchet Mountains, and grades upward into fissile calcareous shale. Dolomitic shale shows rare, very thin (.5 mm), medium to coarse silty quartzose lenticular laminae in a matrix of clay. Laminations are undisturbed and no fauna was found. Clay matrix consists of illite and dolomicrite. A few of the dolomite rhombs are .012 to .015 mm in diameter (Fig. 21). Clay greatly predominates over silt, which forms only 1 to 2 percent of most samples.

"Basal" Lithofacies 8 - Fissile Calcareous Shale

About 10.5 m of light gray (N 7) weathering to grayish yellow (5 Y 8/4), fissile, calcareous shale occur at the Big Hatchet Mountains. The shale shows very thin (.5 - 1 mm), lenticular laminae, consisting of coarse silty quartz and lutite-sized skeletal hash, in a matrix of illitic clay and micrite. Laminae are undisturbed and no <u>in situ</u> fauna was found. Clay greatly predominates over silt, which forms no more than 5 to 6 percent of the shale.

"Basal" Lithofacies 9 - Platy Calcareous Shale

Gradationally overlying the fissile calcareous shale at the Big Hatchet Mountains is 10.5 m of light gray (N 7) weathering to grayish yellow (5 Y 8/4), platy, calcareous shale, which grades upward into the shale lithofacies (Fig. 22). Platy calcareous shale differs from the underlying fissile shale by its platy bedding and internal structure. Internally, the shale is very thinly (.5 - 1 mm) laminated with a regular alternation of clayey laminae and silty quartz and lutite-sized skeletal hash. Although clay predominates over silt, the abundance of silt has increased from the underlying dolomitic shale and fissile calcareous shale to about 30 percent in the platy calcareous shale. No indigenous fauna occurs in this lithofacies.

Shale Lithofacies

The shale lithofacies represents that sequence of shale overlying the "basal deposits" and below the zone where carbonate lenses become prominent. At the northern sections, the shale lithofacies consists of 44 to 60 m of dark, fissile shale. At the Big Hatchet Mountains, the shale lithofacies consists of 31 m of calcareous shale.

In internal structure and mineralogy, the shale lithofacies is laterally and vertically gradational. In the northern sections, a change in lithofacies occurs upward as the shale lightens in color, current-formed structures increase in abundance, and a benthic fauna is established. From the northern sections southward to the Big Hatchet Mountains, the shale becomes more calcareous, gains a benthic fauna, and shows an increased abundance of current-formed structures. Upward in the lithofacies at the Big Hatchet Mountains, current-formed structures and the benthic fauna become even more abundant than lower in the lithofacies. Figure 23 illustrates these vertical and lateral trends in the shale lithofacies.

In the northern sections, the lower part of the shale lithofacies consists of dark greenish gray (5 GY 4/1) or dark gray (N 3) to medium gray (N 5), fissile shale (Fig. 24). Internally, the shale is faintly laminated with dark-colored and light-colored, very thin to thin (.03 - 1.5 mm) laminations (Fig. 25). Dark-colored laminae dominate and consist of clay with a concentration of carbonaceous material. Carbonaceous material consists primarily of "tasmanoid bodies", with some minor plant material (Fig. 26). The "tasmanoid bodies" are very similar to the black, flattened disks reported throughout Upper Devonian black shales and are commonly referred to as Tasmanites or megaspores (Schopf, 1969). Canright (1977, personal communication) states that the black disks found in the Percha are too poorly preserved to make specific identifications. Most of the light-colored laminae are clay units with only minor carbonaceous material. Rarely, some of the light-colored laminae are single, flat lenticular structures 3 to 6 mm long consisting of concentrations, a few grains thick, of quartz silt and very finely to finely crystalline dolomite rhombs.

Laminae in the lower part of the shale lithofacies are undisturbed by bioturbation and no evidence of a benthic fauna was found. The total megafauna found in the lower part of the shale lithofacies consists of one straight cephalopod found at Bear Mountain.

Figure 23. Vertical and lateral trends in the shale of the shale, and lens and shale lithofacies. The arrows indicate the direction of increasing abundance or degree.

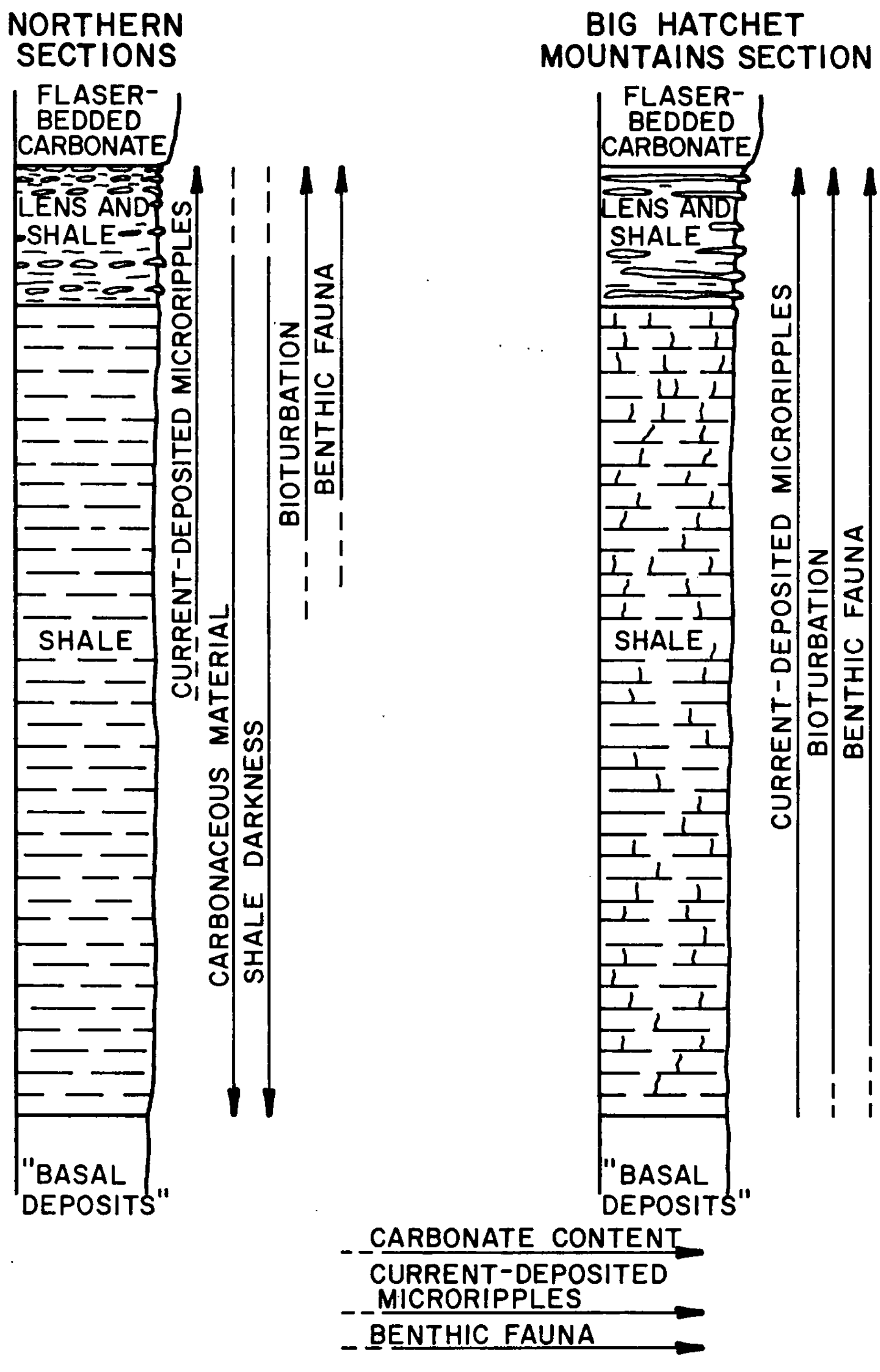
NORTHERN SECTIONS
FLASER-BEDDED CARBONATE
LENS AND SHALE
SHALE
"BASAL DEPOSITS"
CURRENT-DEPOSITED MICRORIPPLES
CARBONACEOUS MATERIAL
SHALE DARKNESS
BIOTURBATION
BENTHIC FAUNA
BIG HATCHET MOUNTAINS SECTION
FLASER-BEDDED CARBONATE
LENS AND SHALE
SHALE
"BASAL DEPOSITS"
CURRENT-DEPOSITED MICRORIPPLES
BIOTURBATION
BENTHIC FAUNA
CARBONATE CONTENT
CURRENT-DEPOSITED MICRORIPPLES
BENTHIC FAUNA

In the northern sections, the shale lithofacies changes character upward. Carbonaceous material and carbonaceous laminations become less abundant. In accord, the shale lightens in color to greenish gray (5 GY 6/1) Silty lenticular laminae become more abundant and better formed. Clay, however, still greatly predominates over silt. A benthic fauna gradually occupied the site of deposition of the shale and bioturbation features occur. The lowermost evidence of a benthic fauna, in the form of small brachiopod imprints occurs in the upper one-third of the lithofacies. Upward, small linguloid brachiopods occur. Small spiriferid brachiopods occur near the top of the lithofacies.

In lithology, the shale lithofacies in the northern sections grades upward from carbonaceous, chloritic-illitic clay-shale to quartz-bearing medium to coarse silty, chloritic-illitic clay-shale or quartz-bearing medium to coarse silty, dolomitized, chloritic-illitic clay-shale. In the lower part of the lithofacies, illitic and chloritic clay plus carbonaceous material accounts for up to 97 percent of the shale. Illite dominates over chlorite by about 4 to 1 (Appendix). Quartz silt rarely accounts for more than 5 percent of the shale. Upward, as silty lenticular laminae become more common, quartz may form up to 20 percent of the shale. Dolomite is present throughout most of the lithofacies as a product of diagenesis. At the base of the lithofacies, dolomite is generally absent, but occurs upward over a few meters as very finely crystalline rhombs forming a few percent of the shale. Dolomite rhombs generally increase in size and abundance upward. Near the top of the lithofacies, dolomite, present as finely to medium crystalline rhombs randomly distributed throughout the shale, comprises about 7 to 10 percent of the shale.

Within the shale lithofacies and the overlying lens and shale lithofacies are the only occurrences of chlorite in the Percha Formation (Fig. 27). The clays in the underlying "basal deposits" are entirely illitic. Chlorite decreases in abundance upward in the lens and shale lithofacies, and only illite persists into the flaser-bedded carbonate lithofacies. The overall behavior of the chlorite fraction in x-ray diffraction patterns indicates a Fe-chlorite interlayered with an expandable component. Oriented clay samples show the typical chlorite peaks at 7Å and 14Å. On many samples, the 7Å peak is the more prominent. After heating in glycol vapor, the 14Å peak expands slightly on some samples. After heating at 600° C for 1 - 2 hours, the 14Å peak generally merges with the 10Å illite peak forming a single broad peak. The 7Å peak is lost.

The shale lithofacies at the Big Hatchet Mountains consists of light gray (N 7), fissile, calcareous shale beds a few centimeters to tens of centimeters thick interbedded with slightly more resistant, thin (1 - 3 cm) beds of silty, calcareous mudstone. Mudstone beds are laterally discontinuous over 1 - 2 m of outcrop and commonly merge without a decrease in bed thickness with fissile calcareous shale. Less commonly, mudstone beds are lenticular and pinch to zero laterally.

Internally, both shale and mudstone show very thin to thin (<1 - 3 mm), commonly lenticular, silty laminae in a clay matrix. Silty laminae are concentrations of silty quartz and lutite-sized skeletal hash. The clay matrix is a sparsely fossiliferous mixture of illite and micrite. The abundance of silty laminae differs greatly from shale to mudstone beds. In the shale beds, clay greatly predominates over silt, and silty lenticular laminae are rare. Silty lenticular laminae are much more abundant in mudstone beds, where silty quartz and lutite-sized skeletal hash form up to 35 percent of individual thin-sections.

Vertical trends in the lithofacies described for the northern sections are similar to those at the Big Hatchet Mountains. Terrigenous clay content decreases upward. The overall unit becomes more resistant as silty quartz and skeletal hash laminae become increasingly abundant. Lenticular laminae are more commonly disrupted by bioturbation upward.

Figure 27. Mineralogy of the clay fraction of the Percha lithofacies. Where both illite and chlorite are present, the percentage of each, determined by x-ray analysis, is given.

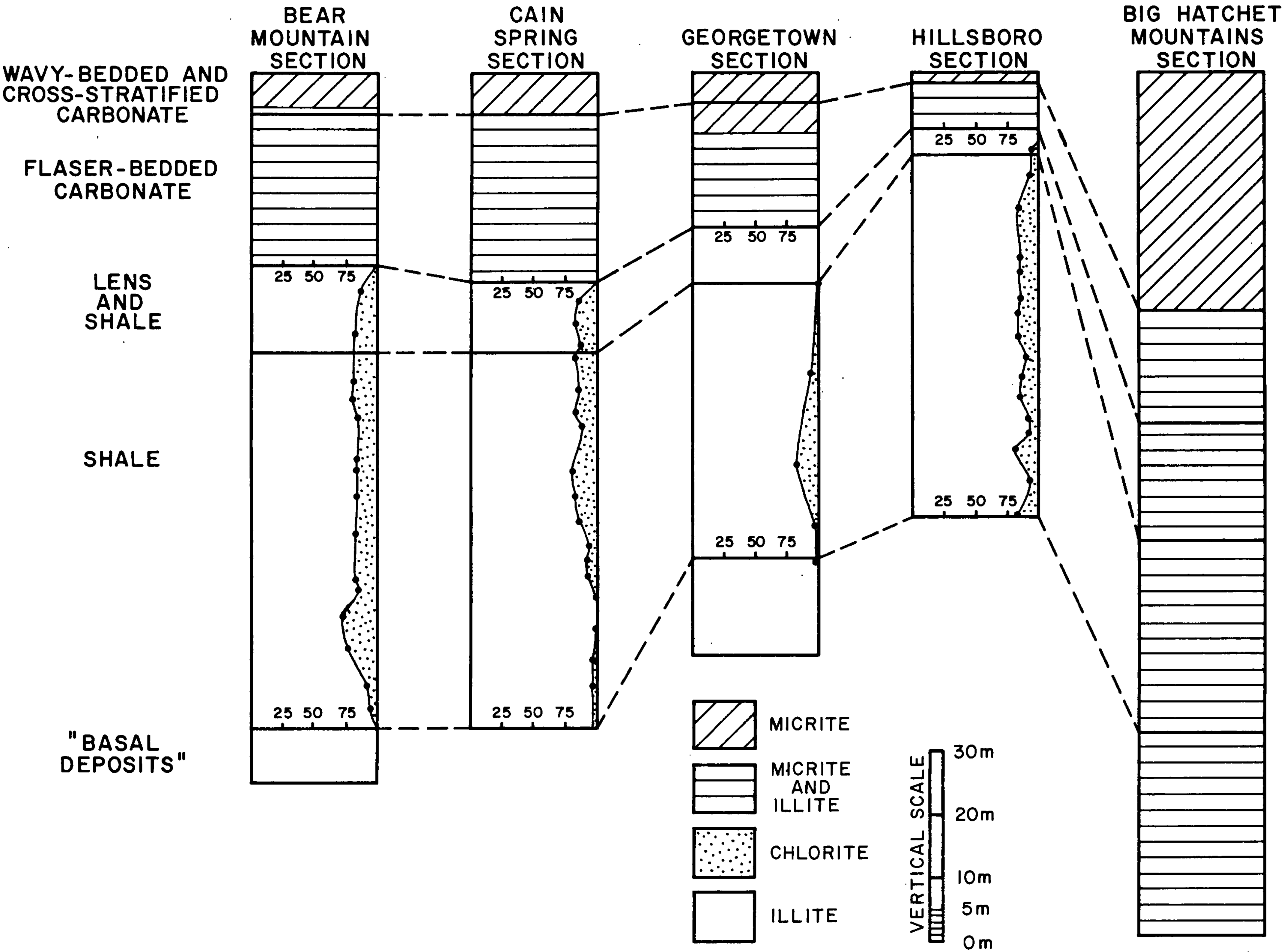
BEAR MOUNTAIN SECTION
CAIN SPRING SECTION
GEORGETOWN SECTION
HILLSBORO SECTION
BIG HATCHET MOUNTAINS SECTION
WAVY-BEDDED AND CROSS-STRATIFIED CARBONATE
FLASER-BEDDED CARBONATE
LENS AND SHALE
SHALE
"BASAL DEPOSITS"
25 50 75
MICRITE
MICRITE AND ILLITE
CHLORITE
ILLITE
VERTICAL SCALE
30m
20m
10m
5m
0m

Lens and Shale Lithofacies

Lens and shale lithofacies consists of shale interbedded with either carbonate layers or horizontal rows of discrete carbonate lenses. From a thickness of 14 m at the Silver City Range, the lithofacies thickens southward to 18.3 m at the Big Hatchet Mountains and thins eastward to 4 m at Hillsboro.

The lens and shale lithofacies is gradational with the underlying shale and overlying flaser-bedded carbonates. Initially, carbonate beds occur as thin ($<$ 1 cm), laterally discontinuous layers vertically separated by approximately 1 m of shale (Fig. 28). Upward, layers and rows of lenses become thicker and more abundant, and the thickness of shale between layers or rows of lenses is reduced to a few tens of centimeters or less. Near the top of the lithofacies, shale units are reduced to a few centimeters or less in thickness, and carbonate beds become even more abundant and grade into flaser-bedded carbonates.

Carbonate beds occur in two distinct forms. At the northern sections, horizontal rows of discrete carbonate lenses occur (Fig. 29). Individual rows are discontinuous laterally over several meters of outcrop. Individual lenses are most commonly flat ellipsoids (Fig. 30). Less common are pod-shaped lenses (Fig. 31), and irregular channel-shaped layers with an undulating undersurface (Fig. 32). In the Silver City Range, lenses average 5 to 7.5 cm thick and 15 to 25 cm long with an overall size range of 1 to 12 cm thick and 1.5 cm to 1 m long. East of the Silver City Range, lenses are, on the average, smaller and less well-developed. At Georgetown and Hillsboro, lenses average 1 to 2.5 cm thick

Figure 21 Photomicrograph showing the edge of a thin-section, under x-nicols, from the dolomitic shale lithofacies, showing a scattering of very finely crystalline (up to 0.015 mm) dolomite rhombs within the clay matrix. Big Hatchet Mountains section.

Figure 22 Outcrop of the platy calcareous shale lithofacies, showing the platy nature of the bedding. This platy bedding contrasts with the fissile nature of the underlying calcareous shale, but is similar to the bedding of the interbedded siltstone and mudstone lithofacies (Fig. 12). Big Hatchet Mountains section.

Figure 24 Outcrop of the shale lithofacies, showing the dark, fissile shale typical of this lithofacies in the northern sections. Bear Mountain section.

Figure 25 Photomicrograph of a thin-section from the shale lithofacies, showing poorly defined laminations consisting of concentrations of carbonaceous material. The laminations are undisturbed by bioturbation. Hillsboro section, X31.

Figure 26 Tasmanoid bodies form the bulk of the carbonaceous material within the shale lithofacies. Individual disks are about .3 to .4 mm in diameter. Rhombic holes in the disks are sites where dolomite crystals grew. Bear Mountain section biological mount.

Figure 28 Outcrop of initial carbonate layer within the lens and shale lithofacies.

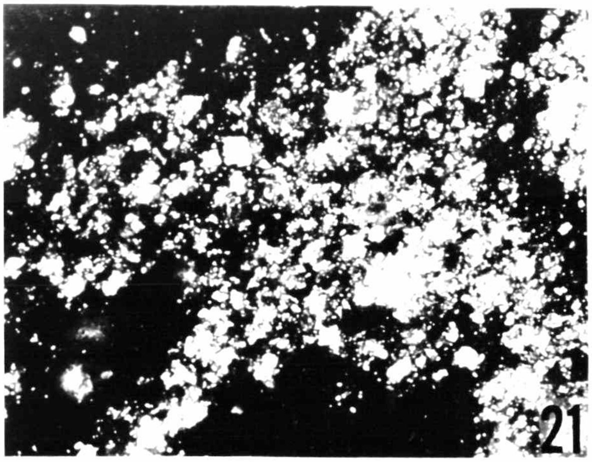
21

22

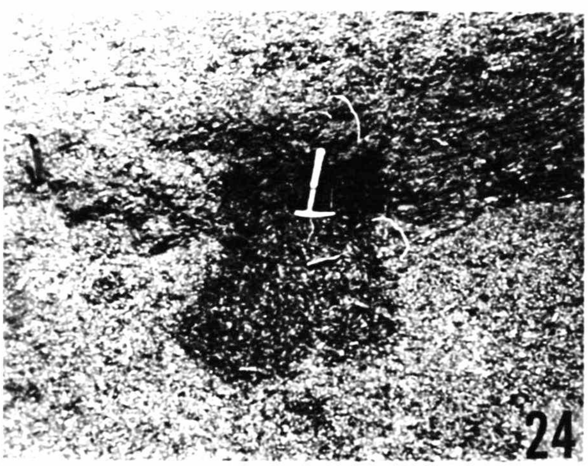
24


25

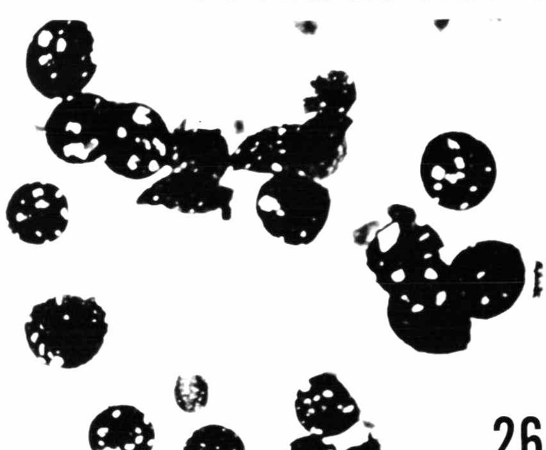
26

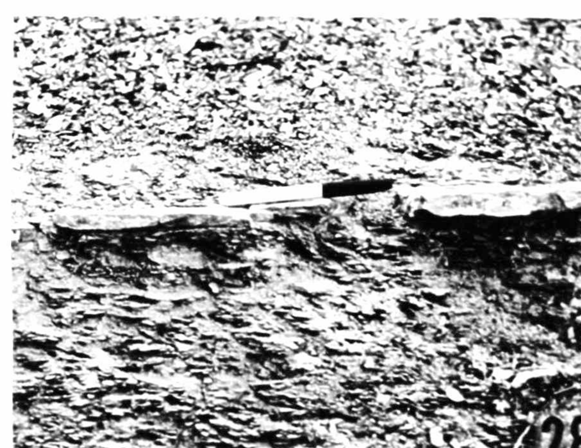
28

and 7.5 to 12.5 cm long. At the Big Hatchet Mountains, however, carbonate units occur as 1 to 3 cm thick layers traceable for up to 10 m of outcrop before either the layer thins to zero or the outcrop is covered (Fig. 33, 34).

Internally, carbonate layers and lenses consist of homogeneous, medium gray (N 5), skeletal calcilutite. Internal structure is poorly defined but may consist of burrows and laminations (Fig. 35). Thin (1 mm) laminations occur as terrigenous clay laminae in carbonate matrix near the base of the lithofacies. Upward, clay laminae are absent, and the only laminae present consist of medium to coarse skeletal calcilutite slightly coarser than the surrounding carbonate sediment.

Carbonate lenses and layers vary in lithology from illitic clayey, quartz-bearing coarse silty, skeletal calcilutite near the base of the lithofacies to skeletal calcilutite or dolomitized skeletal calcilutite upward in the lithofacies. Initial carbonate layers consist of a mixture of calcareous skeletal debris, illitic clay, and quartz silt. Upward, the terrigenous component rapidly decreases, and carbonate layers and lenses consist entirely of skeletal calcilutite or dolomitized skeletal calcilutite (Fig. 36). Skeletal components are generally too fine to recognize, but uncommon coarser skeletal fragments consist of fragments of crinoids, calcareous brachiopods, bryozoans, ostracodes, and phosphatic shell material (Fig. 37, 38). Sand-sized clay clasts also occur.

Carbonate lenses at the Silver City Range are partially replaced by dolomite, which occurs as very finely to medium crystalline rhombs replacing up to 65 percent of the original skeletal material. Dolomite becomes more

Figure 29 Outcrop of rows of carbonate lenses surrounded by shale, typical of the lens and shale lithofacies at the northern sections. Bear Mountain section.

Figure 30 Ellipsoidal lens, the most common shape of the carbonate lenses in the lens and shale lithofacies at the northern sections. Rule is 15 cm for scale. Bear Mountain section.

Figure 31 Pod-shaped lens cropping out in the lens and shale lithofacies. Bear Mountain section.

Figure 32 Channel-shaped lens cropping out in the lens and shale lithofacies. This lens pinches to zero laterally from a maximum thickness of 12 cm in about 1 m of outcrop. Bear Mountain section.

Figure 33 Outcrop of carbonate layers separated by shale in the lens and shale lithofacies at the Big Hatchet Mountains section. Individual layers can be traced laterally for several meters before pinching to zero. The occurrence of carbonate layers within this lithofacies at the Big Hatchet Mountains contrasts with rows of discrete carbonate lenses within this same lithofacies at the northern sections.

Figure 34 Close-up of the lens and shale lithofacies at the Big Hatchet Mountains, showing a resistant carbonate layer interbedded with fissile shale.


29


30

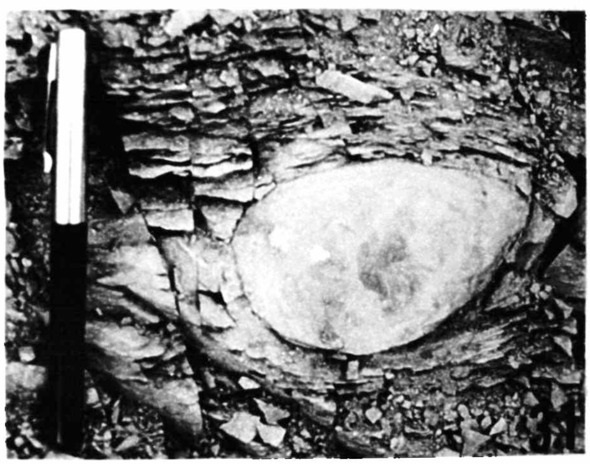
31

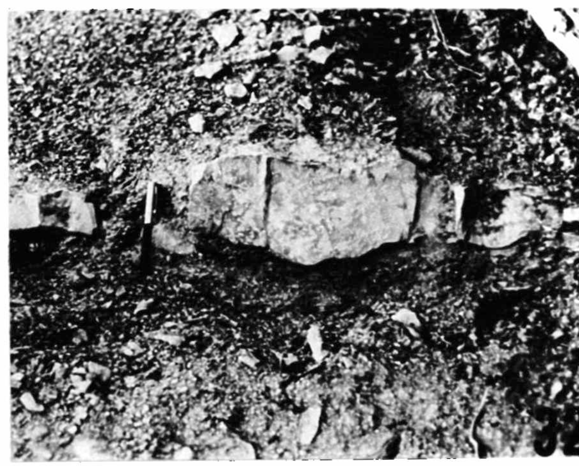
32

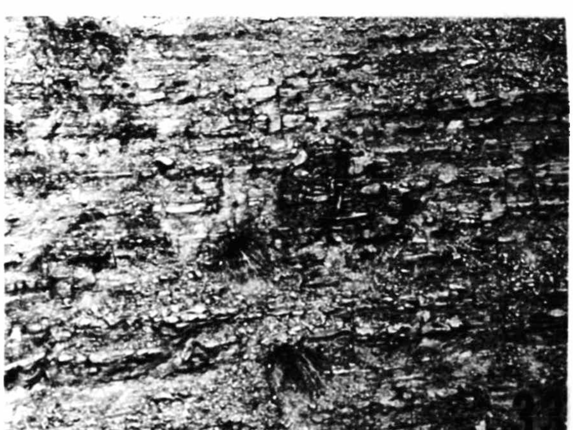
33

34

abundant upward in the lithofacies, as the overall section becomes more dolomitized upward.

Carbonate layers and lenses are also commonly altered by neomorphism of skeletal calcilutite to microspar and pseudospar. The process proceeds from the exterior of the lens inward. During neomorphism, primary skeletal texture is destroyed, giving lenses an internal "graded texture" from a core of unaltered skeletal calcilutite to a mosaic of coarsely crystalline pseudospar near the periphery of the lens (Fig. 39). Where growing neomorphic spar crystals are in contact with terrigenous shale, such as along the lens-shale contact, or where carbonate material surrounds terrigenous clay clasts (Fig. 40), fibrous pseudospar crystals up to 0.2 mm long form, commonly showing fabric expansion and distortion of adjacent material (Fig. 41, 42).

Fissile greenish gray (5 GY 6/1) shale occurring between carbonate layers and lenses represents a continuation of deposition of sediment similar to the shale in the underlying shale lithofacies. Trends in internal structure and mineralogy established in the shale lithofacies are continued into the shale of the lens and shale lithofacies (Fig. 23).

In the northern sections, shales show bioturbated, thin (1 - 2 mm), single, flat lenticular, quartz silty laminae several millimeters long in a matrix of clay. Carbonaceous materials, such as "tasmanoid bodies", are uncommon, poorly preserved, and commonly replaced by hematite. Mud matrix, however, predominates greatly over silty lenticular structures.

In lithology, shales in the northern section are quartz-bearing coarse silty, chloritic-illitic clay-shale and quartz-bearing coarse silty, dolomitized, chloritic-illitic, clay-shale. Quartz silt and skeletal fragments constitute 10 percent of the shale. The remainder of the shale is illite and chlorite clay in a ratio of 4 to 1. Near the top of the lithofacies, which is gradational into flaser-bedded carbonates, chlorite disappears. Dolomite occurs as finely crystalline rhombs randomly distributed throughout the shale and forms up to 12 percent of the shale at the Silver City Range, but only 1 to 2 percent at Hillsboro and Georgetown.

At the Big Hatchet Mountains, shale in the lens and shale lithofacies is also a continuation of the underlying shales of the shale lithofacies. In internal structure, however, these shales differ greatly from the shales at the northern sections by having a greater abundance of current-formed structures. Low in the lithofacies, thin (2 - 3 mm), single to connected, flat lenticular laminae several centimeters long are abundant (Fig. 43, 44). Upward, the lenticular structures become even more abundant and the shale consists of an interlaminated sequence of 2 to 3 mm thick lenticular laminae several centimeters long and equally thick irregular clay laminations.

In lithology, these shales are quartz-bearing coarse silty, fossil hash-bearing, calcareous, illitic clay-shale. Illite is rare near the top of the lithofacies.

Figure 35 Slab (about 6 cm high) of a carbonate lens from the lens and shale lithofacies, showing abundant burrows and bioturbation features. Silver City Range.

Figure 36 Photomicrograph showing the skeletal lutite-sized fragments that compose the carbonate lenses in the lens and shale lithofacies. Georgetown section, X31.

Figure 37 Photomicrograph showing coarse calcarenite-sized fragments of crinoids and calcareous brachiopods occurring in a carbonate lens from the lens and shale lithofacies. Hillsboro section, X12.5.

Figure 38 Photomicrograph showing coarse calcarenite-sized (0.75 mm) bryozoan fragment occurring in a carbonate lens from the lens and shale lithofacies. Silver City Range.

Figure 39 Photomicrograph showing progressive neomorphism of a carbonate lens from the lens and shale lithofacies. From the left side unaltered skeletal lutite-sized material grades to neomorphic spar in the right side. Bear Mountain section, X12.5.

Figure 40 Photomicrograph showing a clay intraclast, about .55 mm in diameter, surrounded by neomorphic spar. Neomorphic spar growth within lenses of the lens and shale lithofacies commonly attains maximum growth where it is adjacent to terrigenous clay. Georgetown section, X31.

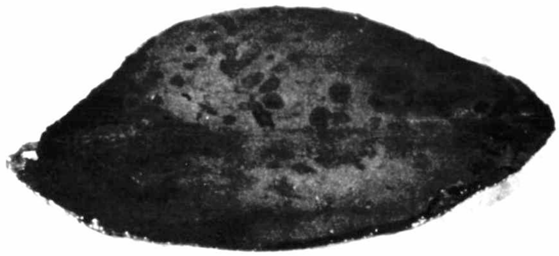

35

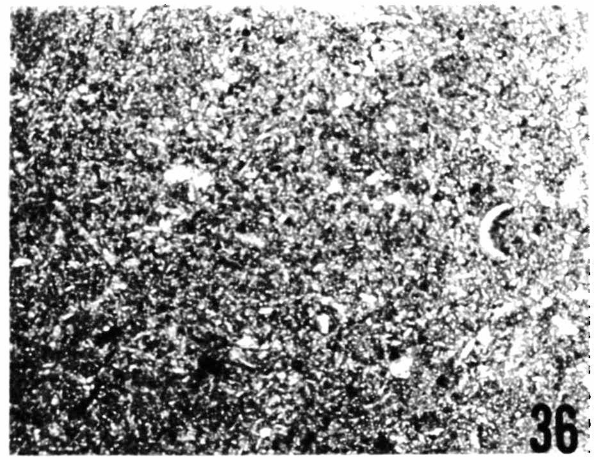

36

37

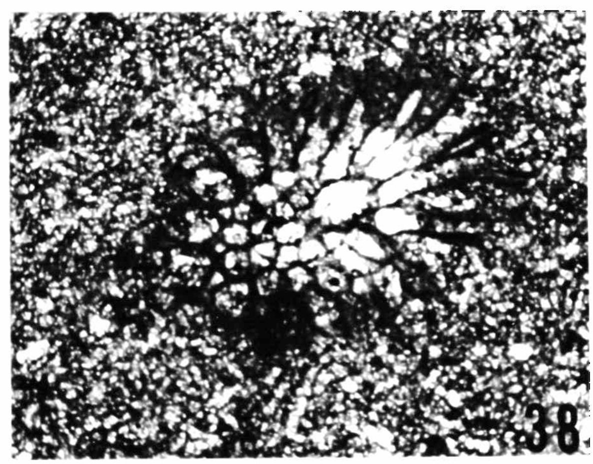

38

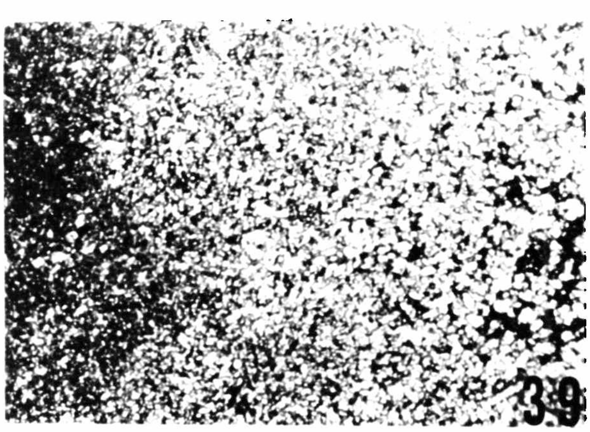

39

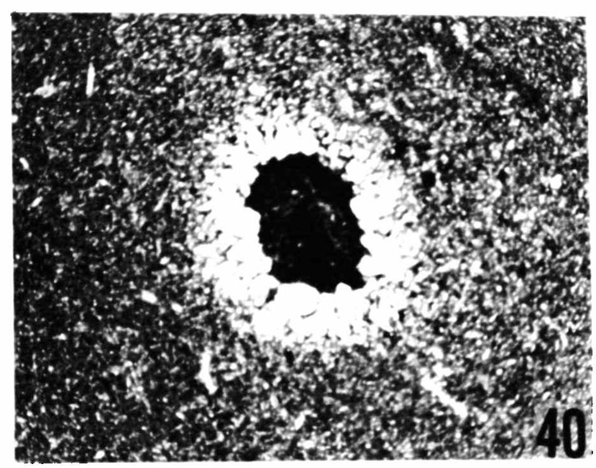

40

Flaser - Bedded Carbonate Lithofacies

The flaser-bedded carbonate lithofacies consists of light gray (N 7), flaser-bedded limestone and dolomitized limestone interbedded with numerous more resistant limestone beds. The lithofacies is thickest in the Silver City Range, where it is 28.5 m thick, and thins both south and east to 18 m at the Big Hatchet Mountains and 20 m at Georgetown to 7.5 at Hillsboro. Flaser bedding gradationally overlies the lens and shale lithofacies, and flaser bedding and lenses occur intercalated over the basal few meters of the flaser-bedded carbonate lithofacies. Through this transitional inverval, the mud component changes from dominately terrigenous to dominately carbonate (Fig. 27). Flaser-bedded carbonates either grade upward into the wavy-bedded and cross-stratified carbonate lithofacies, or, at some locales, is abruptly truncated by basal beds of the upper lithofacies.

The dominant features of this lithofacies are ripples separated by thin mud flasers (Fig. 45, 46). Individual ripples range in size from 1 cm high and 2 cm long to 6 cm high and 30 cm long, with an average size of 2 cm high and 7.5 cm long. At Georgetown, ripples are generally smaller than the mean and average 1.5 cm high and 5 cm long. At the Big Hatchet Mountains, ripples are generally larger than the mean and average 3 cm thick and 9 cm long. Ripples tend to be segregated into vertical zones according to size, with ripples of a fairly uniform size forming a zone. As a very general trend, overall ripple size increases upward in the lithofacies.

Ripples consist of poorly washed crinoidal biosparite, poorly washed dolomitized crinoidal biosparite and poorly washed intrasparite

(Fig. 47). Allochems comprise up to 70 percent of some thin-sections from the carbonate ripples. Crinoidal fragments, consisting primarily of disarticulated columnals and calyx plates, comprise up to 60 percent of individual ripples. Crinoids are followed in abundance by bio-micritic intraclasts, which form up to 30 percent of some ripples, and are identical to the biomicritic flasers separating individual ripples. Bryozoan and calcareous brachiopod fragments are common, followed in abundance by rugosan corals, sponge spicules, ostracodes, calcareous gastropods, and phosphatic material. All biological allochems making up the ripples are clastic grains, ranging in size from calcilutite to calcirudite, with a mean near fine calcirudite.

A gradation in the size of the skeletal grains making up the ripples occurs vertically. Near the base of the lithofacies, ripples consist of skeletal calcilutites only slightly coarser than skeletal grains in the underlying lenses of the lens and shale lithofacies (Fig. 48). Upward, skeletal grains coarsen to calcarenite and calcirudite (Fig. 49). Micrite forms up to 15 percent of some ripples, subequal in abundance to sparry cement. Micrite occurs in ripples as a result of the disaggregation of micritic intraclasts upon compaction, infiltration of micrite into the ripple from the overlying mud flaser during deposition, or by micrite adhering to allochems within the ripple. Dolomitization within this lithofacies occurs primarily in the Silver City Range, where finely to medium crystalline rhombs form up to 15 percent of some thin-sections from this lithofacies. Quartz silt to very fine sand is generally sparse, rarely forming over 5 percent of the ripple.

Figure 41 Photomicrograph showing fabric expansion of terrigenous clay by neomorphic spar within a carbonate lens from the lens and shale lithofacies. Georgetown section, X31.

Figure 42 Photomicrograph showing neomorphic spar crystals up to .2 mm in length. The largest spar crystals within carbonate lenses from the lens and shale lithofacies occur adjacent to terrigenous clay. Georgetown section, X31.

Figure 43 Slab, about 4 cm high, showing very common lenticular laminae occurring within shale from the lens and shale lithofacies at the Big Hatchet Mountains section.

Figure 44 Photomicrograph of a thin-section made from the slab pictured in Figure 43. The lenticular laminae consist of skeletal hash with some quartz, X31.

Figure 45 Outcrop of well-formed flaser bedding in which skeletal sand ripples are separated by thin mud flasers. Rule is 15 cm for scale. Big Hatchet Mountains section.

Figure 46 Outcrop of flaser bedding as it commonly appears. Ripples are irregular in shape and commonly truncated by the overlying ripple. Big Hatchet Mountain section.

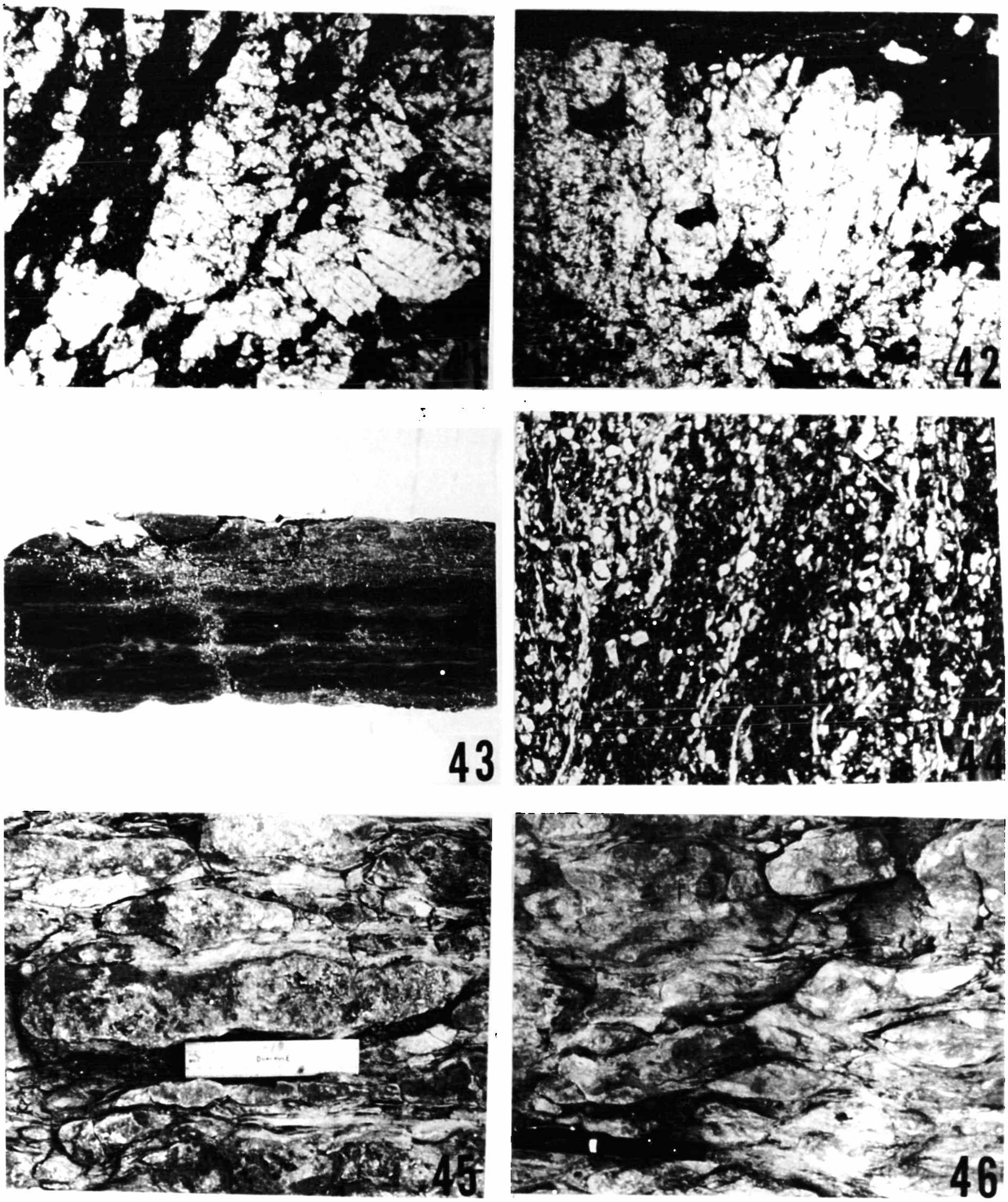
42
43
45
46

Ripples are separated by carbonate mud flasers averaging 1 to 2 cm thick. Individual mud flasers are wavy, generally filling troughs between ripples and draping over ripple crests, but are rarely laterally continuous over a few centimeters before they are truncated by overlying ripples. In general, the thickness of mud flasers is inversely proportional to ripple size. Zones of larger ripples have thinner, less abundant, and less laterally continuous mud flasers than zones of smaller ripples. At Georgetown, where ripples, in general, are smaller than average, mud units are up to 13 cm thick and ripples occur as isolated structures in carbonate mud (Fig. 50). In such thicker mud zones, ripples are commonly deformed as result of vertical sinking of coarse skeletal sand into the mud substrate.

Where mud dominates over ripples, the mud is highly bioturbated and shows no distinct internal structure. Indigenous fossils are abundant. Crinoids with tens of attached columnals, delicate cryptostome bryozoans, and rhynchonellid, spiriferid and strophomenid brachiopods in life position are common. Thin mud flasers are less bioturbated and show very thick (.5 cm), lenticular laminae up to 5 cm long consisting of skeletal sand.

Muds in this lithofacies are illitic clayey, packed biomicrite, or dolomitized biomicrite or biomicrite. Skeletal allochems consist dominantly of crinoids, bryozoans, and brachiopods, which form up to 65 percent of some thin-sections. Illite clay occurs predominantly near the base of the lithofacies and disappears upward.

An average of 4 or 5 resistant limestone beds per section protrude out from the flaser bedding. These beds average 25 cm thick, but may be up to 1 m thick. Most of these resistant beds are continuous across the outcrop with little change in bed thickness. Less commonly, beds are lenticular (Fig. 51).

Resistant beds consist of rippled carbonates, but with the average ripple size being considerably larger than in the adjacent flaser bedding. Also, the thickness of the mud flaser is much less, ranging from zero, there ripples directly overlie each other, to 1 cm thick. These beds are more resistant by virtue of having a greater predominance of skeletal sand over mud than in the adjacent flaser bedding. In lithology and nature of the skeletal component, ripples in the resistant beds are identical to the overall flaser bedding.

In the larger resistant beds, a distinct vertical gradation in the size of the ripples making up the bed occurs. From the base of the bed upward, ripple size decreases systematically (Fig. 52). In accord, the thickness of the mud flaser increases upward. For example, at Bear Mountain, one resistant bed about 1 m thick shows a decrease in ripple size from 6 cm high and 30 cm long at the base to 3 cm high and 20 cm long to 1.5 cm high and 15 cm long at the top of the bed. At the base of the bed, mud is absent, but near the top, mud flasers 1 cm thick separate individual ripples.

Figure 47 Slab, about 6 cm high, of a ripple from the flaser-bedded carbonate lithofacies. White fragments are crinoidal debris. Clay intraclasts are also common. A hint of internal ripple cross-stratification is present. Bear Mountain section.

Figure 48 Photomicrograph showing lutite-sized skeletal sediment typical of ripples low in the flaser-bedded carbonate lithofacies. Georgetown section, X31.

Figure 49 Photomicrograph showing the typical components of a ripple from the flaser-bedded carbonate lithofacies. Calcarenaceous crinoidal fragments are the most common skeletal component. Hillsboro section, X12.5.

Figure 50 Outcrop of the flaser-bedded carbonate lithofacies at the Georgetown section. Compared to Figs. 45 and 46, the increased mud content and smaller size of the ripples at this locale is apparent.

Figure 51 Outcrop of two resistant beds within the flaser-bedded carbonate lithofacies. The lower bed is lenticular, but the upper bed could be traced across the outcrop. Bear Mountain section.

Figure 52 Close-up of an outcrop of a resistant bed within the flaser-bedded carbonate lithofacies, showing the vertical sequence of ripples making up the bed. Larger ripples occur at the base of the bed and ripple size decreases upward. Bear Mountain section.

47

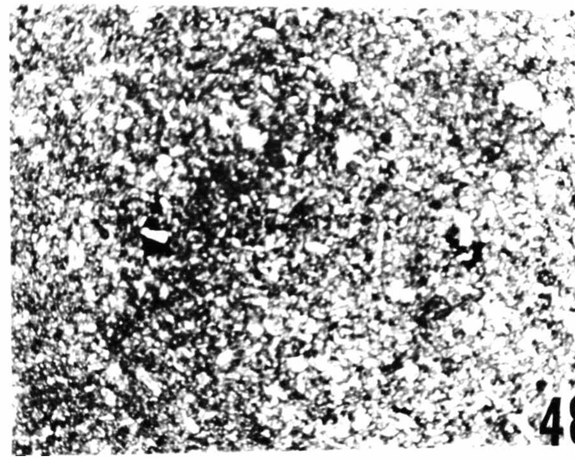

48

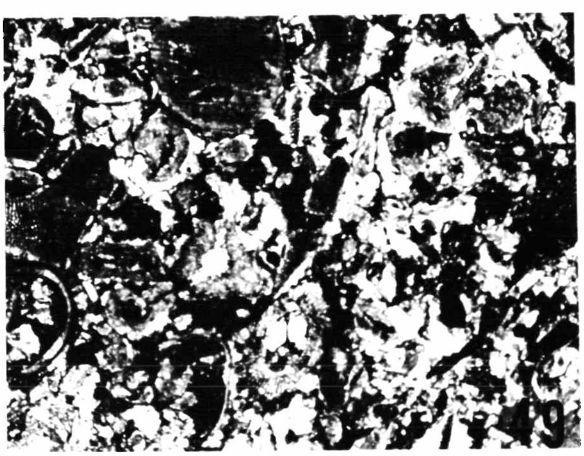

49

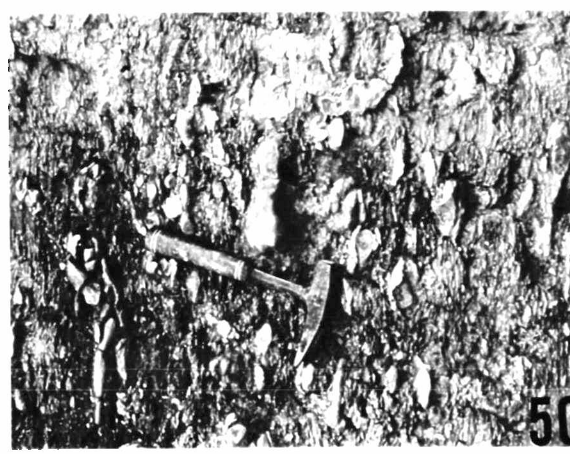

50

51

52

Wavy - Bedded and Cross - Stratified Carbonate Lithofacies

The uppermost lithofacies of the Percha Formation consists of resistant, medium light gray (N 6), thin to thick beds of cross-stratified; wavy-, flaser-, and lenticular-bedded; and parallel-laminated skeletal sandy limestone and dolomitized limestone. Thin to medium beds of nonresistant carbonate mud occur between resistant beds, especially in the lower part of the lithofacies. The lithofacies is 5 to 6 m thick in the northern sections, with the exception of Hillsboro, where only 1.5 m of quartz and skeletal sandy limestone occurs. In all northern sections measured, the lithofacies is overlain by dense resistant biomicrite of the Alamogordo Member of the Lake Valley Formation. In the Big Hatchet Mountains, 38 m of the lithofacies were measured and the section arbitrarily ended at the base of the first oolite bed in the Escabrosa Formation. Zeller (1965) reports 65.8 m of skeletal sandy limestone overlain by dense black limestone above the oolite horizon.

Resistant limestone beds, ranging in thickness from a few centimeters to 1 m, are skeletal sand bodies showing distinct features indicating a high energy of deposition. Individual beds are commonly laterally discontinuous over a few meters of outcrop (Fig. 53). Other beds are more continuous and traceable over the outcrop for many meters but generally show considerable thickening and thinning. Individual beds are most commonly either trough cross-stratified (Fig. 54), or wavy-bedded with ripples separated by thin mud layers (Fig. 55). Other common sedimentary structures include parallel laminations (Fig. 56), and flaser and lenticular bedding (Fig. 57). Upward in the lithofacies, beds have fewer mud flasers and, therefore, appear more massive.

This lithofacies is best developed at the Big Hatchet Mountains. In the lower part of the lithofacies, individual beds are highly discontinuous laterally and, for example, pinch to zero from a thickness of several tens of centimeters in only 1 or 2 meters of outcrop. Trough cross-stratification predominates over other sedimentary structures. On the average, beds are 15 to 30 cm thick and separated by 1 to 20 cm of carbonate mud. Beds become more massive upward in the lithofacies and average 50 cm to 1 m thick.

In the northern sections, with the exception of Hillsboro, wavy bedding predominates over trough cross-stratification. Individual ripples making up the wavy beds average 3 to 8 cm high and 10 to 40 cm long. Mud layers a few millimeters thick separate individual ripples within single wavy beds. Beds range in thickness from 7.5 to 75 cm and are separated by a few centimeters to tens of centimeters of carbonate mud. In general, beds become more massive upward and the mud component is reduced.

Resistant skeletal sandy limestone beds range in lithology from poorly washed, crinoidal-bryozoan biosparite to well-sorted, crinoidal-bryozoan biosparite or dolomitized biosparite (Fig. 58, 59). Calcarenite to calcirudite skeletal fragments consist of crinoids, cryptostome bryozoans, calcareous brachiopods, tentaculites, gastropods, and ostracodes. Skeletal allochems account for 60 to 70 percent of sand beds in the lower part of the lithofacies, where the average skeletal fragment size is a calcirudite, to 85 to 90 percent of sand beds higher in the lithofacies in more massive beds. In these more massive strata, skeletal fragment size is fine calcarenite and closer packing occurs (Fig. 60). Crinoidal fragments constitute the largest percentage of the skeletal component, accounting for up to 65 percent of some thin-sections. Locally, bryozoan fragments are extremely common and form the bulk of individual thin-sections. Calcarenite-sized biomicritic intraclasts occur in the lower sand beds, but rarely comprise more than 5 to 7 percent of individual samples. Micrite matrix forms up to 5 percent of some sand beds low in the lithofacies, but does not occur in the better sorted, more massive beds higher in the lithofacies. Sparry cement always predominates over micrite in the sand beds. Dolomitization of sand beds occurs primarily in the Silver City Range, where 4 to 5 percent of some samples consist of medium crystalline dolomite rhombs after spar. Some dolomite rhombs are being dedolomitized, as evidenced by iron-oxide stain outling the dedolomitized rhomb (Fig. 61).

Mud layers between individual sand beds range in thickness from 1 cm to tens of centimeters. Thicker mud beds are generally dissected by skeletal sand in the form of isolated ripples and channel-fills (Fig. 62). Mud layers consist of packed biomicrite or dolomitized packed biomicrite. Skeletal allochems make up over 50 percent of most mud beds. Allochems consist primarily of crinoids and lacy and twiggy bryozoans. No sorting of allochems is evident, and an _in situ_ origin seems likely. Crinoidal columns, consisting of 30 to 50 columnals, and delicate fenestrate bryozoans are common. Bedding surfaces are littered with these fossils (Fig. 63). Burrows are common, especially at the Big Hatchet Mountains.

Dolomitization of the biomicrite is more common than in the biosparites. In some samples in the Silver City Range, medium crystalline dolomite has completely replaced the biomicrite.

At Hillsboro, those characteristics described above for this lithofacies are not present, and the lithofacies consists of 1.2 m of quartz and skeletal sandy limestone. The outcrop is very poor because of weathering, faulting, and associated brecciation, and very few sedimentary structures were evident. In general, however, the lithofacies consists of a lower 0.6 m thick non-resistant bed and an upper 0.6 m thick more resistant bed.

The lower bed is a quartz fine sandy, poorly washed biosparite. Skeletal fragments, consisting of calcarenite- to calcirudite-sized fragments of crinoids, bryozoans, and brachiopods account for 45 percent of the biosparite. Crinoidal columns consisting of up to 20 columnals occur. Fine quartz sand accounts for 41 percent of the bed. Micrite and spar cement occur in subequal amounts. Within the lower bed, the only sedimentary structures observed were isolated skeletal sand ripples 1 cm high and 20 cm long.

The upper bed shows a hint of wavy bedding and some well-developed, isolated ripples 8 cm high and 30 cm long consisting of skeletal sand. The lithology of the bed is similar to the lower bed except that the amount of quartz sand is reduced to about 33 percent.

Figure 53 Outcrop of the wavy-bedded and cross-stratified carbonate lithofacies showing the irregularity and lateral discontinuity of the beds. Big Hatchet Mountains section.

Figure 54 Outcrop of a cross-stratified skeletal sand bed in the wavy-bedded and cross-stratified carbonate lithofacies. Big Hatchet Mountains section.

Figure 55 Slab, about 12 cm high, showing a wavy-bedded sand bed consisting of skeletal sand ripples separated by thin mud laminae. Bear Mountain section.

Figure 56 Parallel-laminated skeletal sand bed in the wavy-bedded and cross-stratified carbonate lithofacies. Big Hatchet Mountains section.

Figure 57 Skeletal sand bed consisting of sandy, lenticular, structures separated by more muddy laminae. Wavy-bedded and cross-stratified carbonate lithofacies, Big Hatchet Mountains section.

Figure 58 Photomicrograph of a biosparite typical of the skeletal sand beds of the wavy-bedded and cross-stratified carbonate lithofacies. Pictured are crinoidal fragments with encrusting bryozoans. Big Hatchet Mountains section, X31.

53

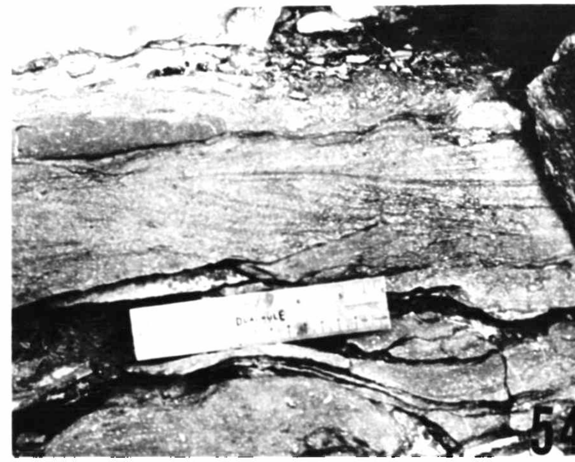

54

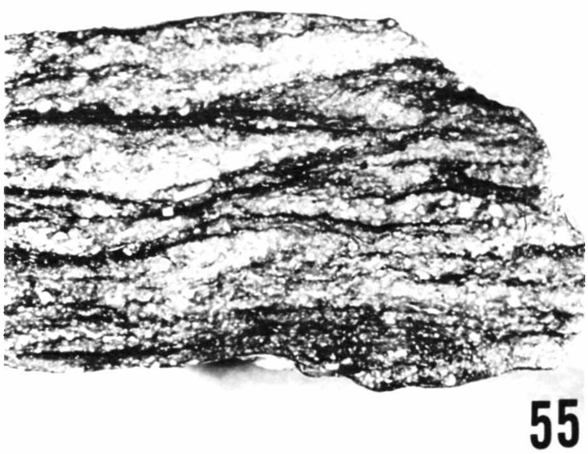

55

56

57

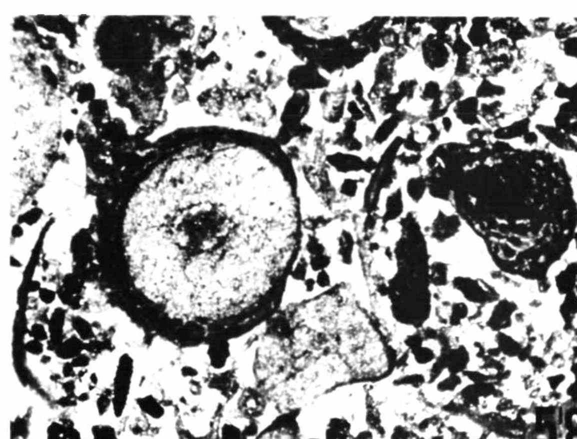

58

Figure 59 Photomicrograph showing crinoidal-bryozoan biosparite, typical of the sand beds within the wavy-bedded and cross-stratified carbonate lithofacies. Cain Spring section, X12.5.

Figure 60 Photomicrograph showing the close packing of skeletal fine calcarenite-sized fragments occurring in massive sand beds near the top of the wavy-bedded and cross-stratified carbonate lithofacies. Big Hatchet Mountains section, X31.

Figure 61 Photomicrograph showing numerous medium crystalline dolomite rhombs undergoing dedolomitization, evidenced by an iron-oxide rim. Big Hatchet Mountains section, X125.

Figure 62 Outcrop of a muddy unit occurring between two skeletal sand beds. The unit is dissected by small sand beds. Big Hatchet Mountains section.

Figure 63 Bedding plane, about 9 cm in length, showing abundant crinoids, bryozoans, and rugosan corals. Bear Mountain section.

Figure 70 Basal skeletal sand bed within the wavy-bedded and cross-stratified carbonate lithofacies, showing the occurrence of phosphatic pebbles as a lag at the base of this sand bed. Georgetown section.


59


60


61


62

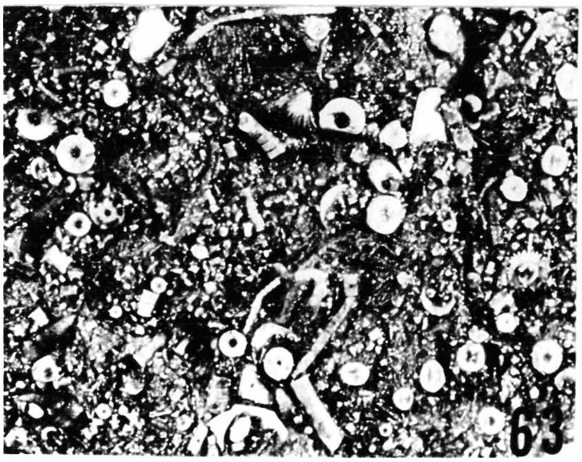
63


70

ENVIRONMENTS OF DEPOSITION OF THE PERCHA LITHOFACIES

Introduction

The lithofacies of the Percha were deposited in a transgressive sequence grading laterally and vertically in the section from tidal complex to lagoon to offshore carbonate platform (Fig. 64). The Percha lithofacies and their environments of deposition are:

(1) "basal deposits" - tidal complex

(2) shale - lagoon

(3) lens and shale - channeled outer lagoon

(4) flaser-bedded carbonate - inner carbonate platform

(5) wavy-bedded and cross-stratified carbonate - outer carbonate platform

"Basal Deposits" - Tidal Complex

"Basal deposits" formed in a tidal complex consisting of a suite of adjacent, shifting subenvironments, expressed in the rock record as distinct, laterally discontinuous, thin lithofacies. The basal lithofacies and their environments of deposition are:

(1) basal shale - shallow ponds

(2) shale and dolomite - upper tidal flat

(3) interbedded siltstone and mudstone - lower tidal flat

(4) rhythmically laminated carbonaceous limestone - isolated lagoons

(5) sandstone - transgressive beach

(6) grayish black shale - subtidal lagoon

(7) dolomitic shale - upper tidal flat

(8) fissile calcareous shale - upper tidal flat

(9) platy calcareous shale - lower tidal flat

"Basal" Lithofacies 1: Basal Shale - Shallow Ponds

The basal shale was deposited in a series of very shallow ponds above the tidal flat. In the initial transgression ponds formed in pre-existing low areas on the Montoya erosional surface. Depressions filled by the shale have probably retained their original configuration and, therefore, ponds were only a few centimeters deep. Ponds were flooded and eventually filled with silt and clay by higher than normal tides and surface run-off. The occurrence of unoxidized carbonaceous material in the shale indicates prevailing reducing conditions, probably resulting from pond stagnation and a surplus of organic material.

The occurrence of chitinozoans within these sediments is interesting, as chitinozoans have generally been cited in the literature as marine biota (Jenkins, 1970). Within the Percha, however, chitinozoans occur within ponds above the tidal flat, but are absent from subtidal sediments rich in other carbonaceous material, indicating that the chitinozoans are an _in situ_ pond biota.

An alternate possibility is that the basal shale is only a remnant of a more extensive, earlier period of marine deposition, which was removed by erosion before deposition of the Percha. But as no evidence of a more widespread deposition or any evidence of erosion at the contact

Figure 64. Idealized facies tract of the Percha lithofacies.

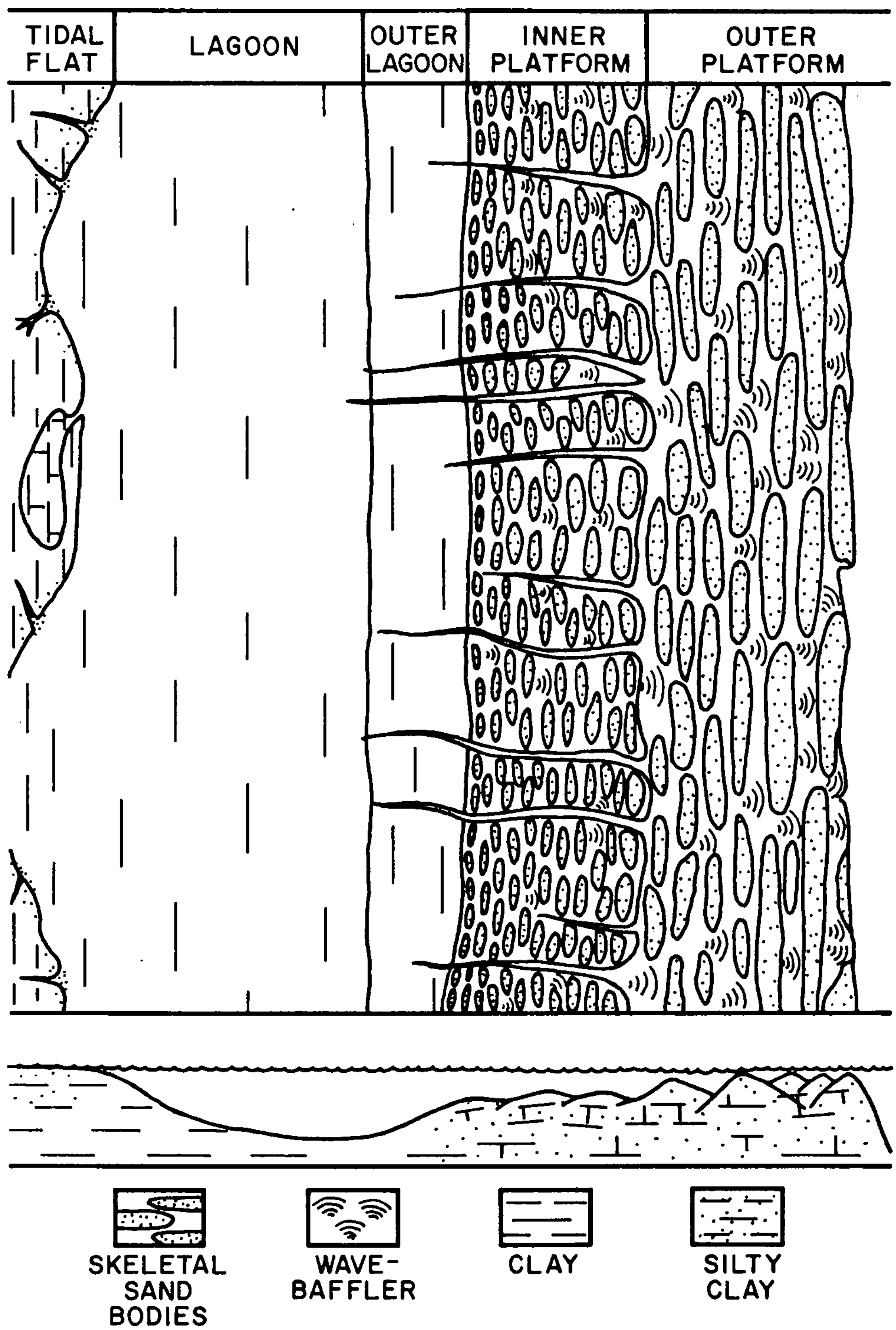
TIDAL FLAT
LAGOON
OUTER LAGOON
INNER PLATFORM
OUTER PLATFORM
SKELETAL SAND BODIES
WAVE-BAFFLER
CLAY
SILTY CLAY

of the basal shale and the overlying shale and dolomite could be found, this possibility seems unlikely.

"Basal" Lithofacies 2: Shale and Dolomite - Upper Tidal Flat

The shale and dolomite lithofacies was deposited on an upper tidal mud flat near the high water line. The irregularly alternating silty lenticular laminae and clay laminae are tidal in origin. Silty lenticular laminae were deposited by very small isolated ripples traveling over the mud flat during flood periods. Clay laminae formed during slack water as clay flocculated out of suspension.

The predominance of clay and clayey laminae over silt and silty laminae results from a typical paucity of silt or sand in the upper tidal flat. Reineck (1967) and Thompson (1968) found mud concentrated on the upper tidal flats of German Bay and the Colorado River tidal delta, respectively. This concentration of mud on the upper tidal flat has been explained by van Straaten and Kuenen (1958) and Reineck (1967) as a result of frictional drag on wave currents. Wave currents are strongest on the lower tidal flat and decrease up the inclined tidal flat. The net result is a decrease in grain size from sandy lower tidal flat to muddy-sandy mixed flat to muddy upper tidal flat.

Plant material and spores found within the shale and dolomite lithofacies were derived from adjacent land areas. Protoslavinia has been interpreted as a marine alga by Schopf and Schwietering (1970). This alga was indigenous to the Percha upper tidal flat. The reddish color of the shale and replacement of much of the organic material by hematite is indicative of overall oxidizing conditions at the time of deposition resulting from periodic subaerial exposure.

"Basal" Lithofacies 3: Interbedded Siltstone and Mudstone - Lower Tidal Flat

Interbedded siltstone and mudstone were deposited on the lower tidal flat. As a result of more regular, pronounced tidal currents lower on the tidal flat, as compared to the upper tidal flat, a more regular alternation of silty and clayey laminae occurs with silt and clay being subequal, or with silt predominating over clay.

Sandy channels in the upper part of the lithofacies are tidal channels regularly flushed by currents and kept free of muddy sediments. The common occurrence of burrows on the bottom of some channel-fills, compared to the general lack of burrows in the adjacent flat, suggests that the channels regularly contained water and presented a more hospitable environment for organisms than the adjacent flat, which experienced a higher rate of sedimentation and periodic exposure.

The development of tidal channels in the lower tidal flat and their general absence higher in the flat is fairly typical of some modern tidal complexes. Reineck (1972) found tidal channels best developed in the lower part of the German Bay tidal flats. Similarly, van Straaten (1954, 1961) found the lower tidal flats of the Netherlands cut by tidal channels, with the upper tidal flat generally free of channels.

"Basal" Lithofacies 4: Rhythmically Laminated Carbonaceous Limestone - Isolated Lagoons

Rhythmically laminated, carbonaceous limestone was deposited in isolated, stagnant, reducing lagoons cut off from the adjacent tidal flat. These carbonaceous limestones are essentially free from terrigenous sediment, but are overlain, underlain, and laterally adjacent to dominantly terrigenous tidal deposits. Deposition of these limestones must have occurred in small basins cut off or blocked by some type of barrier from the influx of terrigenous material. The regularly alternating continuous laminae of calcite and carbonaceous material clearly were not the result of "current deposition", but rather formed by a settling from suspension of material over the breadth of the lagoon.

The carbonate and carbonaceous material probably originated within the lagoon itself. A regular, cyclic change in the material available for deposition is indicated by the cyclic pattern of the laminations. Bottom conditions were reducing, as indicated by the preservation of organic material, lack of a benthic fauna, and lack of bioturbation.

Similar deposits, consisting of an alternation of calcite, and carbonaceous or detrital continuous laminae are reported from several environments, ranging from deep inland sea to evaporitic sequence to shallow ephemeral lake. Conditions shared in common by these diverse environments are stagnant water circulation, low oxygen conditions, and a periodic, usually seasonal, change in sediment supply.

The classic example of varved, deep inland sea rhythmites is from the Black Sea. There laminae consist of calcite and detrital sediment. Müller and Baschke (1969) report that the calcite layers consist primarily of coccoliths, diatoms, and calcite grains.

Anderson and Kirkland (1960) report calcite-carbonaceous rhythmites from the base of a few evaporite deposits. An apparent clastic-organic-evaporite cycle exists in basins slowly undergoing terrigenous starvation. According to Anderson and Kirkland, the idealized sequence of varved laminae is from bottom to top, clastic-organic laminae, organic-calcite laminae calcite-anhydrite laminae, anhydrite laminae, and, finally, halite. This cycle occurs most notably in the Permian Castile Formation of New Mexico (Anderson and others, 1972) and in the Jurassic Todilto Formation of New Mexico (Anderson and Kirkland, 1960). The origin of calcite, anhydrite, and halite is by precipitation from solution.

Anderson and Kirkland (1969) also report calcite-carbonaceous rhythmites from the Pleistocene Rita Blanca lake-fill on the High Plains of Texas. The authors attribute the calcite laminae primarily to direct precipitation of calcium carbonate from solution during summer months when maximum stagnation and evaporation occurred. Elevated temperatures reduce the amount of carbon dioxide in solution, thereby reducing the capacity of the water to hold calcium bicarbonate in solution and, as a result, calcium carbonate is precipitated. Plants and bacteria also aid the precipitation of calcium carbonate by removing carbon dioxide from the system.

Calcite laminae within the carbonaceous limestone of the Percha are particularly interesting because the calcite occurs as rhombs. Precipitated calcite laminae within both the Todilto and Rita Blanca deposits are micritic, but rhombic calcite comprises the calcite layers within the Castile.

Folk (1974b) argues that only in freshwater environments, relatively free of "pollutant ions", will rhombic calcite occur. Clearly, freshwater origins for the calcite rhombs occurring in the Castile and Percha are highly unlikely.

The origin of the calcite rhombs within the Percha appears to have only three possible causes. First, the rhombs could have been dolomite later dedolomitized. Secondly, rhombic calcite could have replaced an earlier material during freshwater diagenesis. Third, rhombic calcite could have been directly precipitated.

The dedolomitization of a pre-existing dolomite seems unlikely here. Dedolomitization, as described by Chafetz (1972), is a surface alteration feature. The carbonaceous limestone in the Percha is a distinctly unweathered, dense, hard rock. At Bear Mountain, for example, carbonaceous limestone beds overlie highly weathered dolomitic shale. The weathered dolomitic shale contains unaltered dolomite rhombs. It is unlikely that the carbonaceous limestone beds have been selectively more altered than surrounding deposits. In addition, no evidence of dedolomitization, such as iron oxide rings, could be found. No evidence of a pre-existing phase of dolomitization could be found either. Dolomitization commonly destroys original textures.

The occurrence of even, undisturbed laminae and lenticular structures, originating as isolated ripples, argue against any phase of earlier dolomitization.

The second possibility of rhombic calcite replacing an earlier material during freshwater diagenesis is unlikely for several of the same reasons. Replacement or recrystallization would tend to obliterate primary textures. Primary textures, however, appear to be unaltered.

A direct precipitation of rhombic calcite is indicated. Not only are primary textures preserved, but ripple-deposited lenticular laminae within single calcite laminae show rhombs of calcite behaving like clastic particles. These lenticular laminae consist of calcite rhombs coarser than the surrounding rhombic matrix, indicating their existence as rhombs at the time of deposition. This occurrence of precipitated rhombic calcite, however, has yet to be reconciled to ideas expressed by Folk (1974b) regarding conditions under which rhombic calcite occurs.

"Basal" Lithofacies 5: Sandstone - Transgressive Beach

The sandstone lithofacies occurring at the Big Hatchet Mountains is a transgressive beach deposit. The thinness of the deposit, plus its lack of lateral continuity, indicates that beach development was not extensive and formed only locally as a transgressive linear strandline deposit. Byrne and others (1959) report a similar transgressive beach sand a few centimeters to 30 cm thick, underlying Holocene sediments of Louisiana. Similarly, Thompson (1968) reports a basal transgressive beach sand 1 m or less thick along the Colorado Delta, Baja California, which developed as a result of the Late Wisconsin sea level rise.

"Basal" Lithofacies 6: Grayish Black Shale - Possible Subtidal Lagoon

Because of very poor outcrop and a consequent lack of information, a precise environment of deposition for the grayish black shale at the Big Hatchet Mountains was not determined. Deposition of clay, rich in organic material and pyrite requires quiet, restricted conditions. In addition, within the context of its occurrence, the entire basal sequence, it seems likely that the shale originated in restricted lagoons or bays along the coastline.

"Basal" Lithofacies 7 and 8: Dolomitic and Fissile Calcareous Shales - Upper Tidal Flat

The dolomitic and fissile calcareous shale lithofacies were deposited on the upper tidal flat. These calcareous lithofacies are analogous to the more terrigenous shale and dolomite lithofacies in the northern sections. As at the northern sections, laminae typical of the upper tidal flat are developed. Thin, commonly lenticular, silty laminae deposited by small ripples during flow periods alternate with clay laminae deposited during slack water. As at the northern sections also, clay greatly predominates over silt and no in situ fauna was found.

The primary difference between the mud flats developed at the northern sections compared to those at the Big Hatchet Mountains is the diminished abundance of terrigenous sediment and introduction of carbonate sediment at the Big Hatchet Mountains. The dolomite occurring within the dolomitic shale at the Big Hatchet Mountains has some of the earmarks of penecontemporaneous dolomite associated with supratidal zones. Dolomite crystals are extremely fine, rarely over 0.010 or 0.015 mm. In addition, a loss of dolomite occurs from the dolomitic shale upward into the fissile calcareous shale. In other words, a loss of dolomite occurs from the upper tidal flat to the lower tidal flat, a likely occurrence with penecontemporaneous dolomite confined to areas above or near the high water line. The thin, finely laminated dolomitic crusts that Shinn and others (1965) cite as the mode of occurrence of dolomite in the supratidal zones of the Bahamas, however, were not found within the Percha.

"Basal" Lithofacies 9 - Platy Calcareous Shale - Lower Tidal Flat

Platy calcareous shale lithofacies at the Big Hatchet Mountains was deposited on the lower tidal flat and is analogous to the interbedded siltstone and mudstone lithofacies at the northern sections. As at the northern sections, the regular alternation of silty and clayey laminae within the lithofacies are the result of tidal currents. An *in situ* fauna is absent as well.

Tidal Sequence at the Big Hatchet Mountains Section

The overall sequence of lithofacies in the "basal deposits" of the Big Hatchet Mountains is a transgressive tidal complex. The initial part of the transgression was accompanied by tidal flat progradation. Initial deposition consisted of "high energy" beach sand. Beach sand does not grade vertically into subtidal deposits, but rather into "low energy" upper tidal flat deposits. Terrigenous sediment becomes less abundant through this same sequence.

A similar situation occurred at the Colorado River tidal delta in Baja California, as described by Thompson (1968). A basal transgressive sand is overlain by mud flat deposits. Sediment supply from the Colorado River outpaced the Late Wisconsin transgression. A seaward mud flat progradation occurred during an overall sea level rise and tidal flat sedimentation maintained the mud flat surface near the high tide line.

The triggering mechanism for the tidal flat progradation in the Percha may have been the diminishing supply of terrigenous sediment, which allowed carbonate production. With carbonate production occurring under favorable conditions, tidal flat deposits built out over the initial transgressive beach sand. The transgression gradually outpaced carbonate production. Upper tidal flat dolomitic shale with isolated lagoons grades vertically into calcareous shale into platy calcareous shale deposited on the lower tidal flat.

The cause of the diminished supply of terrigenous sediment at the Big Hatchet Mountains is unclear, but may be related to local source area supply. Whatever the cause, carbonates play a much more significant role in both tidal flat and the overlying subtidal accumulations in the southern area than at the northern sections. Figure 65 illustrates the tidal tract developed at the Big Hatchet Mountains.

Tidal Sequence at the Northern Sections

"Basal deposits" at the northern sections consist of a transgressive tidal flat complex. Shallow pond-fills, deposited in low areas landward of the tidal flat, grade vertically in the section into upper tidal flat deposits. Upper tidal flat deposits grade upward into lower tidal flat deposits, which grade upward into subtidal lagoonal deposits. Lagoons and ponds adjacent to the tidal flat commonly became isolated from a terrigenous sediment supply and were sites of calcium carbonate precipitation.

The tidal flats developed at the northern sections were clearly "low energy". Flaser bedding or herringbone structures associated with some modern tidal flats did not develop on the Percha tidal flat. Tidal currents on the Percha tidal flat were apparently insufficient to generate these higher energy structures. In addition, the number of tidal channels on the lower tidal flat is small, presumably because the exchange of water between tides was neither large nor energetic. Figure 66 illustrates an idealized facies tract of the tidal flat at the northern sections.

Figure 65. Idealized facies tract of the tidal sequence at the Big Hatchet Mountains.

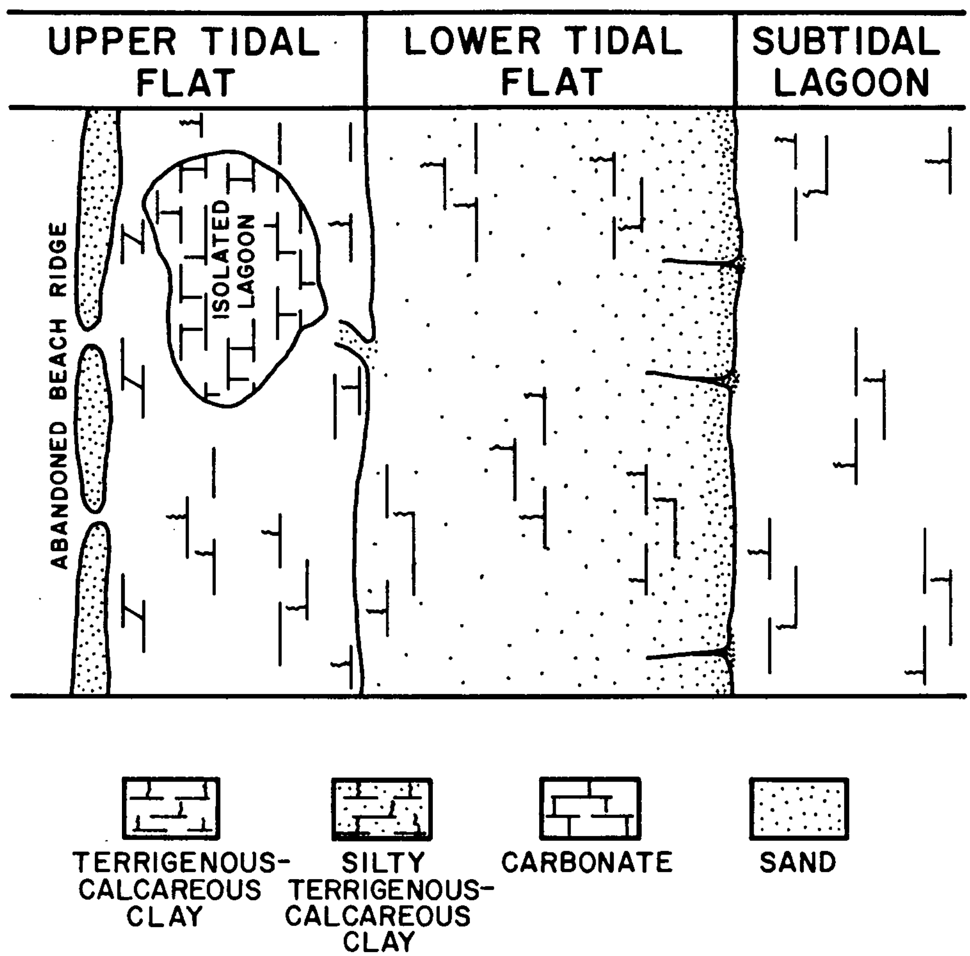

UPPER TIDAL FLAT
LOWER TIDAL FLAT
SUBTIDAL LAGOON
ABANDONED BEACH RIDGE
ISOLATED LAGOON
TERRIGENOUS-CALCAREOUS CLAY
SILTY TERRIGENOUS-CALCAREOUS CLAY
CARBONATE
SAND

Figure 66. Idealized facies tract of the tidal sequence at the northern sections.

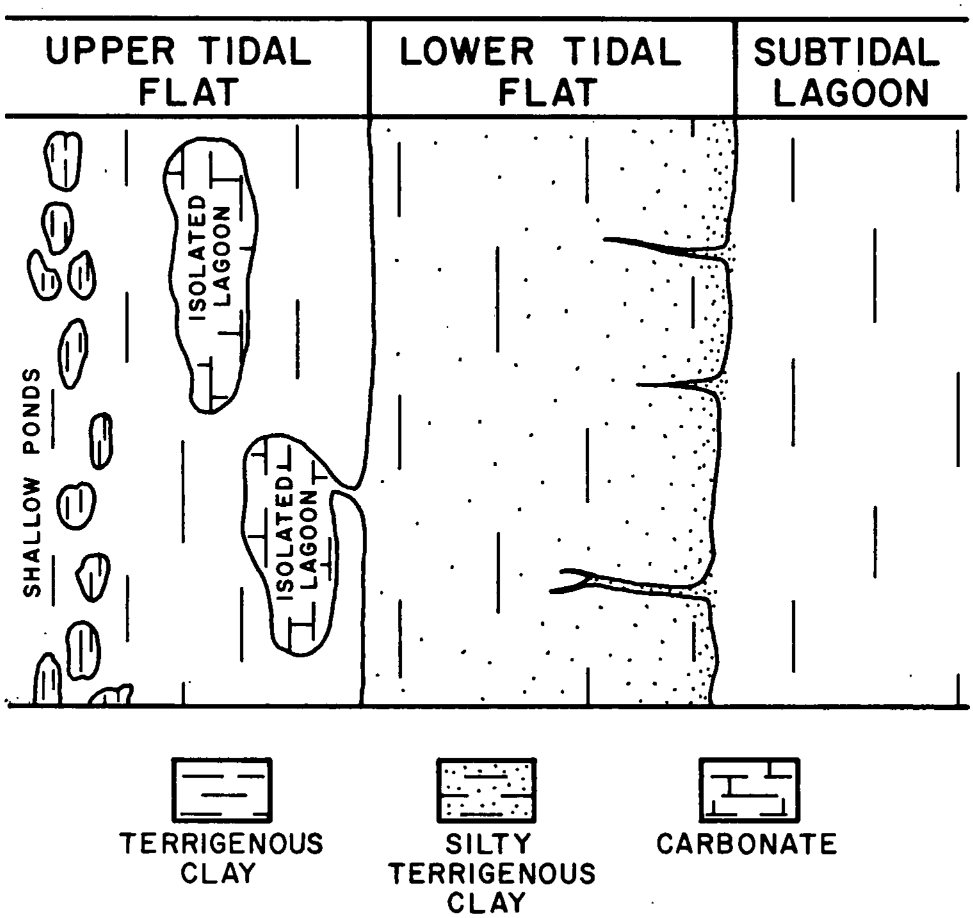
UPPER TIDAL FLAT
LOWER TIDAL FLAT
SUBTIDAL LAGOON
SHALLOW PONDS
ISOLATED LAGOON
ISOLATED LAGOON
TERRIGENOUS CLAY
SILTY TERRIGENOUS CLAY
CARBONATE

Shale Lithofacies - Lagoon

The shale lithofacies was deposited as part of a transgressive sequence in a restricted shallow lagoon situated between a tidal flat and an offshore carbonate buildup (Fig. 64). Restricted conditions were the result of the offshore carbonate buildup and prevailing shallow water conditions over the lagoon. The offshore buildup acted as a barrier and prevented the high energy waves of the open marine basin to the south from affecting the sediment accumulating in the lagoon. The nature of the sediment accumulated in the lagoon changes from terrigenous at the northern sections to terrigenous and carbonate at the Big Hatchet Mountains.

The broad lagoon developed at the northern sections during the Percha transgression was the site of terrigenous mud accumulation under, initially, highly restricted conditions. The lower shale shows a general absence of "current-deposited" structures. Terrigenous clay and organic material settled out of suspension, forming poorly defined laminae as periodic changes occurred in the availability of the clay and organic detritus. The laminae that formed are well-preserved. No benthic fauna was available to destroy the laminae.

Upward in the section, ripple-deposited, silty lenticular laminae become increasingly abundant with the advent of weak currents that occurred in the lagoon. These weak currents help to oxygenate the bottom and a benthic fauna was slowly established and bioturbation features occur. The decrease in abundance of carbonaceous material may be because oxygenated conditions did not favor the preservation of organic material, the benthic fauna may have fed on the organic detritus, and the less stagnant conditions may have been unfavorable to the bulk of the marine vegetation that provided the carbonaceous material. In acccrd with reduced carbonaceous content, the shale lightens in color. The vertical shale sequence, therefore, shows a transgressive lagoon, which grade from restricted conditions to less restricted conditions approaching the offshore carbonate buildup.

The inner Percha lagoon that developed at the northern sections is unlike most modern subtidal environments because it lacks a benthic fauna and displays an abundance of primary sedimentary structures. The subtidal zone normally supports an abundant fauna and sedimentary structures are usually destroyed by burrowing organisms. For example, Moore and Scruton (1957) found sedimentary structures destroyed by burrowing organisms along the nearshore Gulf of Mexico except near the Mississippi River delta. At the delta, the rate of sedimentation was greater than the burrowing ability of those few organisms capable of surviving the intense sediment rain, and primary structures were preserved.

Apparently, a benthic fauna did not inhabit the Percha lagoon becuase of prevailing euxinic conditions. Euxinic conditions are indicated by the lack of "current-formed" structures, preservation of carbonaceous material, and the dark color of the shale.

Recent euxinic environments have been broadly grouped by Byers (1973) as occurring in open ocean, semi-enclosed sea, and local lagoon and estuary. Within the open ocean, euxinic conditions are unusual because of global water circulation and exist only where the Oxygen Minimum Zone intersects the bottom. Byrne and Emery (1960) and Calvert (1964) report euxinic bottom conditions at a depth of 600 m in the Gulf of California where rhythmites of diatom ooze and clay laminae form in stagnant reducing conditions free from a benthic fauna.

Semi-enclosed seas and deep coastal fjords barred from open circulation by a sill also have euxinic bottom conditions. For example, water is exchanged and oxygenated in the Black Sea through the Bosporus to a depth of 200 m (see Deuser, 1974). Below this zone, conditions are euxinic and Muller and Blaschke (1969) have demonstrated the occurrence of undistrubed rhythmites of detrital and coccolith-rich laminae in portions of the Black Sea.

Some coastal lagoons have euxinic bottom conditions. Zangerl and Richardson (1963) noted euxinic conditions developed in restricted shallow ponds and lagoons with a floating mat of vegetation along the coast of Louisiana.

None of the recent euxinic environments, however, are directly analogous to the broad Percha lagoon. Clearly, the Percha lagoon, situated on the craton and developed on top of tidal flat deposits and/or an erosional surface, was not the site of deep water deposition. It is equally clear that no modern euxinic coastal conditions are as broad as the Percha lagoon.

Broad euxinic conditions in the Percha lagoon were the result of a broad, offshore carbonate buildup paralleling the shelf edge. The lagoon was locked between the cratonic strandline and a carbonate bank that was near or at wave base. Upwelling currents were diminished over the broad carbonate buildup and only weak currents persisted into the outer reaches of the lagoon.

Lagoonal depth must have been sufficiently shallow such that strong currents did not form because of surface drag over the lagoon. Lagoonal depth, however, must not have been so shallow that the bottom was aggitated by minor wind-generated waves.

The lagoon developed at the Big Hatchet Mountains during the Percha transgression differs from the lagoon developed at the northern sections by containing carbonates, more abundant current features, and a benthic fauna with associated bioturbation features. Carbonate production was initiated by the diminished influx of terrigenous sediment during the tidal flat deposition and was responsible for tidal flat progradation during an overall transgression. Tidal flat progradation slowly gave way to subtidal conditions as the seas transgressed more rapidly than sediment accumulated. Carbonate production continued, however, and the lagoon bottom was maintained at a very shallow depth. Small wind-generated waves were capable of stirring the bottom. The net result was an oxygenated lagoonal bottom showing abundant current features and a benthic fauna. The lagoon that developed at the Big Hatchet Mountain area was, therefore, more oxygenated, less stagnant, and shallower than the lagoon developed at the northern sections.

The occurrence of chlorite solely in the lagoonal shales at the northern sections, where euxinic conditions prevailed, suggests a diagenetic alternation of nonchloritic clays to chlorite within the lagoon. Work with recent clays has suggested similar trends (Grim and Johns, 1953; Powers, 1953, 1957; Brown and Ingram, 1954; and Griffin and Ingram, 1955). The most convincing example is from Grim and Johns (1953), who found chlorite selectively concentrated in bays in the vicinity of Rockport, Texas. The chief sediment transported by the Guadalupe River into the area is montmorillonite with minor amounts of illite, and kaolinite and/or chlorite. The bays of the area (San Antonio, Mesquite, and Aransas Bays) show a decrease in the amount of montmorillonite and an increase in illite and chlorite. In the adjacent open Gulf, montmorillonite again increases in abundance and chlorite becomes less abundant. Grim and Johns attribute the increase in chlorite in the bays to diagenetic alternation of nonchloritic clay minerals to chlorite.

Clay mineral trends in the Percha suggests a similar mode of occurrence of chlorite in the lagoonal deposits, but the role of diagenesis in clay mineralogy is far from settled. A strict reliance on source area to account for the observed clay mineralogy trends seems unlikely, as abrupt source area changes would have had to occur after deposition of the "basal deposits" and again after deposition of the shale lithofacies.

Lens and Shale Lithofacies - Channeled Outer Lagoon

The lens and shale lithofacies was deposited along the outer edge of the lagoon behind the carbonate buildup (Fig. 64). Sediment deposited in this area consisted of both terrigenous sediment derived from land sources and carbonate sediment derived from the offshore carbonate buildup. The shale of this lithofacies was deposited as a continuation of lagoonal mud accumulation. Carbonate lenses and layers were deposited as fill in the feather-edges of channels transporting fine skeletal debris into the lagoon from the offshore carbonate bank. The gradational nature of the lens and shale lithofacies into the overlying flaser bedding is a result of the continued transgression of the Percha depositional complex.

Vertical trends established in the shale lithofacies are continued through the shales of the lens and shale lithofacies. Both at the northern and Big Hatchet Mountains sections, the increasing abundance of a fauna, with associated bioturbation, and ripple-deposited lenticular laminae upward in the shale lithofacies and into the shale of the lens and shale lithofacies occur as a result of continued transgression of the Percha depositional complex. As in the shale lithofacies, the shales of the lens and shale lithofacies at the Big Hatchet Mountains show considerably more abundant ripple-deposited lenticular laminae than at the northern sections, indicating that bottom conditions were considerably more agitated.

The channel-fill origin of the carbonate lenses and layers is derived from their morphology and lithology. The sediment making up the lenses and layers (lutite- to arenite-sized skeletal fragments of crinoids, bryozoans, ostracodes, and calcareous brachiopods) are not found in the adjacent shale, where the fauna consists of linguloid brachiopods. These skeletal fragments were, therefore, not derived from the immediate area, but have been transported into the area. Evidence of transport is clearly seen in the texture of the skeletal material making up the lenses and layers. The lenses and layers consist of a mass of fine abrasional fragments and no _in situ_ fauna or even whole fossils were found. The same suite of organisms, whose fragments make up the lenses and layers, occurs _in situ_ and in great abundance in the overlying carbonates. At the time of deposition, these organisms were inhabiting the carbonate buildup adjacent to the outer edge of the lagoon where the carbonate lens and shale lithofacies accumulated. Material making up the lenses and layers consists of pulses of fine skeletal debris transported into the lagoon by currents.

These pulses of fine skeletal debris transported into the outer lagoon were confined to channels. The fragments making up the debris are coarser than the surrounding clay-shale. Currents capable of transporting this debris are probably also capable of scouring the liquified mud substrate. Evidence that scouring did occur is seen in the terrigenous clayey rip-up clasts found within the carbonate lenses and layers. Scouring would have produced a shallow channel to be filled by the skeletal debris being transported. Had channeling not occurred, this fine skeletal debris would most likely have been distributed laterally in very thin sheets, which is not the case, as the debris is confined to distinct, laterally discontinuous beds a few centimeters thick.

The laterally discontinuous carbonate layers at the Big Hatchet Mountains show the original form of the channels. The rows of carbonate lenses in the northern sections were originally deposited in channels of similar configuration, but have been modified by loading. Channel-fill was coarser than the liquified mud substrate, which was incapable of supporting this coarser material. Portions of the channel-fill began to sink into the underlying mud. The eventual breakup of the channel-fill into horizontal rows of discrete lenses was the net result (Fig. 67).

Whether or not the channel-fill broke up into discrete lenses or not was a function of the surrounding shale. Shale surrounding carbonate lenses at the northern sections is predominantly clay. A distinct contrast existed, therefore, in the size of the particles making up the channel-fill and the surrounding substrate. The substrate was incapable of supporting the fill and the layer of carbonate channel-fill broke up into discrete lenses. At the Big Hatchet Mountains, however, there was less contrast between the carbonate channel-fill and the surrounding substrate, because the muddy substrate contained a considerable amount of silt and fine sand. The substrate was capable of supporting the channel-fill, and break up of the carbonate layer did not occur.

Similar lens-shaped, nonconcretionary structures described in the literature are sedimentary boudinage, load casts, and ball and pillow structures. Lenses in the Percha are only superficially similar to sedimentary "boudinage". Sedimentary "boudinage" is a diagenetic product that occurs during compaction. Percha lenses are clearly not "boudinage" structures because they do not have any sign of lateral spreading during diagenesis, such as tensional gashes. Instead, Percha lenses appear to have formed soon after deposition, while the carbonate material was unconsolidated and the surrounding substrate was hydroplastic.

Percha lenses do not, however, show the highly irregular shape commonly associated with load casts. Load casts are formed during deposition when soft hydroplastic mud is unequally loaded with sand and yields to the weight of the sand, and the sand sinks into the mud (Shrock, 1948, p. 156; Potter and Pettijohn, 1963, p. 145-148, 152).

Percha lenses most closely resemble ball and pillow structures. Ball and pillow structures are formed after the initial deposition of sand over mud (Potter and Pettijohn, 1963, p. 148-152). The sand layer later sinks into the mud, breaking up into isolated cells with mud squeezing around and over the sand. A triggering mechanism, such as an earthquake, was suggested as being necessary by Kuenen (1958, 1965) who produced structures similar to ball and pillow experimentally by applying a mild shock to an aquarium containing mud with an overlying sand layer.

Ball and pillow formation occurs soon after deposition of the sand over mud. For example, Kaye and Power (1954) cite ball and pillow structures that could be no older than 10 years. A sand layer had broken up into lenses surrounded by mud on a small delta in F.D. Roosevelt Lake, Washington. The part of the delta on which the ball and pillow structure formed had not existed prior to the building of the reservoir only 10 years earlier.

Lens structures in the Percha depart somewhat from typical ball and pillow structures. Most commonly, ball and pillow structures are confined to one bed (Potter and Pettijohn, 1963, p. 148). Lenses in the Percha are a common occurrence in a particular lithofacies from section to section where a distinct difference in the consistency of channel-fill and surrounding substrate occurs. The only triggering mechanism necessary was a critical "load factor" of coarse material versus the competency of the surrounding substrate.

Figure 67. Idealized sequence showing the formation of carbonate lenses from channel-fill as a result of loading.

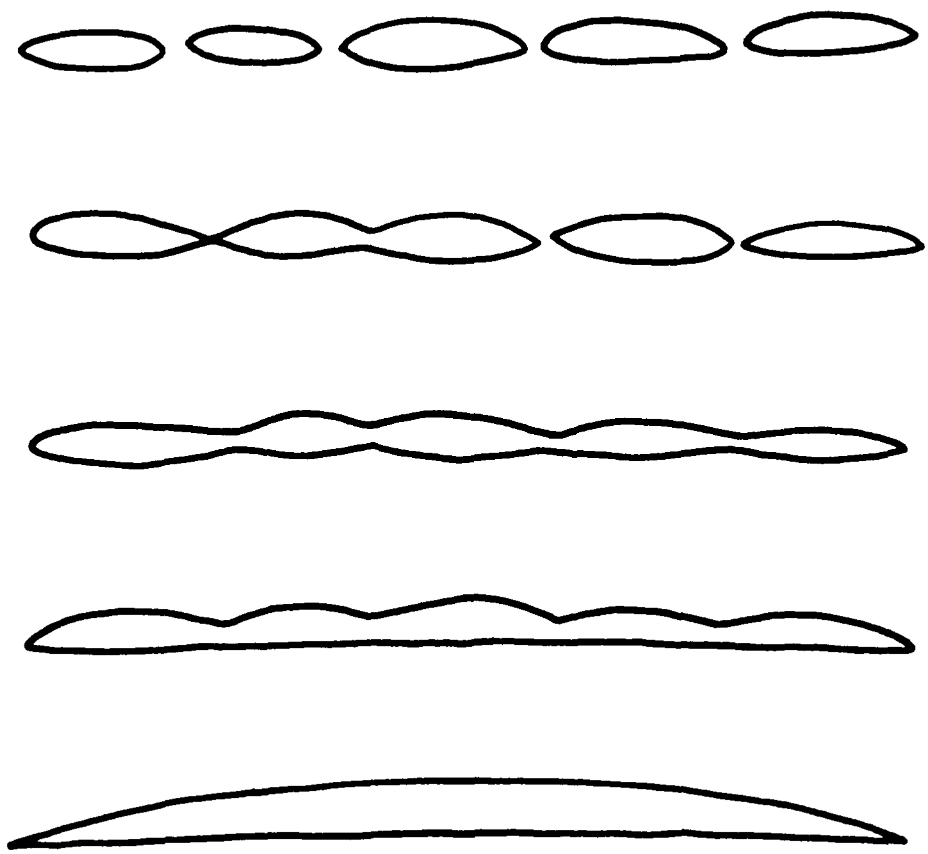

Flaser-Bedded Carbonate Lithofacies - Inner Carbonate Platform

The flaser-bedded carbonate lithofacies was deposited on the inner carbonate platform (Fig. 64). The inner platform was a zone of moderate energy consisting of shifting, rippled skeletal sands and muddy patches with flourishing life. The zone was cut by migrating shallow channels.

Skeletal sand deposited as ripples was derived both from the high energy outer carbonate platform and within the inner platform itself. Crinoidal and bryozoan skeletal sand, a product of mechanical abrasion in the high-energy outer platform was transported lagoonward by currents. Skeletal sand was also derived from the immediate area by the mechanical abrasion of the local fauna, which consisted chiefly of brachiopods, bryozoans, and crinoids.

Mud was abundant in the area, and currents were insufficient to winnow it out completely. As with the sand fraction, carbonate mud was derived both from the better winnowed outer platform and from <u>in situ</u> production within the inner platform. Very little of the mud was terrigenous in origin. Much of the mud was deposited within clusters of organisms acting as organic bafflers.

Resistant beds occurring in the lithofacies were deposited in shallow, migrating channels, Resistant beds are laterally confined zones of higher energy deposits, as evidenced by larger ripple size and less abundant mud flasers than in the surrounding flaser bedding. Individual ripples making up these beds are separated by thin mud flasers, indicating the filling of the channels over a period of time and under a variety of energy conditions. Channel migration is evidenced by the regular decrease upward in ripple size in some of the larger resistant beds. As a channel migrated laterally, so did the zone of highest energy. A vertical section through a migrating channel filled by rippled sand, therefore, shows an upward fining of ripple size. Channel migration is also evidenced by the broad lateral extent of most of these resistant beds across the outcrop. The extension of these beds across many meters of outcrop resulted from the migration of the channel through a period of time and does not reflect the lateral extent of the actural channel at any one time. These channels occurring in the flaser bedded carbonate lithofacies are probably the more offshore extension of the smaller channels in the lens and shale lithofacies.

The depositional environment of the inner carbonate platform of the Percha is analogous to the blanket sediment of the interior platform of modern reef tracts. For example, Multer (1975) describes the area behind the outer reef tract in Florida as a zone of loose clean rippled sand with patches of grassy muddy areas with a rich variety of life.

Wavy-Bedded and Cross-Stratified Carbonate Lithofacies - Outer Carbonate Platform

The wavy-bedded and cross-stratified carbonate lithofacies was deposited in a crinoidal and bryozoan bank occupying the outer part of the carbonate buildup paralleling the shelf edge (Fig. 64). The bank began during the initial part of the transgression as a shelf-margin garden taking advantage of upwelling currents. A carbonate buildup ensued. The buildup lacked a framework constituent among the organisms occupying the buildup. Vertical growth was accomplished, therefore, primarily by the accumulation of skeletal debris in winnowed sand bodies. In addition, mud patches, densely populated by crinoids and bryozoans, acted as trapping agents of fine sediment and contributed to the sediment accumulation. Vertical growth was accompanied by a lateral extension of the garden over the craton as the transgression continued. This lateral spreading was contingent upon the presence of satisfactory conditions of water depth and paucity of terrigenous sediment.

Once established, this outer bank maintained itself at or near wave base and acted as a major current baffler in a zone of high energy. Mechanical processes broke up skeletal material after the death of the organism. Fine material was winnowed and transported lagoonward, while coarse skeletal debris was locally distributed as sand bodies, resulting in the deposition of wavy-bedded and cross-stratified skeletal sand beds.

Muddy units in this lithofacies originated as patches between sand bodies were the mass of organisms was sufficient to act as a trapping agent for fine sediment. Muddy zones were cut by small sand channels during channel migration.

Variations in the lithofacies thickness and nature of the bedding from section to section resulted from differences in the proximity to the shelf edge. The initial buildup of the skeletal bank began on the shelf edge located to the south of the Big Hatchet Mountains section. With continued transgression, satisfactory conditions for crinoidal and bryozoan garden growth were extended northward. The initial point of the buildup continued to accrete vertically as long as rising sea level did not outpace the vertical accumulatinn of the buildup, which was the case in the Percha for a period of time. The Big Hatchet Mountains section is located near the point of bank accumulation. The lithofacies thins over the craton to the northern sections. Similarly, the current energy is diminished northward. Cross-stratified sand bodies grade northward to smaller ripple-deposited wavy beds.

Either the crinoidal and bryozoan bank did not extend as far as the Hillsboro section, or the area where the strata crop out was locally unsuitable for bank development. Because of the large content of quartz sand intermixed with crinoidal debris at Hillsboro, it is likely that the area was unsuitable for extensive crinoidal or bryozoan growth because of terrigenous influx. The terrigenous sand could have been derived from a local change in source area or a local regression. Because the underlying flaser-bedded lithofacies also thins northward and eastward to Hillsboro, the area probably was located near the most inland extension of the outer crinoidal and bryozoan bank.

Modern analogies to the crinoidal and bryozoan bank occur along carbonate shelf margins where reef complexes are typically developed at the platform edge. For example, the outer Florida reef tract consists of a high energy zone of coral boundstone with intervening rippled calcarenite- and calcirudite-sized skeletal sands derived from the mechanical abrasion of the reef (Ginsburg, 1956). The coarsest rubble is located directly behind the outer reef at a depth of 1.5 to 4.5 m (Multer, 1975).

The Percha crinoidal and bryozoan bank differed in one major respect from the Florida reef tract. The primary bank-forming organisms of the Percha bank, unlike the corals of the Florida reef, did not provide a structural framework for reef development. The lack of a major boundstone wave barrier has significant consequences on the lateral extension of the bank as well as the distribution of skeletal debris. First, because currents were not immediately stopped by a boundstone barrier but only slowly diminished inward over the wave-baffling crinoidal and bryozoan garden, moderate to strong nutrient-bearing currents persisted over a broad area, providing optimal conditions for growth of this community. Hence, the Percha bank was not a narrow structure confined to the shelf edge, as is the outer reef tract off Florida, but rather, extended from the shelf edge inward over a broad area. Secondly, unlike the Florida reef tract where skeletal sand is confined to a rather narrow zone behind the reef, the Percha bank debris was transported great distances into the inner platform and lagoon. As a result, grain size decreased lagoonward regularly as currents diminished over the broad platform. Ginsburg (1956) and Swinchatt (1965) report a somewhat analogous situation in those areas of the outer reef tract off Florida where no boundstone is present. In such areas there is considerably more transport of sediment from the outer reef into the back reef. In addition, the outer reef subenvironment has a greater landward extension, and conditions only gradually change to the back reef subenvironment.

PERCHA DEPOSITIONAL COMPLEX

The Percha Formation is an Upper Devonian- Lower Mississippian shale-carbonate unit consisting of five lithofacies extending over the study area in southwestern New Mexico (see cross-sections figs. 68, 69). The lithofacies were deposited in a transgressive sequence grading laterally and vertically in the section from tidal complex to lagoon to carbonate platform. This sequence of environments forms a single, terrigenous-carbonate, depositional package with cause and effect (Fig. 64).

Tidal flat development occurred with the initial episode of the generally northward transgression over an erosional surface. The tidal flat sequence is transgressive, grading upward in the section from upper tidal flat to lower tidal flat to subtidal lagoon. Terrigenous tidal flat development was complicated, however, by paleoslope and local currents. A highly variable sequence of coastal subenvironments occurred laterally. Lagoons cut off from the terrigenous sediment supply became sites of carbonate precipitation. At the Big Hatchet Mountains area, terrigenous influx was generally diminished, triggering carbonate production and tidal flat progradation under overall transgressive conditions.

Tidal deposits grade upward into shallow, restricted lagoonal deposits. Restricted and atypically euxinic subtidal conditions prevailed over the lagoon, because the lagoon was cut off from open circulation by a broad offshore carbonate buildup, and because water depth in the lagoon was sufficiently shallow that frictional drag prevented strong currents.

Less euxinic lagoonal conditions occurred at the Big Hatchet Mountains area, because carbonate production, initiated during tidal flat deposition, continued and maintained the lagoon bottom at a very shallow depth. Wind-generated waves and currents were able to mix the water and stir the shallow bottom sediments. The outer edge of the lagoon was channeled by influxes of fine skeletal debris transported from the carbonate platform into the lagoon.

The offshore carbonate buildup consisted of an inner and outer platform. The carbonate buildup was unlike most modern buildups because it lacked a major boundstone wave barrier at the outer platform edge. The outer Percha platform was the site of a broad garden of wave-baffling crinoids and bryozoans maintained at or near wave base. instead of upwelling currents along the platform edge being diminished along a narrow boundstone wave barrier, as occurs in most modern platform edge buildups, upwelling currents at the edge of the Percha platform were only slowly diminished as they moved across the platform.

As a result, outer bank crinoidal and bryozoan gardens took advantage of upwelling nutrients in this zone of high energy and extended from the shelf edge inward over a broad area. Currents were gradually reduced by the wave-baffling gardens from the outer platform, characterized by large shifting sand bodies; to the inner platform, characterized by rippled sand and channels; to the outer lagoon, characterized by small channels and micro-ripples. Inward, the shallow, stagnant lagoon existed, locked between the cratonic strandline and the broad offshore carbonate buildup.

The broad inward extension of the outer platform depositional environment during the transgression was accompanied by continued vertical growth of the outer platform skeletal bank. Vertical growth continued until carbonate production was outpaced by rising sea level. The net result is a northward-thinning skeletal bank deposit. Speculation concerning the cause of the thick deposit of micrite overlying skeletal bank deposits in this area includes a rapid rise in sea level with drowning of the crinoidal and bryozoan garden or migration of the gardens to shallower areas north of the study area.

Figure 68. East-west cross-section through the northern sections.

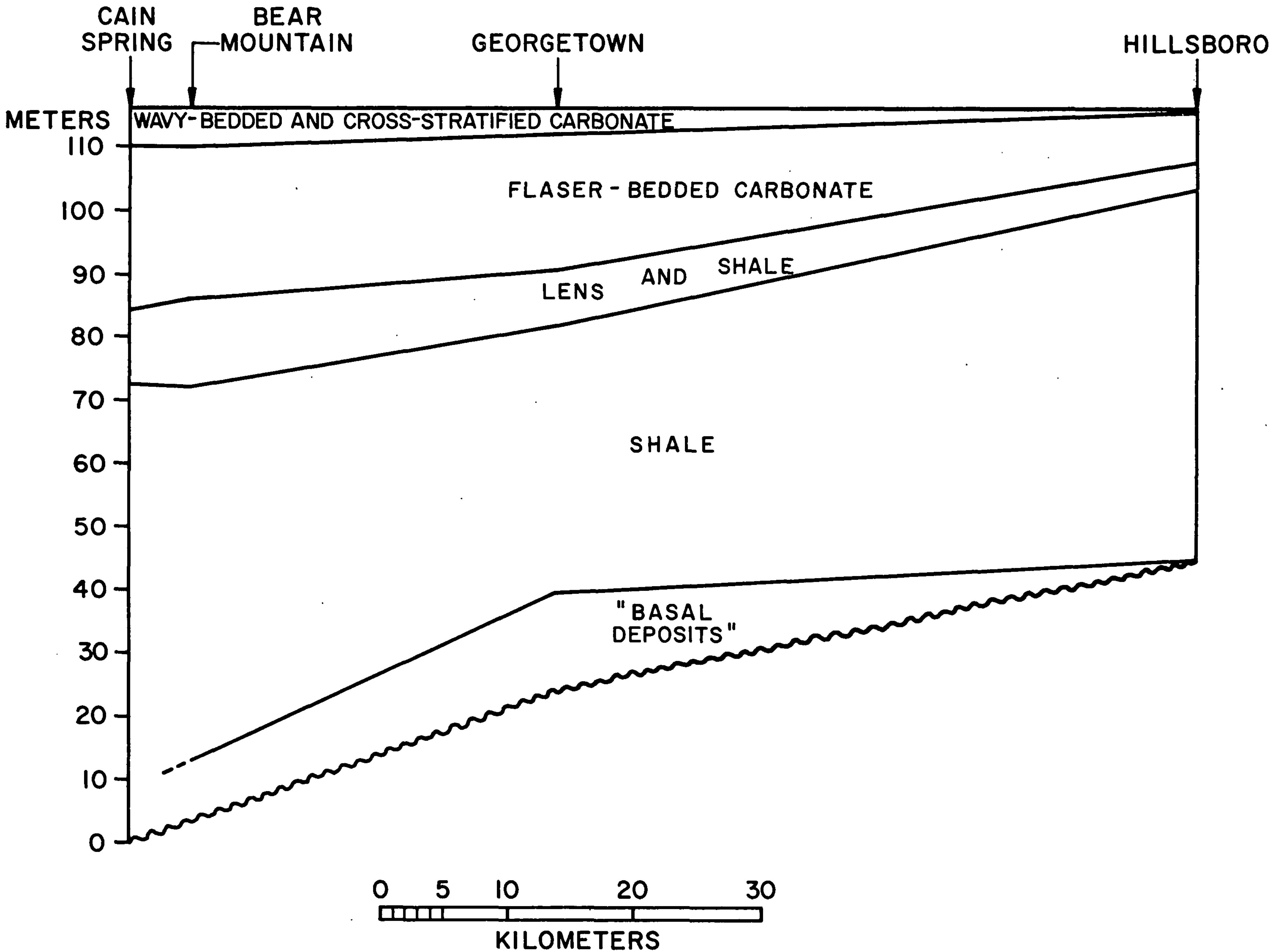
CAIN SPRING
BEAR MOUNTAIN
GEORGETOWN
HILLSBORO
METERS
WAVY-BEDDED AND CROSS-STRATIFIED CARBONATE
FLASER-BEDDED CARBONATE
LENS AND SHALE
SHALE
"BASAL DEPOSITS"
110
100
90
80
70
60
50
40
30
20
10
0
0 5 10 20 30
KILOMETERS

Figure 69. North-south cross-section from the Bear Mountain section to the Big Hatchet Mountains section.

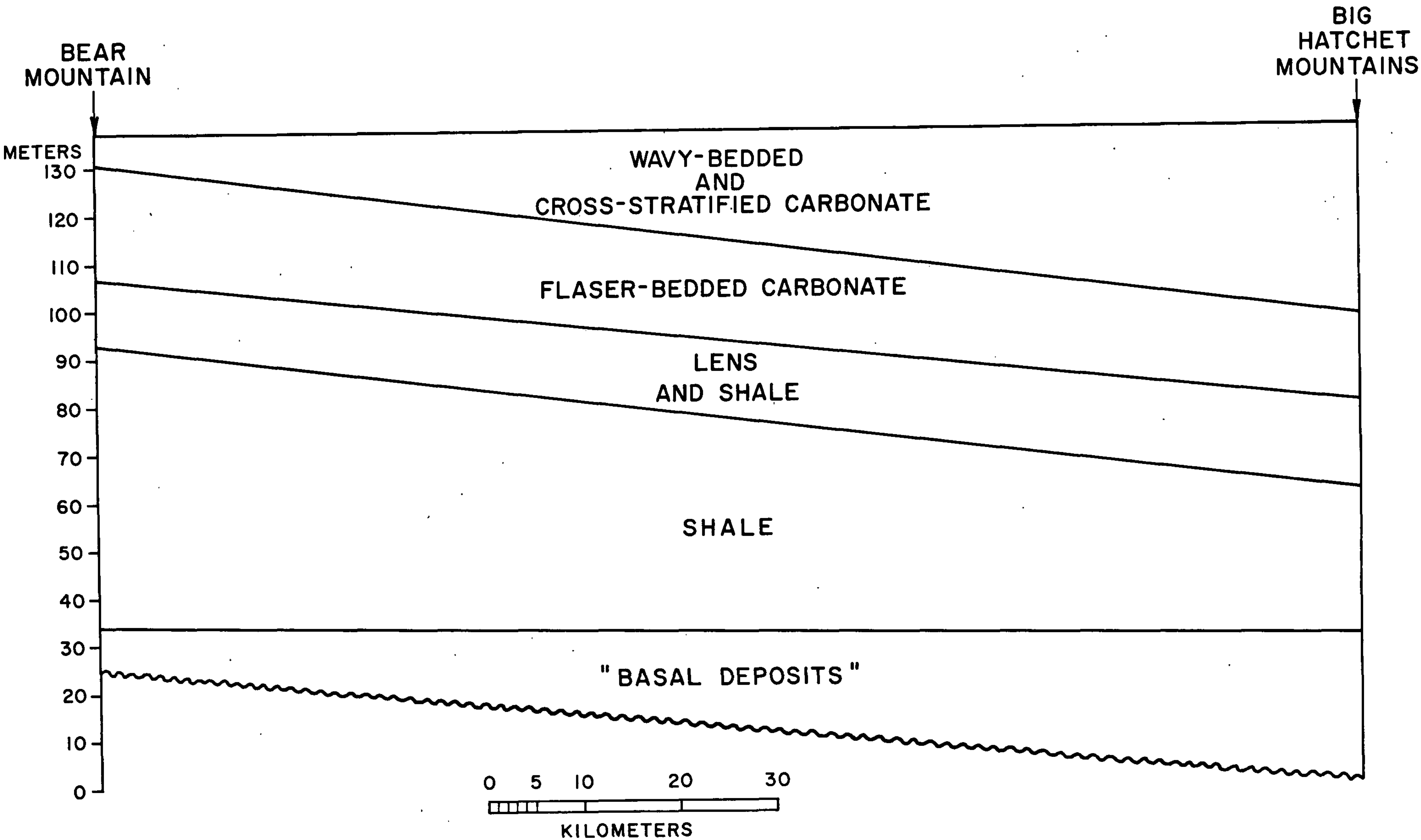
BEAR MOUNTAIN
BIG HATCHET MOUNTAINS
METERS
130
120
110
100
90
80
70
60
50
40
30
20
10
0
WAVY-BEDDED AND CROSS-STRATIFIED CARBONATE
FLASER-BEDDED CARBONATE
LENS AND SHALE
SHALE
"BASAL DEPOSITS"
0 5 10 20 30
KILOMETERS

DEVONIAN - MISSISSIPPIAN UNCONFORMITY

An unconformity has been cited as existing between the Percha and the overlying Escabrosa and Lake Valley Formations (most notably by Laudon and Bowsher, 1941, 1949; Stevenson, 1945; Armstrong, 1962; and Schumacher and others, 1976). Within the terminology of this study, the unconformity occurs between the flaser-bedded carbonate, and wavy-bedded and cross-stratified carbonate lithofacies. Working in the Sacromento Mountains of New Mexico, Laudon and Bowsher (1941) state that the lithologic expression of the unconformity is an oxidized horizon containing phosphatic concretions and, locally, fish teeth. In an expanded work covering much of the Mississippian strata of southwestern New Mexico, Laudon and Bowsher (1949) state that the fauna of the Caballero Formation is similar to the Kinderhookian fauna of the Chouteau Formation of the Mississippi Valley and that the fauna of the Lake Valley Formation is Osage in age. Lane (1974), working with conodonts, found the Caballero and Lake Valley Formations of southeastern New Mexico to range in age from middle to late Kinderhookian. Schumacher and others (1976), studying conodonts from outcrops in eastern Arizona and parts of southwestern New Mexico, state that the topmost beds of the Percha Formation are late but not latest Famennian, the overlying Caballero is Kinderhookian, and the Lake Valley is Osagian. Although all of these previous workers indicate that an unconformity is present, none deemed it necessary to qualify his usage of the term unconformity. Unqualified, the term means only a surface of nondeposition or erosion. It is highly important, however, to state whether this nondeposition or erosion was subaerial or submarine.

A consideration of the overall Percha depositional package indicates that an unconformity may have resulted from submarine erosion, but there is no evidence whatsoever to indicate subaerial weathering. The contact between the lithofacies is gradational, and the vertical sequence of lithofacies clearly indicates a transgression. A shoaling of water depth occurred during the transition from the deposition of the flaser-bedded carbonates to the deposition of the wavy-bedded and cross-stratified carbonates. This shoaling was the result of a lateral shift of depositional environments from the inner carbonate platform to the outer bank at or near wave base. This sequence is transgressive, and no regression is involved.

The lithologic evidence cited by Laudon and Bowsher (1941), moreover, does not indicate an unconformity. This author is at a loss to comprehend the significance of fish teeth in indicating an unconformity. Everywhere this author found the "oxidized zone" within the study area, the reddish color was a surface feature formed by the weathering of the phosphatic concretions and was not present on a fresh surface. Phosphatic pebbles were found to occur as channel-lag in the bases of the lower skeletal sand bodies and channel-fill in wavy-bedded and cross-stratified lithofacies (Fig. 70). The phosphatic pebbles were x-rayed and determined to be carbonate-apatite. Their presence, however, does not indicate an unconformity.

Work on presently-forming phosphates indicates that they are associated with areas of upwelling nutrient-rich and biologically productive waters (Baturim, 1971; Summerhayes and others, 1973; Manheim and others, 1975; and Summerhayes and others, 1976). For example, Manheim and others (1975) found contemporary phosphates forming along the upper continental slope in the zone of maximum upwelling nutrient-rich water off Peru and Chili. Phosphate was occurring as a replacement of foraminiferal tests in organic-rich sediment. Similarly, Summerhayes and others (1976) report contemporary phosphate forming off southwestern Africa concentrated on the outer continental shelf. Phosphates are uncommon on the inner shelf and slope.

The association between upwelling zones and phosphate formation results because areas of upwelling cause high biological production, and the resulting organic-rich sediment provides conditions favorable for the diagenetic growth of phosphate. According to Manheim and others (1975), and Summerhayes and others (1976), phosphate formation is also enhanced by a low rate of terrigenous sedimentation.

Those conditions associated with the formation of phosphate have already been described as existing along the outer carbonate platform, which is where the phosphatic pebbles occur in the Percha. Upwelling currents occurred at the platform edge and extended over the bank, with crinoid and bryozoan gardens taking advantage of the nutrients in these currents. Terrigenous sediment was negligible in this zone, except at Hillsboro, where the rate of sedimentation is uncertain.

Considering the nature of sedimentation along the outer carbonate platform, it is not surprising that conodont faunal zones may be missing. The initial transgression of high energy bank conditions may have reworked or removed existing substrate. In addition, the nature of sedimentation on the bank was such that a high degree of reworking and movement of sediment occurred without a great deal of net deposition in any particular area.

APPENDIX - CLAY MINERALOGY OF THE PERCHA FORMATION

Clay Mineral Sample Preparation and X-ray Diffraction Analysis Procedure

Washed shale or mudstone samples were finely ground with a mortar and pestle forming a slurry. The slurry was poured on a glass slide and allowed to dry for 24 hours in order for clay particles to orient themselves. The clay mount was then scanned at 2 θ per minute from 40° to 0° 2θ in order to get a preliminary identification of the clay minerals present. When a 12 to 14 Å peak was present, the mount was placed in a container with ethylene glycol and heated at 60 degrees C for 3 hours. The mount was then scanned from 16° to 0° 2θ. Montmorillonite-type clay displays a shift after glycolation from 12 to 14 Å to about 16 to 18 Å. When a 7 Å peak was present, the mount was scrapped from the glass slide and water was added to make a slurry. This slurry was poured on heat-proof slides and heated at 600° C for 1 to 2 hours. The mount was then again scanned from 16° to 0° 2θ. Kaolinite becomes amorphous and the 7 Å peak is lost. Some Fe-rich chlorites behave like kaolinite upon heating.

Quantification Procedures

Clay minerals in the Percha are illite and chlorite and were "semi-quantified" according to Hawkins (1970). Hawkins, using methods developed by Shell Research, Houston, determined the relative percentage of 10 Å versus 7 Å material by the equation:

$$\%\ 10\ \text{Å} = \frac{100\ (\text{ht. } 10\ \text{Å peak})}{\text{ht. } 10\ \text{Å peak} + (\text{ht. } 7\ \text{Å peak} / 2.5)}$$

Peak heights were measured from the diffractograph of the glycolated mounts. The amount of 7 Å material could be simply determined by 100% - % 10 Å material, because all Percha terrigenous clay consisted of illite or illite and chlorite. Hawkins states that the method is accurate within $\pm$ 10 percent.

Mineralogy of the Clay Fraction of the Percha Formation

The tables on the following pages list the mineralogy of the clay fraction occurring within the Percha Formation by samples x-rayed. Samples are listed according to their number of meters above the base of the formation. Where illite and chlorite are both present, the relative percentages of each is listed. Where thin-section work indicated the presence of micrite, an "x" is placed in the column headed "micrite".

MINERALOGY OF THE CLAY FRACTION OF THE PERCHA FORMATION:

BEAR MOUNTAIN SECTION

# m above base	Illite	Chlorite	Micrite	Litho-facies
111.8	0	0	x	Wavy-bedded and cross-stratified carbonate
108.2	0	0	x	
106.9	x	0	x	
94.8	0	0	x	Flaser-bedded carbonate
91.7	0	0	x	
78.0	85	15	x	Lens and shale
71.9	82	18	0	
64.3	78	22	0	Shale
61.3	76	24	0	
58.3	84	16	0	
52.1	81	19	0	
49.1	82	18	0	
46.1	81	19	0	
39.9	80	20	0	
33.8	82	18	0	
30.8	86	14	0	
27.8	74	26	0	
21.6	75	25	0	
15.4	88	12	0	
12.5	92	8	0	
3.0	x	0	0	"Basal deposits"
.7	x	0	0	
.03	x	0	0	

MINERALOGY OF THE CLAY FRACTION OF THE PERCHA FORMATION:

CAIN SPRING CANYON SECTION

# m above base	Illite	Chlorite	Micrite	Litho-facies
100.3	0	0	x	Wavy-bedded and cross-stratified carbonate
67.4	85	15	0	Lens and shale
64.3	83	17	0	
61.0	87	13	0	
59.8	80	20	0	
54.9	86	14	0	Shale
51.9	82	18	0	
48.9	87	13	0	
42.7	78	22	0	
36.5	79	21	0	
33.5	86	14	0	
29.8	90	10	0	
27.4	89	11	0	
24.4	89	11	0	
21.3	100	0	0	
16.8	100	0	0	
11.9	96	4	0	
6.1	94	6	0	

MINERALOGY OF THE CLAY FRACTION OF THE PERCHA FORMATION:

GEORGETOWN SECTION

# m above base	Illite	Chlorite	Micrite	Litho-facies
88.4	0	0	x	Wavy-bedded and cross-stratified carbonate
86.9	0	0	x	Flaser-bedded carbonate
83.5	0	0	x	
80.8	x	0	x	
76.2	x	0	x	
68.8	x	0	x	
67.4	x	0	x	
65.5	x	0	0	Lens and shale
58.8	x	0	0	
44.2	90	10	0	Shale
30.5	79	21	0	
21.3	96	4	0	
15.0	98	2	0	"Basal deposits"
9.0	x	0	0	
6.1	x	0	0	
3.0	x	0	0	
.3	x	0	0	
.3	x	0	0	

MINERALOGY OF THE CLAY FRACTION OF THE PERCHA FORMATION:

HILLSBORO SECTION

# m above base	Illite	Chlorite	Micrite	Litho-facies
67.0	x	0	x	Flaser-bedded carbonate
64.0	x	0	x	
62.2	x	0	x	
60.9	x	0	0	Lens and shale
57.9	95	5	0	
54.9	91	9	0	
50.3	82	18	0	
42.7	82	18	0	
39.7	83	17	0	
35.0	83	17	0	
32.0	82	18	0	
28.9	80	20	0	Shale
25.9	87	13	0	
22.9	85	15	0	
19.8	83	17	0	
16.7	88	12	0	
13.7	90	10	0	
10.7	80	20	0	
6.1	91	9	0	
.6	84	16	0	

MINERALOGY OF THE CLAY FRACTION OF THE PERCHA FORMATION:

BIG HATCHET MOUNTAIN SECTION

# m above base	Illite	Chlorite	Micrite	Litho-facies
132.6	0	0	x	Wavy-bedded and cross-stratified carbonate
109.7	0	0	x	
106.7	0	0	x	
103.7	0	0	x	
94.5	x	0	x	Flaser-bedded carbonate
85.3	0	0	x	
72.5	x	0	x	Lens and shale
26.8	0	0	x	
51.8	x	0	x	Shale
42.7	x	0	x	
39.7	x	0	x	
35.0	x	0	x	
30.0	x	0	x	"Basal deposits"
25.0	x	0	x	
20.0	x	0	x	
18.0	x	0	x	
9.0	x	0	x	
6.1	x	0	x	
3.5	x	0	0	

References

Amsden, T.W., W.M. Caplan, P.L. Hilpman, E.H. McGlasson, T.L. Rowland and O.A. Wise, Jr. 1967. Devonian of the southern midcontinent area, United States in D.H. Oswald ed., International Symposium on the Devonian System, Alberta Soc. Pet. Geol., Calgary. 1: 913-932.

Anderson, Roger Y. and Douglas W. Kirkland. 1960. Origin, varves and cycles of Jurassic Todilto Formation, New Mexico. Amer. Assoc. Pet. Geol. Bull. 44: 37-52.

Anderson, Roger Y. and Douglas W. Kirkland. 1969. Paleoecology of an early Pleistocene lake on the High Plains of Texas. Geol. Soc. Amer. Mem. 113: 215 pp.

Anderson, Roger Y., Walter E. Dean, Jr., Douglas W. Kirkland and Henry I. Snider. 1972. Permian Castile varved evaporite sequence, West Texas and New Mexico. Geol. Soc. Amer. Bull. 83: 59-86.

Armstrong, Augustus K. 1962. Stratigraphy and paleontology of the Mississippian System in southwestern New Mexico and adjacent southeastern Arizona. New Mexico State Bureau of Mines and Mineral Resources, Mem.: 99 pp.

Baturim, G.N. 1971. Stages of phosphorite formation on the ocean floor. Nature (Lond.) 232: 61-62.

Bowsher, Arthur L. 1967. The Devonian System of New Mexico. Tulsa Geol. Soc. Digest 35: 258-276.

Brown, Charles Q. and Roy L. Ingram. 1954. The clay minerals of the Neuse River Sediments. Jour. Sed. Petr. 24: 196-199.

Byers, Charles Wesley II. 1973. Biogenic structures of black shale paleoenvironments. Dissertation, Yale University: 134 pp.

Byrne, John V., Duane O. LeRoy and Charles M. Riley. 1959. The chenier plain and its stratigraphy, southwestern Louisiana. Gulf Coast Assoc. Pet. Geol. 9: 237-260.

Bryne, John V. and K.O. Emery. 1960. Sediments of the Gulf of California. Geol. Soc. Amer. Bull. 71: 983-1010.

Calvert, S.E. 1964. Factors affecting distribution of laminated diatomaceous sediments in the Gulf of California in Marine Geology of the Gulf of California - A symposium. Amer. Assoc. Pet. Geol. Mem. 3: 311-330.

Campbell, C.V. 1967. Lamina, laminaset, bed and bedset. Sedimental. 8: 7-26.

Chafetz, Henry S. 1972. Surface diagenesis of limestone. Jour. Sed. Petrol. 42: 325-329.

Collinson, Charles, Leroy E. Becker, Marvin P. Carlson, Fred H. Dorheim, Gerard W. James, John W. Koenig and David H. Swann. 1967. Devonian of the north-central region, U.S. in O.H. Oswald, ed. International Symposium on the Devonian System, Alberta Soc. Calgary. 1: 933-972.

Darton, M.H. 1917. A comparison of Paleozoic sections in southern New Mexico. U.S. Geol. Surv. Prof. Paper 108-C; 31-55.

Deuser, W.G. 1974. Evolution of anoxic conditions in Black Sea during Holocene in E.T. Degenes and D.A. Ross, eds. The Black Sea - Geology, Chemistry and Biology. Amer. Assoc. Pet. Geol. Mem. 20: 133-136.

Dunham, K.C. 1935. The geology of the Organ Mountains. New Mexico State Bureau of Mines and Mineral Resources, Bull. 11: 272 pp.

Folk, Robert L. 1962. Spectral subdivision of limestone types. Amer. Assoc. Pet. Geol. Mem 1: 62-84.

Folk, Robert L. 1974a. Petrology of Sedimentary Rocks. Hemphill Publ. Co., Austin, Texas. 182 pp.

Folk, Robert L. 1974b. The natural history of crystalline calcium carbonate: effect of magnesium content and salinity. Jour. Sed. Petro. 44: 40-53.

Fritz, M.A. 1944. Upper Devonian bryozoa from New Mexico. Jour. Paleo. 18: 31-41.

Ginsburg, R.N. 1956. Environmental relationships of grain size and constituent particles in some South Florida carbonate sediments. Amer. Assoc. Pet. Geol. Bull. 40: 2384-2427.

Gordon, C.H. 1907. Mississippian (Lower Carboniferous)Formation in the Rio Grande Valley, New Mexico. Amer. Jour. Sci. 24: 60-62.

Griffin, George M. and Roy L. Ingram. 1955. Clay minerals of the Neuse River estuary. Jour. Sed. Petrol. 25: 194-200.

Grim, Ralph E. and William O. Johns. 1953. Clay mineral investigation of sediments in the northern Gulf of Mexico in Ada Swineford and Norman Plummer, eds. Clays and Clay Minerals. Nat. Research Council Publ. 327: 81-103.

Hawkins, Gayle Patrick. 1970. The stratigraphy and mineralogy of the Lewisville Member of the Cretaceous Woodbine Formation in the Arlington, Tarrant County, Texas area. Master thesis, University of Houston. 199 pp.

Ingram, Roy L. 1954. Terminology for the thickness of stratification and parting units in sedimentary rocks. Geol. Soc. Amer. Bull. 65: 937-938.

Jenkins, W.A.M. 1970. Chitinozoa. Geoscience and Man 1: 1-21.

Kaye, Clifford, A. and Walter R. Power Jr. 1954. A flow cast of very recent date from northeastern Washington. Amer. Jour. Sci. 252: 309-310.

Kindle, E.M. 1909. Devonian fauna of the Ouray Limestone. U.S. Geol. Surv. Bull. 391: 60 pp.

Kottlowski, Frank E. 1963. Paleozoic and Mesozoic strata of southwestern and south-central New Mexico. New Mexico State Bureau of Mines and Mineral Resources, Bull. 79. 100 pp.

Kuenen, Ph. H. 1958. Experiments in geology. Trans. Geol. Soc. Glasgow 23: 1-28.

Kuenen, Ph. H. 1965. Value of experiments in geology. Geologie en Mijnbouw 44: 22-36.

Lane, H. Richard, 1974. Mississippian of southeastern New Mexico and West Texas - A wedge-on-wedge relation. Amer. Assoc. Pet. Geol. Bull. 58: 269-282.

Laudon, L.R. and A.L. Bowsher, 1941. Mississippian formations of Sacramento Mountains, New Mexico. Amer. Assoc. Pet. Geol. Bull. 25: 2107-2160.

Laudon, L.R. and A.L. Bowsher. 1949. Mississippian formations of southwestern New Mexico Geol. Soc. Amer. Bull. 60: 1-88.

Msnheim, Frank, Gilbert T. Rowe and Don Jipa. 1975. Marine phosphorite formation off Peru. Jour. Sed. Petrol. 45: 243-251.

Matthews, R.K. 1966. Genesis of recent lime mud in southern British Honduras Jour. Sed. Petrol. 36: 428-454.

McGlasson, E.H. 1967. The Siluro-Devonian of West Texas and southeast New Mexico in O.H. Oswald, ed. International Symposium on the Devonian System. Alberta Soc. of Pet. Geol. Calgary. 11: 937-948.

Miller, A. and C. Cullison. 1951. A clymenoid ammonoid from New Mexico. Amer. Jour. Sci. 249: 600-603.

Moore, D.G. and P.C. Scruton. 1957. Minor internal structures of some recent unconsolidated sediments. Amer. Assoc. Pet. Geol. Bull. 41: 2723-2751.

Muller, G. and R. Blaschke. 1969. Zur entstehung des Tiefsee-Kulkschlammes im Schwarzen Meer. Naturwissenschaften 56: 561-562.

Multer, H. Gray. 1975. Field guide to some carbonate rock environments. Dept. of Earth Sciences, Fairleigh Dickinson University Contrib. 40. 175 pp.

Pool, F.G., D.L. Baars, H. Drewes, P.T. Hayes, K.B. Ketner, E.D. McKee, C. Tiechert and J.S. Williams. 1967. The Devonian of the southwestern United States in O.H. Oswald, ed. Internation Synposium on the Devonian System. Albert Soc. of Pet. Geol. Calgary. 1: 879-912.

Potter, Paul Edwin and F.J. Pettijohn. 1963. Paleocurrents and Basin Analysis. Academic Press, N.Y. 296 pp.

Powers, Maurice C. 1953. Clay diagenesis in the Chesapeake Bay area in Ada Swineford and Norman Plummer, eds. Clays and Clay Minerals. Nat. Research Council. Publ. 327: 68-80.

Powers, Maurice C. 1957. Adjustment of land derived clays to the marine environment. Jour. Sed. Petrol. 27: 355-372.

Reineck, Hans-Erich. 1967. Layered sediments of tidal flats, beaches and shelf bottoms of the North in George H. Lauff, ed. Estuaries. Amer. Assoc. Adv. of Sci. Publ. 83: 191-206.

Reineck, Hans-Erich. 1972. Tidal flats in J. Keith Rigby and Wm. Kenneth Hamblin, eds. Recognition of Ancient Sedimentary Environments. S.E.P.M. Spec. Publ. 16: 146-159.

Reineck, Hans-Erich and Friedrich Wunderlich. 1968. Classification and origin of flaser and lenticular bedding. Sedimental. 11: 99-104.

Schopf, J.M. 1969. Early Paleozoic Polynomorphs. in Aspects of Palynology. Robert H. Tschudy and Richard A. Scott, eds. Wiley - Interscience. New York. 163-192.

Schopf, J.M. and J.F. Schwietering. 1970. The Foerstia zone of the Ohio and Chattanooga shale. U.S. Geol. Surv. Bull. 1294-H.: 15 pp.

Schumacher, D. D.P. Witter, S.J. Meader and S.B. Keith. 1976. Late Devonian Tectonism in southeastern Arizona. Ariz. Geol. Soc. Dig. 10: 59-70.

Shinn, Eugene A., R.N. Ginsburg and R. Michael Lloyd. 1965. Recent supratidal dolomite from Andros Island, Bahamas in L.C. Pray and R.C. Murray, eds. Dolomitization and Limestone Diagenesis. S.E.P.M. Spec. Publ. 13: 112-123.

Shrock, R.R. 1948. Sequences in Layered Rocks. McGraw-Hill Book Co. New York. 507 pp.

Stainbrook, M.A. 1947. Brachiopoda of the Percha Shale of New Mexico and Arizona. Jour. Paleo. 21: 297-328.

Stevenson, Frank. 1945. Devonian of New Mexico. Jour. Geol. 53: 217-245.

Straaten, L.M.J.U. van. 1954. Composition and structure of recent marine sediments in the Netherlands. Leidse Geol. Mededal. 19: 1-110.

Straaten, L.M.J.U. van. 1961. Sedimentation in tidal flat areas. Alberta Soc. Pet. Geol. 9: 203-226.

Straaten, L.M.J.U. van. and Ph. H. Kuenen. 1958. Tidal action as a cause of clay accumulation. Jour. Sed. Petrol. 28: 406-413.

Summerhayes, Colin P., G.F. Birch, J. Rogers and R.V. Dongle. 1973. Phosphate in sediments off southwestern Africa. Nature (Lond.) 243. 509-511.

Summerhayes, Colin P. Ubirajara de Melo and Henyo T. Barretto. 1976. The influence of upwelling on suspended matter and shelf sediments off southeastern Brazil. Jour. Sed. Petrol. 46: 819-828.

Tennant, C.B. and R.W. Berger. 1957. X-ray determination of dolomite-calcite ratio of a carbonate rock. Amer. Min. 42: 23-29.

Thompson, Robert Wayne. 1968. Tidal flat sedimentation on the Colorado River delta, northwestern Gulf of California. Geol. Soc. Amer. Mem. 107. 133 pp.

Zangerl, Rainer and Eugene S. Richardson. 1963. The paleoecological history of two Pennsylvanian black shales. Fieldiana: Chicago Natural History Museum, Geol. Mem. 4.: 239 pp.

Zeller, Robert A. Jr. 1965. Stratigraphy of the Big Hatchet Mountains area, New Mexico. New Mexico State Bureau of Mines and Mineral Resources, Mem. 16: 128 pp.